INVESTIGATION OF THE ROLE OF GROOVE HYDRATION AND CHARGED NUCLEOSIDES IN DNA CHARGE TRANSFER

A Thesis
Presented to
The Academic Faculty

by

Frank Okezie Onyemauwa

In Partial Fulfillment
of the Requirements for the Degree
Doctor of Philosophy in Chemistry in the
School of Chemistry and Biochemistry

Georgia Institute of Technology
Dec, 2006

INVESTIGATION OF THE ROLE OF GROOVE HYDRATION AND CHARGED NUCLEOSIDES IN DNA CHARGE TRANSFER

Approved by:

Dr. Gary B. Schuster, Advisor
School of Chemistry and Biochemistry
Georgia Institute of Technology

Dr. Leslie Gelbaum
School of Chemistry and Biochemistry
Georgia Institute of Technology

Dr. Christoph Fahrni
School of Chemistry and Biochemistry
Georgia Institute of Technology

Dr. Uzi Landman
School of Physics
Georgia Institute of Technology

Dr. Donald Doyle
School of Chemistry and Biochemistry
Georgia Institute of Technology

Date Approved: 07/25/2006

This work is dedicated to my physically late father Mr. Benjamin Akazi Onyemauwa who taught me the value of education, responsibility and diligence.

ACKNOWLEDGEMENTS

The work described herein could not have been possible without the help and support of several people. I wish to thank Professor Gary Schuster my Ph.D. advisor for his guidance and for giving me the opportunity to learn in his laboratory by doing the work described below. I will also like to thank all my committee members for their useful advice. Special thanks to Dr. Sriram Kanvah for being the friend and the help that was readily available when ever I needed it. I will like to thank Dr. Abraham Joy for the laughs and his friendly advice during the course of this work. Also, I will like to extend my gratitude to Dr. Joshy Joseph for his help and interest in seeing that the last project describe herein came to conclusion by giving useful suggestions that enabled the incorporation of the modified monomer into DNA strands. Thanks to Gozde Guler, Avik Gosh, Prolay Das, Dr. Bhaskar Datta, Dr. Chu-Sheng Liu and all past members of Schuster group who contributed to my successful completion of this work by their suggestions jokes or teasing. I thank Dr. Cathy Cobb a wonderful friend and my undergraduate advisor for her encouragement, and without whom I could not have thought of going to graduate school for chemistry. Finally, my biggest gratitude goes to my most special friend Erica Jones for her emotional and loving support through my graduate education despite the turbulent times.

TABLE OF CONTENTS

LIST OF TABLES

LIST OF FIGURES

Page

LIST OF SCHEMES

LIST OF SYMBOLS AND ABBREVIATIONS

A	Adenine
Å	Angstrom
AQ	Anthraquinone
AQC	Anthraquinone Carboxyamide
ATP	Adenosine triphosphate
C	Cytidine
CD	Circular dichroism
DCC	Dicyclohexylcarbodiimide
DIPEA	Diisopropyl ethyl amine
DMAP	Dimethyl amino pyridine
DMT	Dimethoxytrityl
DNA	Deoxyribonucleic acid
ESI-MS	Electrospray ionization mass spectrometry
FPG	Formamidopyrimidine glycosylase
G	Guanine
K	Kelvin
k_{hop}	Charge hopping rate constant
k_{trap}	Charge trapping rate constant
MALDI-TOF	Matrix-assisted laser desorption ionization time-of-flight Mass spectroscopy
η	Change in inclination
NMR	Nuclear magnetic resonance
8-oxoG	7,8-Dihydro-8-oxodeoxyguanosine

PAGE	Polyacrylamide gel electrophoresis
PMB	*para*-methoxybenzyl
PNK	Polynucleotide kinase
Py	Pyridine
SAH	S-Adenosyl homosysteine
SAM	S-Adenosyl methionine
T	Thymine
TDT	Terminal dinucleotide transferase
THF	Tetrahydro furan
TFA	Trifluoro acetic acid
T*m*	Melting temperature
UV-vis	Ultraviolet-visible spectroscopy
Ω	Twist angle

SUMMARY

Structural analyses of DNA oligonucleotides indicate the presence of bound water molecules in the major and minor grooves of DNA. These water molecules participate in DNA charge transfer by their reaction with guanosine radical cation to form 7,8-dihydro-8-oxo-guanine (8-oxoG), which when treated with a base leads to DNA strand cleavage. We probed the reaction of guanosine radical cation with water with series of alkyl substituted cytidines and thymidines by incorporating the modified nucleosides into anthraquinone linked DNA duplexes and irradiating them with UV light at 350 nm. The incorporation of these hydrophobic substituents disrupt the DNA spine of hydration, and we have observed that these modifications in the major and minor groove do not effect the trapping or long distance hopping of radical cations in DNA.

The second part of the work reported herein examines the role of charged nucleosides in long range charge transfer in duplex DNA. DNA methylation is a naturally occurring process mediated by enzymes responsible for such functions in biological systems. Hypermethylation of DNA can also occur as a result of environmental alkylating agents leading to mutation of the affected cells. Methylation of the ring nitrogen of a purine base can introduce a positive charge in the ring resulting in the cleavage of the glycosidic bond of the nucleoside.

To understand the role of a charged nucleoside on charge transfer in DNA, we designed and synthesized cationic nucleoside mimics, which were incorporated into anthraquinone-linked DNA strands and irradiated at 350 nm. The presence of the cationic bases on the duplexes inhibits the migrating hole from hopping along the DNA strand,

and induces a prominent local structural distortion of the DNA as a result of the charged nucleobase.

CHAPTER 1

INTRODUCTION

Nucleic acids are polymers of nucleotides joined together by phosphodiester bridges in a 3′ to 5′ linkage. Polynucleotide strands wound together to form long helical molecule as a double helix with the single strands running in opposite directions (antiparallel) and held together by interchain hydrogen bonds (Figure 1.1). In the Watson - Crick Model of DNA, the bases are in the interior of the helix aligned at about 90 degree angle relative to the axis of the helix. Purine bases form hydrogen bonds with pyrimidines, forming a base pair. Experimental evidence indicates that in any given molecule of DNA, the concentration of adenine (A) is equal to thymine (T) and the concentration of cytidine (C) is equal to guanine (G). This means that A will only base-pair with T, and C with G. For Watson-Crick base-pairing, G-C base-pairs contain three H-bonds, whereas those of A-T base pairs contain two H-bonds, making G-C base-pairs more stable than A-T base-pairs (Figure 1.1).

The antiparallel nature of the helix is a result of the orientation of the individual strands. From a given position in the helix, one strand is oriented in the 5' ---> 3' direction and the other in the 3' ---> 5' direction. On its exterior surface of the double stranded DNA, the helix contains two deep grooves between the ribose-phosphate chains. These two grooves are of unequal size and are known as the major and minor grooves (Figure 1.2).

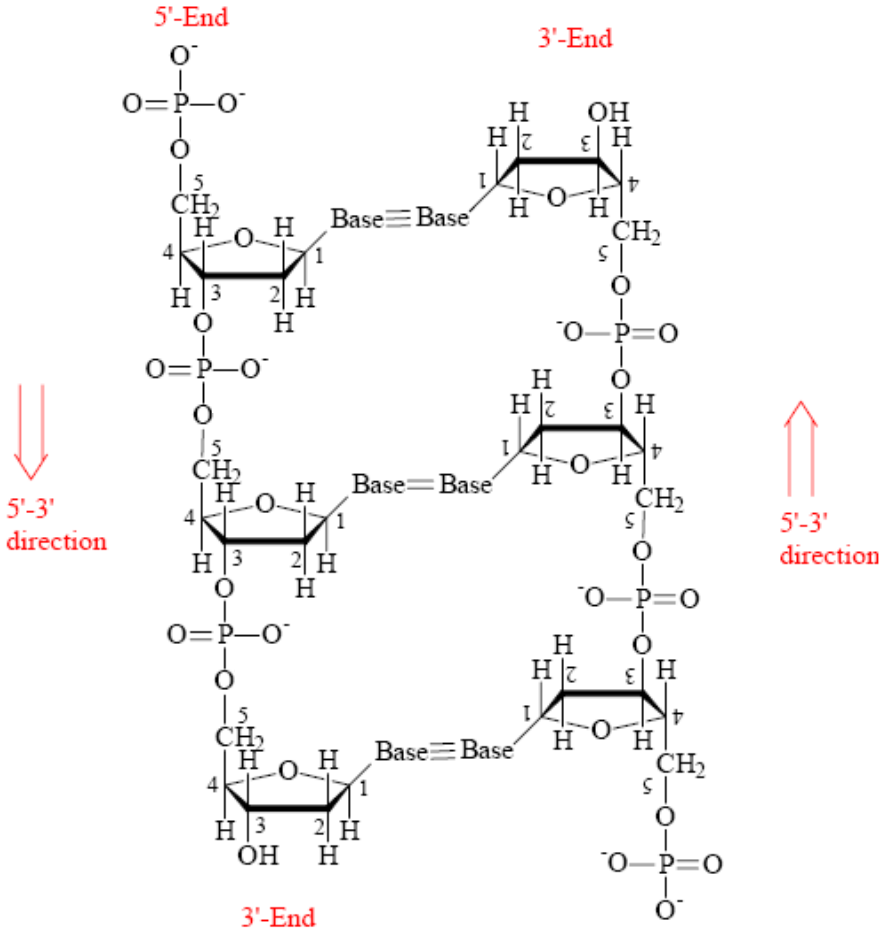

Figure 1.1 Anti-parallel Oligonucleotide Strands of DNA

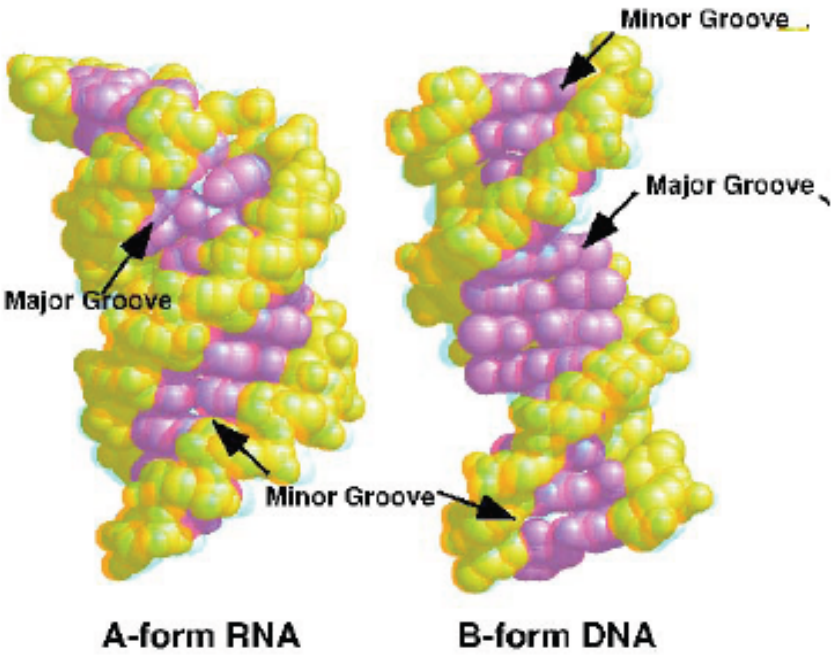

Figure 1.2 Major and Minor Grooves

The difference in their size is a result of the asymmetry of the deoxyribose rings and the structurally distinct nature of the upper surface of a base-pair relative to the bottom surface.

The double helix of DNA has been spectroscopically observed to exist in several different forms, depending upon sequence content and ionic conditions of crystal preparation. The B-form of DNA, which is the biologically dominant form, prevails under physiological conditions of low ionic strength and high degree of hydration. Regions of the helix that are rich in pCpG dinucleotides can exist in a novel left-handed helical conformation termed Z-DNA, and this conformation results from a 180 degree change in the orientation of the bases relative to that of the more common A- and B-DNA (Figure 1.3).

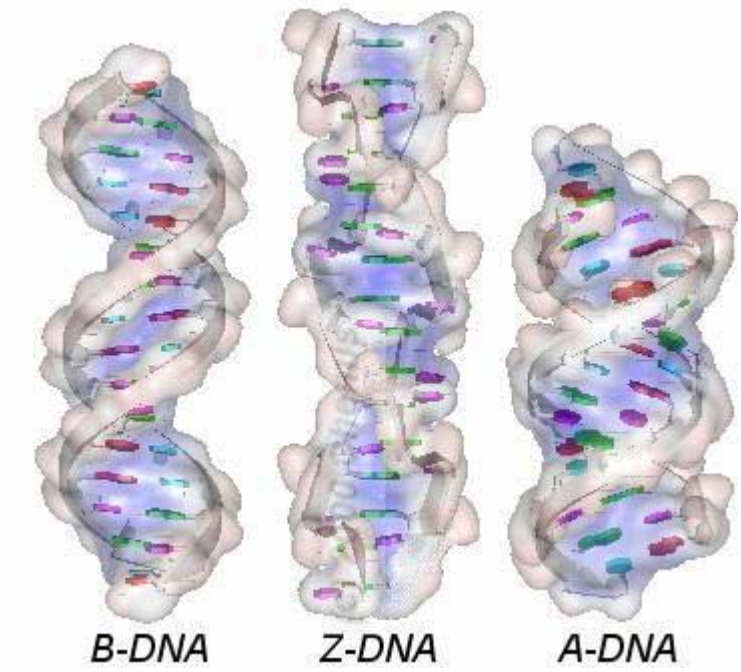

Figure 1.3 Different forms of DNA

The array of aromatic bases in the DNA double helix interact by their π stacking, and scientists have long believed that this π stacking property of DNA double helix can be used to convert DNA strands to molecular wires particularly when this extended solid state π system is doped.[1-3] Unfortunately, the idea of using DNA as a molecular wire has not been realized so far because unlike the regular π stacked bases of a uniform solid state, DNA is constructed from four distinct bases with different redox potentials and assumes its confirmation depending on the degree of hydration and the ionic environment available to it. Nonetheless, the electronic properties of DNA has been studied by scientist and charge migration along DNA bases up to 200Å has been established.[4-9] The extent to which the bridge orbitals of the intervening duplex DNA bases couple electron donor and acceptor is denoted by the symbol β, and the value of β has been reported to range from 0.6-1.3 $Å^{-1}$.[5,6,10-13] Charge transfer processes in DNA are considered in terms

of hole or electron transport. DNA oxidation results in loss of electron and the formation of a base radical cation (hole). The radical cation then migrates through DNA bases causing damage predominantly on the base with the lowest oxidation potential (E_{ox}) or on the base with the highest reactivity of the four bases. The radical cation continues to migrate until it encounters water or oxygen with which it reacts to produce damaged bases.[14]

Synthetic Nucleotide Analogs

Synthetic nucleosides have been used to study charge transfer in DNA. Amongst these are 7-Deazaguanosine, 3-Deazacytidine, 8-Methylguanosine, 5-Fluorouridine, 5-Methylcytidine, 2-Aminopurine, 4′-acylthymidines and 2-Cyanobenzophenone-2′-deoxyuridine.[15] These probes are used either to investigate the inhibition of charge transfer on DNA duplexes or to study the direction of electron transfer in DNA. In any case, the investigation with each of these modified nucleosides has always led to a greater understanding of how radical cation migrates across DNA bases.

The work described in the appendices was done in the laboratory of Dr. Katherine Seley prior to the DNA charge transfer studies and therefore will be introduced briefly below.

Many nucleotide analogues are chemically synthesized for their therapeutic potential. These analogues can be utilized to inhibit specific enzymatic activities. A large family of analogues used as anti-tumor agents, function by interfering with the synthesis of DNA and thereby preferentially killing rapidly dividing cells such as tumor cells. Some of the nucleotide analogues that have been used for chemotherapeutic purposes are

6-mercaptopurine, 5-fluorouracil, 5-iodo-2'-deoxyuridine and 6-thioguanine.[16] Each of these compounds disrupts the normal replication process by interfering with the formation of correct Watson-Crick base-pairing.

Nucleotide analogs also have been targeted for use as antiviral agents. Several analogs are used to interfere with the replication of HIV, such as AZT (azidothymidine**)** and ddI (dideoxyinosine). [17]

The purine analog allopurinol has also been used to treat gout. The structure of allopurinol resembles that of hypoxanthine. Allopurinol inhibits the activity of xanthine oxidase, an enzyme involved in *de novo* purine biosyntheses.[18] Additionally, several other nucleotide analogues are used after organ transplantation to suppress the immune system and reduce the likelihood of transplant rejection by the host.

REFERENCES

(1) Miller, J. S.; Epstein, A. J. *Angew. Chem. Int. Ed*. **1994**, *33*, 385

(2) Fox, M. A. *Acc. Chem. Res*. **1992**, *25*, 569

(3) Marks, T. J. *Science*. **1985**, *227*, 881

(4) Henderson, P. T.; Jones, D.; Hampikian, G.; Kan, Y. Z.; Schuster, G. B. *Proc. Natl. Acad. Sci. USA* **1999**, *96*, 8353

(5) Hall, D. B.; Holmlin, R. E.; Barton J. K. *Nature*. **1996**, *382*, 731

(6) Nŭńez, M. E.; Hall, D. B.; Barton, J. K. *Chem. Biol*. **1999**, *6*, 85

(7) Giese, B. *Acc. Chem. Res*. **2000**, *33*, 631

(8) Nakatani, K.; Dahno, C.; Saito, I. *J. Am. Chem. Soc*. **2000**, *122*, 5893

(9) Takada, T.; Kawai, K.; Cai, X.; Sugimoto, A.; Fujitsuka, M.; Majima, T. *J. Am. Chem. Soc.* **2004**, *126*, 1125

(10) Meggers, E.; Michael-Beyerle, M. E.; Giese. B. *J. Am. Chem. Soc*. **1998**, *120*,12950

(11) Brun, A. M.; Harriman, A. *J. Am. Chem. Soc*. **1992**, *114*, 3656

(12) Meade, T. J.; Kayyem, J. F. *Angew. Chem. Int. Ed. Engl*. **1995**, *34*, 352

(13) Lewis, F. D.; Wu, T.; Zhang, Y.; Letsinger, R. L.; Greenfield, S. R.; Wasielewski, M. R. *Science*. **1997**, *277*, 673

(14) Kasai, H.; Yamaizumi, Z.; Berger, M. Cadet, J. *J. Am. Chem. Soc*. **1992**, *114*, 9692

(15) Wagenknecht, H-A. *Current Organic Chem*. **2004**, *8*, 251

(16) Elion, G. B. *Science*. **1989**, *244*, 42

(17) For new syntetic procedure to AZT and references to the first synthesis of AZT, see Gunthier, C.; Ramondenc, Y. *Tetrahedron*. **2001**, *57*(35), 7513

(18) Gallo, R. C.; Perry, S.; Breitman, T. R. *Biochem. Pharmacol*. **1968**, *17*(10), 2185.

CHAPTER 2

PROBING THE REACTION OF GUANOSINE RADICAL CATION WITH WATER

The importance of water surrounding nucleic acids can never be overemphasized because water is not just a medium to keep the solutes dissolved, but it enables the interaction of different functional groups around the DNA backbone with each other, and the self-assembly of the DNA bases into ordered structures due to hydrophobic forces involving the active participation of water molecules. Detailed solvation studies of DNA molecules is interesting because of its relevance to understanding duplex stability, protein-DNA interaction, interduplex interactions and also to understand the role of ions surrounding the DNA. To this effect, experiments involving sedimentation equilibrium studies, gravimetric investigations, isopiestic measurements, infrared spectroscopic investigations and molecular dynamic simulation studies using high resolution crystal structures of oligonucleotides indicating the position of water molecules along the DNA major and minor grooves are well documented.[1-4] These high resolution structures indicate the presence of extensive hydration throughout the grooves of the DNA duplexes. The conformation of a DNA is determined predominantly by the degree of hydration of the DNA. While high relative humidity favors the B form, low humidity or increased ionic strength results in a transition from the B form to C-, A-, and possibly D- and Z-DNA.[1]

DNA hydration is described in terms of two discrete layers consisting of primary and secondary hydration shells. The primary hydration shell of a double-helical DNA

consist of approximately 11-12 water molecules per nucleotide, which are grouped into three classes according to their binding affinity for phosphate, phosphodiester plus sugar, and base. Spectroscopic information obtained from DNA hydration experiments at less than 65% relative humidity show hydration at phosphate oxygens, with 5-6 water molecules adsorbed per nucleotide.[1] The same experiments also show that below 60% relative humidity, phosphodiester and furanose O4 oxygens also are partly hydrated, while hydration of functional keto, imino, and amino groups of bases is observed above 65% relative humidity with additional 8-9 water molecules. At approximately 80% relative humidity, the primary hydration of DNA duplex is complete with 20 water molecules per nucleotide, which is different from bulk water. From these 20 water molecules, 8-9 are bonded to 11-12 other water molecules found in the inner, primary hydration shell indicating that not all of the 20 water molecules are directly in contact with DNA.[5] The water molecules bonded directly to DNA are impermeable to cations and these water molecules do not freeze into an ice-like state upon cooling to temperatures well below 0°C.[1]

The secondary hydration shell cannot be distinguished from bulk water with regards to permeability to ions, but its structure is slightly different from bulk water that is located further away from the polyelectrolyte DNA.

The different forms of DNA can be identified by using circular dichroism (CD), which measures the difference between the absorption of a left and right handed circularly-polarized light as a function of wavelength. The spectra observed from CD are a measure of the mean residual ellipticity of the DNA duplex. Transitions from one form of DNA to another can therefore be monitored by changes in circular dichroism spectra.

Addition of salt to a B-DNA results in a structural transition from B→C form DNA and further salt addition will result in a sharp cooperative transition between DNA families from C→A or B→A. Changing the polarity of the medium by increasing the amount of ethanol, isopropanol, methanol or dioxane by up to 80% can also change the structure from one form of DNA to the other.

The B-DNA dodecamer d(CGCGAATTCGCG) has been studied in detail,[1] and the crystal structure analysis provides information about the geometrical features of B-DNA with details concerning hydration. Each dodecamer duplex contains approximately 72 ordered water molecules under ambient condition, and a total of 48 more water molecules are observed at defined positions when the concentration of alcohol used for crystallization (2-methyl-2,4-pentanediol) is raised to 60%. At ambient temperature, the phosphate groups are not systematically hydrated except those water molecules that are trapped between thymine methyl group and 5′-phosphate of the same nucleotide. High alcohol concentration at 16K studies[1] however show that more immobilized water molecules bind to phosphate oxygens. There are about one to five solvent molecules per phosphate oxygen, and about 40% of these form bridges between two or more phosphate oxygens. The major groove hydration also shows monodentate binding of water molecules to keto oxygens and amino groups of purine and pyrimidine bases. In the minor groove of the dodecamer there exists an ordered spine of hydration along the central AATT sequence bridging thymine O2 and adenine N3. One layer of water molecules forms a continuous spine followed by a second layer which serves to complete the tetrahedral hydration environment. The water shells of the third and fourth order engage in hydrogen bonding with phosphate groups lining the edge of the minor groove.[1]

A-DNA hydration on the other hand is considerably different from that of B-DNA with no spine of water molecules running along any of the grooves. Nonetheless, phosphate groups of A-DNA are hydrated with a well ordered hydration scheme when compared to B-DNA. Tippin et al[6] reports an average of 10 water molecules per base pair in A-DNA. The vast majorities of the water molecules are found in the first hydration shell and are distributed with 30% in the major groove, 20% in the minor groove and the remaining 50% in the sugar-phosphate backbone.

One of the roles of the hydrating water molecules of DNA is reaction with nucleobase radical cations resulting from photosensitization reactions of endogenous or exogenous sensitizers associated with DNA. The reaction of water with the base radical cation results in the formation of modified nucleosides like 7,8-dihydro-8-oxo-guanine (8-Oxo-G),[7-8] which can be identified and cleaved by repair enzymes like formamidopyrimidine glycosylase (FPG).[9] Hence, water plays a very important role on how far a migrating radical cation can hop along a DNA duplex before getting trapped.

The focus on charge transfer in DNA is because nucleobase radical cations play an important role in oxidative damage leading to mutations and because of the promise of DNA molecular electronics.[10] The reaction of a radical cation in DNA occurs most commonly at guanine because it has the lowest oxidation potential of the four DNA bases (1.29 V).[11] Guanine radical cations in DNA are converted by reaction with water to 7,8-dihydroguanine-8-oxo-guanine (8-Oxo-G).[7-8] Evidence from molecular dynamics simulations and high resolution crystal structures of oligonucleotides indicate that water molecules are specifically associated with normally hydrated DNA oligomers.[3,4,12-14] For B-DNA, on average, each base pair is surrounded by ca. 25-30 water molecules and of

this number, 18-21 water molecules are tightly bound to DNA and the remaining molecules interact more weakly. The tightly bound water molecules are found primarily in the minor and major grooves at specific sites that depend somewhat on base pair sequence.[14] It seems likely that one or more of these specifically bound water molecules is involved in the reaction with guanine radical cations.

Mechanism of Reaction of Anthraquinone Carboxyamide (AQC) Sensitizer in DNA

Following the absorption of light at 350 nm, AQC (Figure 2.1) covalently attached to a DNA is activated to its singlet excited state (AQC^{*1}), which can undergo intersystem crossing to its triplet excited state (AQC^{*3}). Electron transfer from the base nearest to the AQC to the triplet excited AQC generates a triplet contact ion pair or a separated ion pair, and back electron transfer from these species to form ground states is prohibited by spin conservation rules.[15] The contact ion pair reacts with molecular oxygen to regenerate the AQC sensitizer and a nucleobase radical cation, which migrates by thermal motions of the DNA across the bases until trapped by water (Figure 2.2). This hopping mechanism is called polaron-like hopping model.[16] The excited singlet (AQC^{*1}) can also accept an electron from the nearest base to form a singlet contact ion pair, which can back electron transfer to regenerate the AQC and the base in their ground state.[17-18]

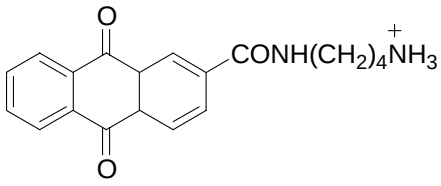

AQC

Figure 2.1 The structure of anthraquinone derivative (used in this study)

Spectroscopic evidence and experiments in the Schuster laboratory show that electron transfer from the base to the AQC is exothermic and rapid, and that the reaction is complete in less than 20 ps.[18] These experiments confirm that both singlet and triplet contact ion pairs are formed, and that the triplet contact pair goes further to react with water and oxygen. Further evidence for the existence of ion pairs is supported by time resolved flash photolysis experiments with antraquinone-2-sulfonate (AQS) by J.-H. Ma et al.[19] The results from the laser flash photolysis experiment further demonstrate that the initial species that are formed from the interaction of AQ sensitizer with nucleotides are ion pairs of base radical cation and AQ radical anion.

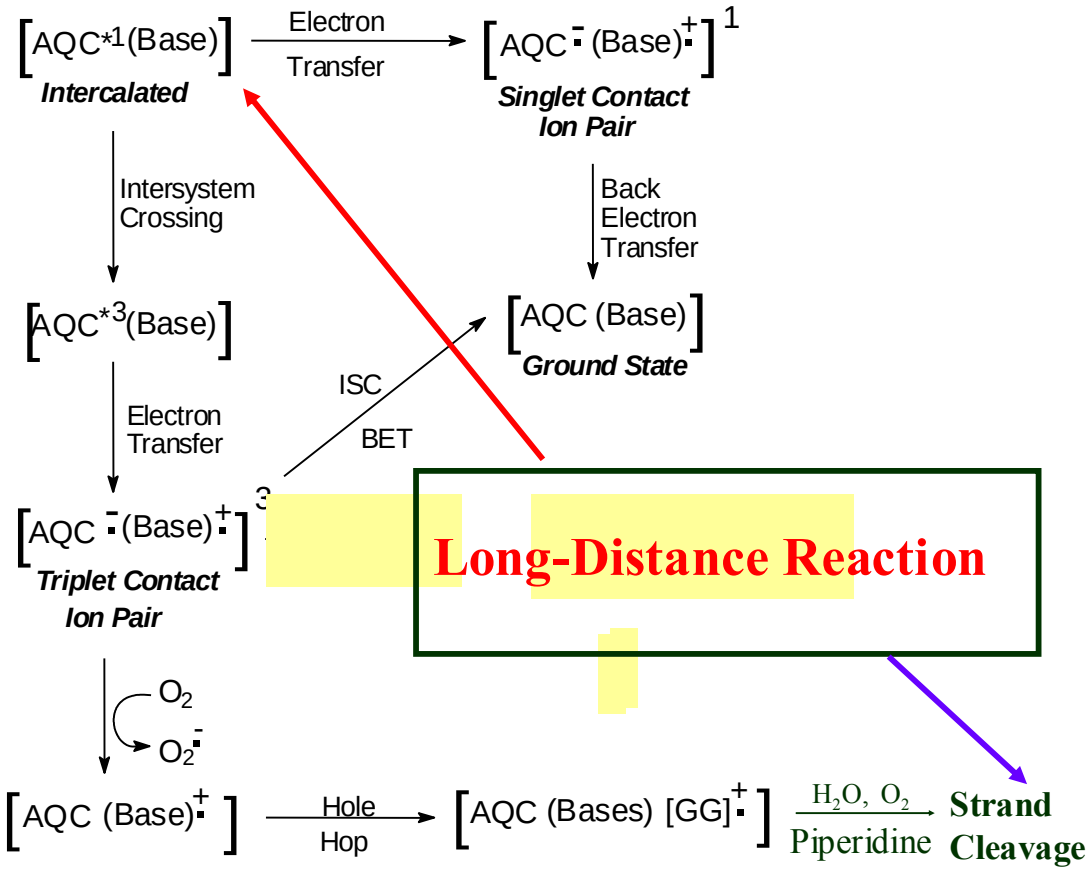

Figure 2.2 The Mechanism of anthraquinone photoexcitation (Schuster et al. *J. Am. Chem. Soc*. 1996, *118*, 36, 8747)

Since guanine bases have the lowest oxidation potential of the four bases and the highest reactivity, the guanosine base is converted to ($G^{\bullet+}$). The reaction of guanosine radical cation ($G^{\bullet+}$) with water to form 8-Oxo-G, which the repair enzymes can recognize, must be faster than charge recombination for DNA to be protected from photochemical damage. Lewis and Fukuzumi [20,21] have determined that fast charge recombination occurs with rate constants > 10^9 s^{-1}. While the absolute rate of the reaction of $G^{\bullet+}$ with water has not been agreed upon, a lifetime of 50 ns has been suggested. [22] Pulse radiolysis and laser photolysis experiments by Candeias et al [23,24] determined that the p*K*a of a free $G^{\bullet+}$ is 3.9, hence at neutral pH the $G^{\bullet+}$ is deprotonated to form the neutral oxidized radical (equation 1)

$$G^{\bullet+} \rightleftharpoons G(-H)^{\bullet} + H^{+} \qquad (1)$$

In comparison, when $G^{\bullet+}$ is formed in a DNA duplex, the proton from the guanosine radical cation is transferred to N3 of the cytosine (C) complementary base. The p*K*a of the N3-protonated C is 4.45, and experimental studies show that this proton is further transferred to the surrounding water. [25-28] This proton transfer has been determined to occur in about 1μs. [21] This means that charge migration across DNA bases is faster than the rate at which proton transfer occurs between guanosine radical cation and the complementary cytosine.

The Phonon-Assisted Polaron-Like Hopping Model

The polaron-like hopping model proposes that the migrating cation or hole act like polaron, and that a structural distortion of the DNA duplex stabilizes and delocalizes the radical cation over several bases. The changes that could lead to distortion include

reduction of the intrabase distance as a result of change in inclination (η) between adjacent base pairs,[29] a decrease in the twist angle (Ω) by rotation around the *z* axis of the DNA which will increase the π electron overlap between bases, thereby stabilizing the radical cation, and thirdly, a shift in the proton donation of the hydrogen bonds that form the base pair will change the p*K*a of the bases carrying the delocalized positive charge, which will in turn shift the hydrogen bonds of the duplex DNA to accommodate the change. These changes will result in a radical ion self-trapped by structural distortion of its containing medium. The polaron can migrate by tunneling only within short distances or it can migrate by phonon-assisted (thermally activated) hopping up 200 Å.[16] The model concludes that the migration of the radical cation occurs by thermal motions of the DNA and its environment when bases are added to or removed from the DNA.[16] This model was proposed by Schuster et al and has been widely accepted among scientist studying charge transfer in DNA.

Major and Minor Groove Hydration Studies

We report herein studies of the effect of water exclusion from the major and minor grooves of DNA on the reactions of nucleobase radical cations. Experiments and modeling studies (Figure 2.3) have shown that thymid[30] and that the N4-position of cytidine points toward the major groove of duplex DNA. We prepared a series of DNA oligomers that contain sugars modified by the covalent attachment of aliphatic alkyl groups at the 4'-position and a second series that contains N4-alkylated cytidines. Because they are hydrophobic, these groups are expected to repel water molecules in their vicinity. Radical cations were introduced into these modified oligomers by

photooxidation and the reaction at selected guanines was compared with that of unmodified DNA oligomers.

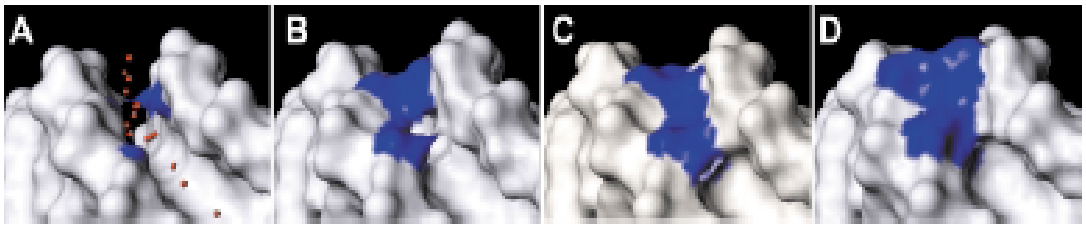

Figure 2.3 Thymidine residues bearing (a) 4′-H, (b) 4′-methyl, (c) 4′-ethyl and (d) 4′-isopropyl group projecting into the minor groove (Marx et al. *Chem. Com*. 2002, 2314)

MATERIALS AND METHODS

ATP radioactive isotopes [α^{32}P and γ^{32}P] and terminal dinucleotide transferase (TDT) were purchased from Amersham Bioscience, and T4 polynucleotide kinase (T4PNK) was purchased from New England Biolabs. DNA oligonucleotides containing anthraquinone and the complementary strands were prepared by standard solid phase methods on an Applied Biosystems DNA synthesizer using phosphoramidite chemistry, and purified by reverse phase HPLC using a C18 Varian Column.

Melting temperature (T_m) measurements of 2 μM duplexes were determined in 10 mM sodium phosphate buffer solution at pH 7.0 using a Cary 1E 3C spectrophotometer. Circular dichroism (CD) measurements were obtained using a JASCO (J-720) CD spectrophotometer. Images from gels were quantified using a Fuji 2340 BAS-image reader. All chemicals and reagents for the synthesis of the modified nucleosides were purchased from either Fisher Scientific or from Sigma Aldrich.

Preparation of radiolabeled DNA. Oligomers were radiolabeled at the 3'-end using α-^{32}P ATP and TDT enzyme while 5'end labeling was performed using γ-^{32}P ATP and T4 PNK enzyme. The single DNA strands were mixed with α-^{32}P ATP or γ-^{32}P ATP and the relevant enzyme. The mixture was diluted to 20 μL and incubated for 45 min at 37^{o}C after which it was purified using a 20% denaturing polyacrylamide gel.

UV Irradiation and analyses. A 5 μM sample of the complementary strand was mixed with 10,000 c.p.m radiolabeled AQ-linked oligonucleotide in a 10 mM sodium phosphate buffer at pH 7.0 and hybridized by heating at 90^{o}C for 10 min, followed by slow cooling to room temperature. Samples were irradiated for 5, 10 or 20 min at ca 30^{0}C in microcentrifuge tubes in a Rayonet Photoreactor equipped with eight 350 nm lamps. Irradiated samples were then precipitated with cold absolute ethanol (100 μL) and glycogen (2 μL), after which the samples were washed twice with 100 μL 80 % ethanol. The samples were dried and treated with 1 M piperidine (100 μL) for 30 min at 90 ^{0}C and afterwards the samples were dried and co-evaporated twice with H_2O (20 μL). Samples were then dissolved in a loading dye and loaded in a 20 % 19:1 acrylamide/bis-acrylamide gel. Drying of gels enabled the visualization of the cleavage sites by autoradiography.

Syntheses of modified nucleosides. The modified nucleosides 4′-isopropylthymidine, 4′-hydroxymethylthymidine, 4N-methylcytidine and 4N-butylcytidine (Figure 2.4) were synthesized according to published procedures.[31-35] 4′-isopropylthymidine

phosphoramidite was synthesized in 16 steps (Scheme 2.1). The 4′-hydroxymethylthymidine was incorporated into the DNA as the benzoyl derivative and was deprotected from the DNA using 30 % ammonia solution in water at 60 ^{0}C for 12 hours. The 4-N alkyl cytidines where synthesized in 5 steps (scheme 2.2)

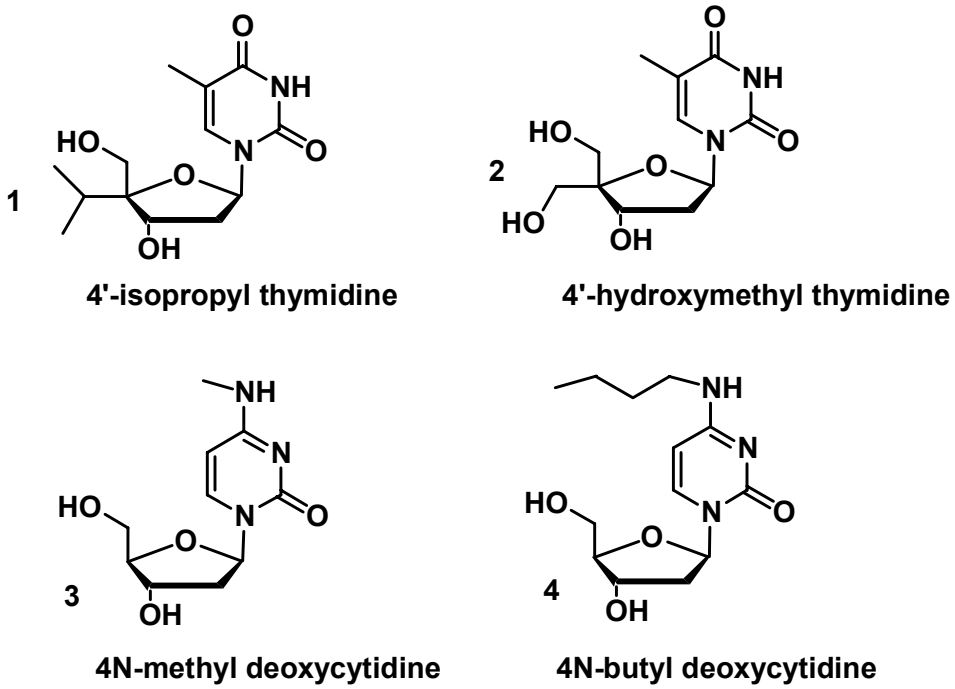

Figure 2.4 Major and Minor Groove Probes

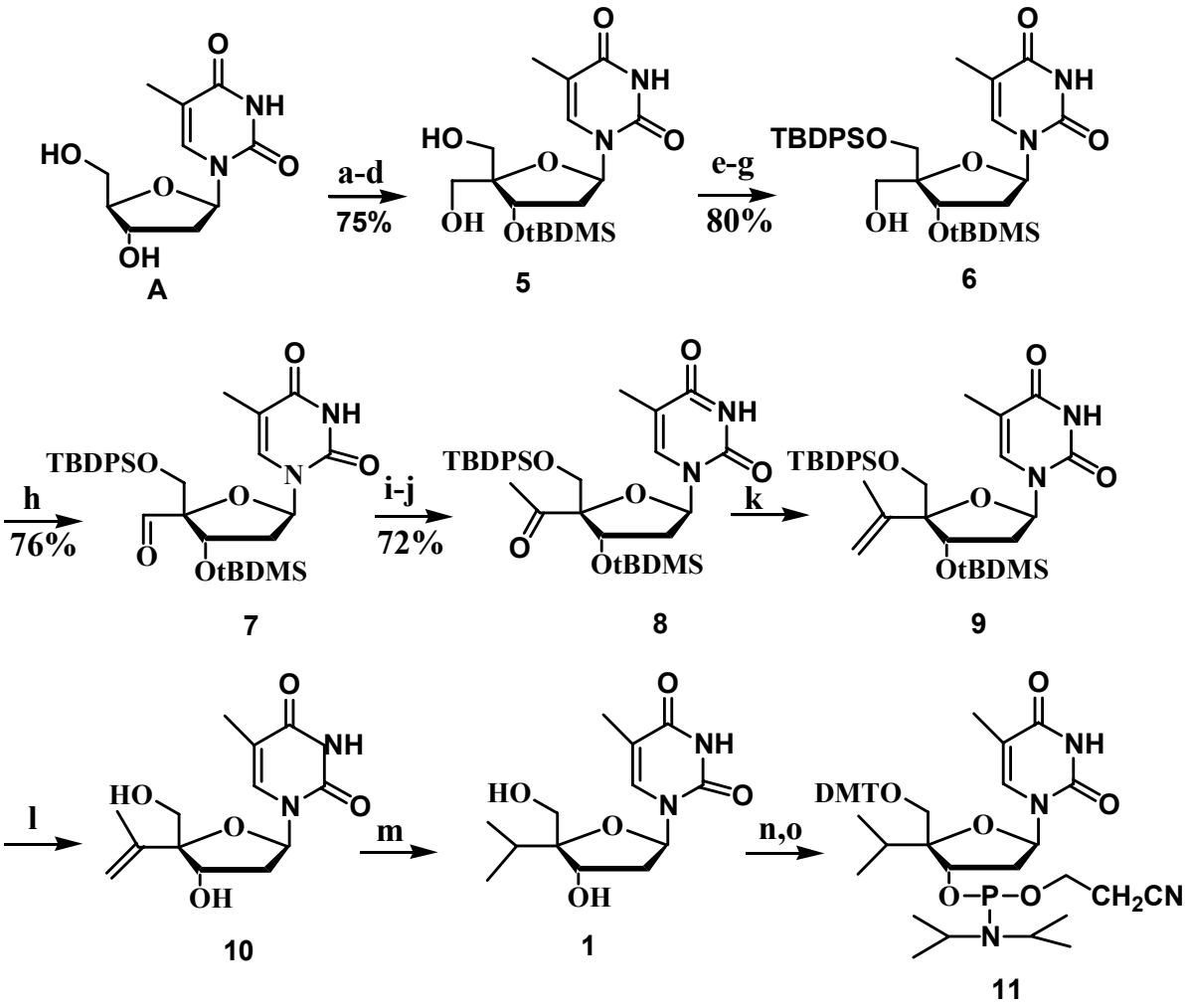

(a) DMTCl, pyridine, DMAP, (b) tBDMSCl, imidazole, DMF (c) 80% AcOH/H_2O, (d) TFA, DCC, DMSO,pyridine/oxalic acid, Tartaric acid, ACOH, NaOH/dioxane, Formaldehyde, $NaBH_4$ (e) DMTCl, DMAP, pyridine, (f) TBDPSCl, imidazole (g) 80%AcOH/H_2O, (h) $C_4Cl_6O_3$, DMSO, CH_2Cl_2 (i) MeMgCl, THF, 0^0C (j) $C_{13}H_{13}IO_8$,CH_2Cl_2 (k) CH_3PPh_3Br, tBuOk/THF (l) TBAF/THF (m) Pd/C, EtOH (n) DMTCl, pyridine (o) 2-Cyanoethyl diisopropylchlorophosporamidite, CH_2Cl_2, DIEA

Scheme 2.1 Synthesis of 4′-isopropylthymidine

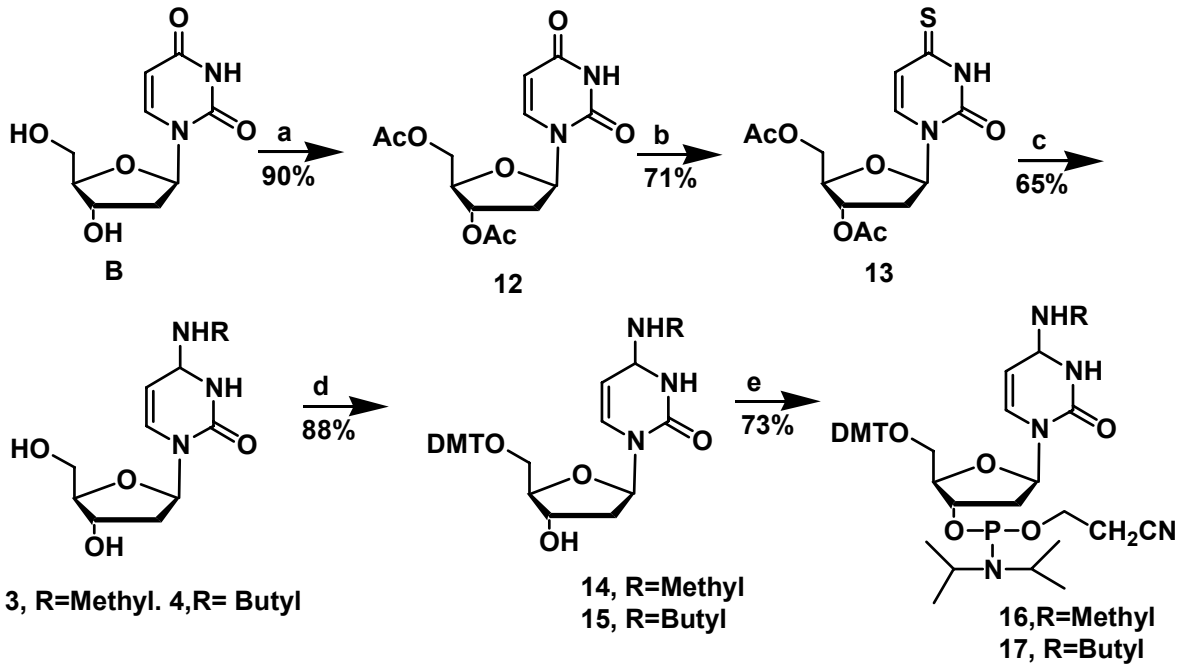

Reagents and Conditions: (a) Acetic anhydride, pyridine, DMAP, rt (b) P_2S_5, pyridine, heat (c) Methylamine/ethanol or butylamine/ethanol, rt (d) DMTCl,DMAP, pyridine (e) DIPEA, CH_2Cl_2, N,N-diisopropyl cyanophosphoramidite chloride, rt

Scheme 2.2 Synthesis of 4N-alkyl modified cytidines

RESULTS AND DISCUSSION

Hydrophobic Groups in the Major Groove.

Water is known to react with the guanosine radical cation in DNA to form 7,8-dihydro-8-oxoguanine (8-oxoG).[7-8] The Schuster group has previously reported that the rate of radical cation hopping (k_{hop}) is much faster than the rate for its irreversible trapping (k_{trap}) in duplex DNA having a $d(AAGG)_n$ sequence of base pairs.[36] In this case, statistically, the radical cation is distributed approximately equally among all of the GG steps of the duplex. Treatment of the irradiated sample with piperidine leads to strand cleavage at the reacted guanines that is detected by autoradiography of samples labeled

with ^{32}P. For $d(AAGG)_n$ sequences, an approximately equivalent amount of strand cleavage is seen at each GG step in the oligomer.

To investigate the effect of exclusion of water from the major groove we modified the N4 position of cytosine by incorporation of either a methyl group (N-MeC) or a butyl group (N-BuC). This modification eliminates one of the N4 protons, which is involved in hydrogen bonding to water while retaining the proton necessary for duplex formation. The modified nucleosides were then incorporated into DNA sequences shown in Figure 2.5a in positions indicated by **M** for 4N-methylcytidine and **B** for 4N-butylcytidine. As a control, sequences were also designed without the modified nucleosides (DNA's **1**, **4**,**7**,**10** and **13**). Several sequences were designed ranging from ones with bases that allowed efficient charge transfer to ones with bases that allowed minimal or no charge transfer in a sequence. DNA **1-3** $(AAGG)_n$ were designed to have the lowest charge transfer barrier by separating the GG steps with AA sequences which have the second lowest oxidation potential of the four DNA bases, and DNA **13-15** $(ATAGG)_n$ were designed with the highest charge transfer barrier by separating the GG steps with ATA sequences since thymine has the highest ionization potential of the four bases.

The modified cytidines are paired with guanosines on the second and third GG steps for DNA **2**, **3**, **5, 6, 14** and **15** and for DNA duplexes **8**,**9**,**11** and **12**, the modified cytidines were paired with guanosines on the second GG step. A sensitizer (anthraquinone) was covalently attached to the 5' position of the opposite strands that did not contain the modification. After purification of the DNA strands by HPLC and determination of the molecular weights by ESI Mass Spectroscopy, the DNA strands with

the anthraquinone were radiolabeled at the 3'-end using α-^{32}P ATP to enable visualization of the strands on the gel. The DNA strands were hybridized and irradiated with 8 UV lamps at 350 nm since this is the wavelength at which the attached sensitizer absorbs light without interference at the absorption wavelength of the DNA. Irradiation was carried out for either 5 or 10 minutes in a sample tube with a second or third sample labeled 0 minutes which was not irradiated as a control.

We assessed the overall structure and stability of the duplexes containing the modified nucleosides by CD spectroscopy, melting temperature (T_m) studies and molecular modeling. As expected, the (T_m) measurements of the modified duplexes are lower than those for the oligomers containing naturally occurring nucleosides (Table 1). The *n*-butyl substituents of DNA oligomers 3, 6 and 15 cause a 6^0C reduction in melting temperature at pH7 when compared to the unmodified sequences (Figure 2.6), while the methyl substituents of DNA oligomers 2, 5 and 14 reduce the Tm by approximately 4^0C at pH7. The reduced stability of the oligomers containing the alkyl substituted cytosines is attributed in part to disruption of hydrogen bonding of water molecules in the major groove and in part to a reduced capability to adopt the *trans*-conformation necessary for base pairing.[37] The CD spectra of the oligomers show that the duplexes containing the N-alkyl substituted cytidines maintain a predominant B-DNA conformation (Figure 2.7).

Figure 2.8 is a molecular model of the AAGG$_2$AA sequence with two N-BuC complementary to the GG step calculated using the Amber force field. It is clear from inspection that the N-BuC groups project into the major groove hindering the approach of water and disrupting the formation of an ordered spine of hydration.

DNA

	5'-AQ-AAG GAA GGA AGG AAG GAA GGA AGG TATA-*3'
1	**3'-TTC CTT CCT TCC TTC CTT CCT TCC ATAT-5'3'-**
2	**3'-TTC CTT MMT TMM TTC CTT CCT TCC ATAT-5'**
3	**3'-TTC CTT BBT TBB TTC CTT CCT TCC ATAT-5'**
	5'-AQ-TTG GTT GGT TGG TTG GTT GGT TGG TATA-*3'
4	**3'-AAC CAA CCA ACC AAC CAA CCA ACC ATAT-5'**
5	**3'-AAC CAA MMA AMM AAC CAA CCA ACC ATAT-5'**
6	**3'-AAC CAA BBA ABB AAC CAA CCA ACC ATAT-5'**
	5'-AQ-ATG GAT GGA TGG ATG GAT GGA TGG ATAT-*3'
7	**3'-TAC CTA CCT ACC TAC CTA CCT ACC TATA-5'**
8	**3'-TAC CTA MMT ACC TAC CTA CCT ACC TATA-5'**
9	**3'-TAC CTA BBT ACC TAC CTA CCT ACC TATA-5'**
	5'-AQ-AAA GGT TAG GAT AGG ATA GGA TTA TAT-*3'
10	**3'-TTT CCA ATC CTA TCC TAT CCT AAT ATA-5'**
11	**3'-TTT CCA ATM MTA TCC TAT CCT AAT ATA-5'**
12	**3'-TTT CCA ATB BTA TCC TAT CCT AAT ATA-5'**
	5'-AQ-ATA GGA TAG GAT AGG ATA GGA TAT CTGT-*3'
13	**3'-TAT CCT ATC CTA TCC TAT CCT ATA GACA-5'**
14	**3'-TAT CCT ATM MTA TMM TAT CCT ATA GACA-5'**
15	**3'-TAT CCT ATB BTA TBB TAT CCT ATA GACA-5'**

Figure 2.5a DNA(2,5,8,11,14) M = 4N-methylcytidine, DNA (3,6,9,12,15) B= 4N-butylcytidine

DNA

	3'-TTT GGA AAG GAA TGG AAT ATA-*5'
16	**5'-AQ-AAA CCT TTC CTT ACC TTA TAT-3'**
17	**5'-AQ-AAA CCT TIC CIT ACC TTA TAT-3'**
	5'-AQ-AAA CCT TAC CAT ACC TTA TAT-3'
18	**3'-TTT GGA ATG GTA TGG AAT ATA-*5'**
19	**3'-TTT GGA AIG GIA TGG AAT ATA-*5'**
	3'-TTT GCG CGC ACA CAC TTT CTT TATAT-5'
20	**5'-AQ-AAA CGC GCG TGT GTG AAA GAA ATATA-*3'**
21	**5'-AQ-AAA CGC GCG hGh GTG AAA GAA ATATA-*3'**

Figure 2.5b DNA (17 and 19) I = 4′-isopropyl thymidine. DNA (21) h = 4′-hydroxymethyl thymidine

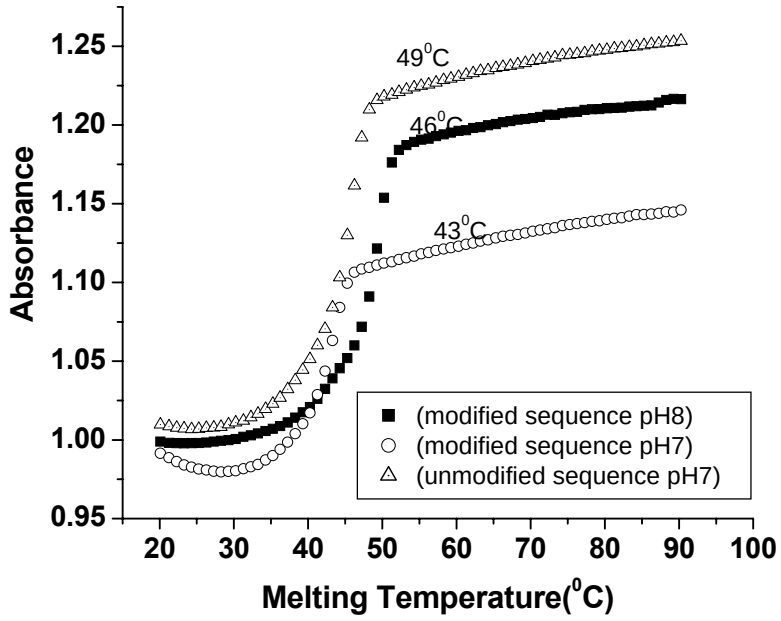

Figure 2.6 Thermal denaturation Curves for DNA's 1 and 3

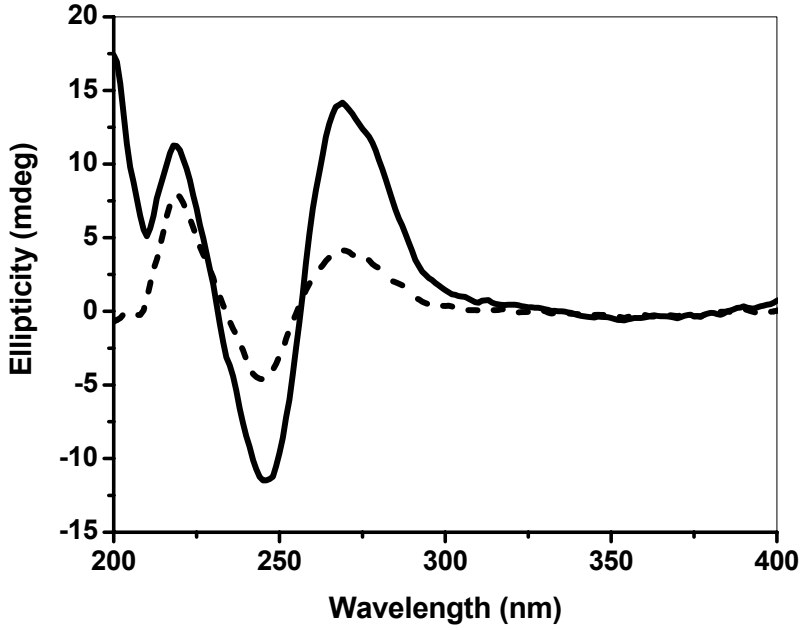

Figure 2.7 Circular Dichroism Spectra of DNA's 1 and 3

Irradiation of these 5′-anthraquinone linked duplexes at 350 nm, a wavelength at which only the anthraquinone group absorbs light and subsequent treatment of the sample

with piperidine leads to strand cleavage at each of the GG steps that is revealed by PAGE and can be analyzed by autoradiography. We showed that at low conversion (single-hit conditions) the relative amount of strand cleavage detected at each of the equivalent GG steps of DNA (1) is approximately the same and that this distribution is independent of irradiation time. In this case, hopping of the radical cation from GG site to GG site is faster than trapping and consequently the radical cation is equally distributed. Similar results are obtained from irradiation of DNA (4) except that there is somewhat less strand cleavage at GG steps farther away from the AQ than for those that are closer, which indicates that k_{hop} and k_{trap} are of similar magnitude. However, the behavior of DNA (13) is significantly different. In this case, only those GG steps closest to the AQ show meaningful strand cleavage. This indicates, as expected, that k_{hop} is slower than k_{trap} when the GG steps are separated by ATA segments. Surprisingly, essentially the same results are obtained when the cytosines opposite GG_2 and GG_3 are alkyl substituted, see Figures 2.9 and 2.10. The amount of strand cleavage at these sites is the same (within experimental error) as it is in the unmodified cases, and so is the relative amount of strand cleavage at the other GG steps in these oligomers. This result means that neither k_{hop} nor k_{trap} are affected by substitution of a methyl or *n*-butyl group for a hydrogen on N4 of the complementary cytosine. The autoradiography analysis indicates that neither the N-MeC nor N-BuC has a significant effect on the amount of reaction observed at the modified sites. For the N-MeC sequences, there is no detectable difference between the amount of strand cleavage for the unmodified sequence compared to the modified sequence (Figure 2.9), while in the case of the N-BuC sequence; there seem to be a lighter damage pattern on the modified AAGG sequence (Figure 2.10). While this result

may indicate a slower reaction of water with guanosine radical cation, it shows that 4N-alkyl substitution does not affect the rate of charge hopping or trapping in DNA.

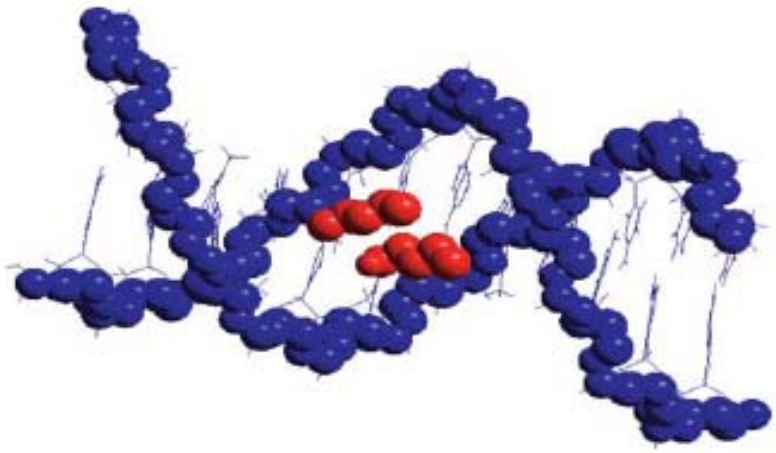

Figure 2.8 Hyperchem model of DNA sequences containing two n-butyl cytidines, shown in red, the sugar phosphate backbone of the DNA are shown as solid blue balls and the nucleobases are represented as blue stick figures. The structure was energy minimized using the amber force field. The n-butyl groups reside in the major groove of the DNA in a parallel orientation.

Table 1: Thermal denaturation studies of DNA duplexes 1-6 and 13-17 in 10 mM sodium phosphate buffer solution at pH 7.0 calculated from the average of three T*m* measurements.

DNA	T_m (°C)
1	49
2	45
3	43
4	49
5	44
6	43
13	48
14	45
15	41
16	39
17	37

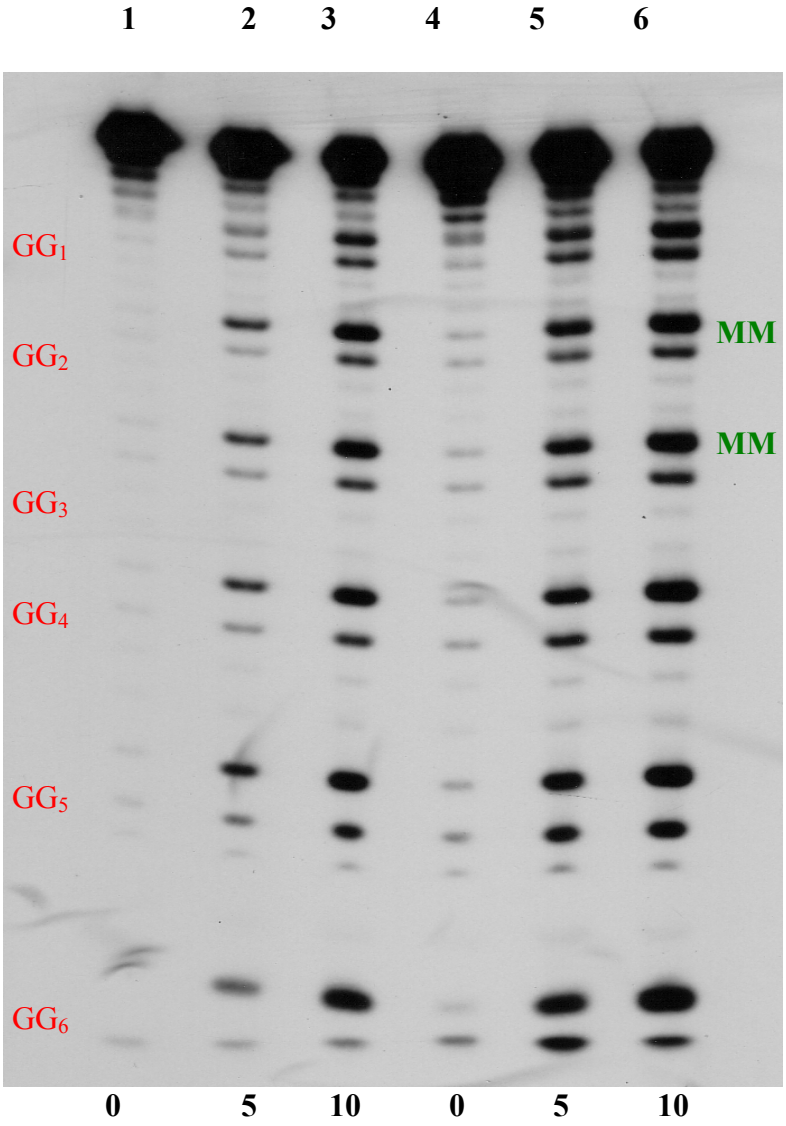

Figure 2.9 Autoradiogram showing the result of irradiation of DNA (1 and 2). The lanes in the gel from left to right correspond to 0, 5, and 10 min of irradiation time for the unmodified sequence to 0, 5 and 10 min for the 4N-methylcytidine modified sequence. M indicates the position of modified nucleoside in the complementary strand.

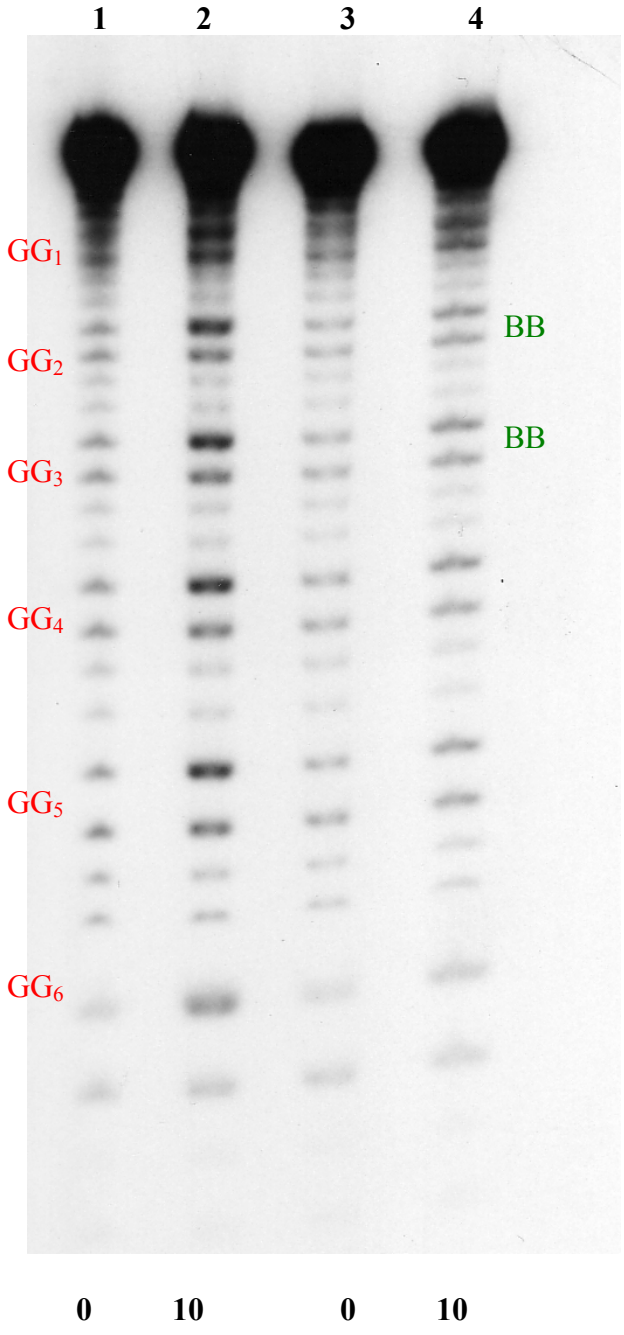

Figure 2.10 Autoradiogram showing the result of irradiation of DNA (1 and 3). The lanes in the gel from left to right correspond to 0, and 10 min of irradiation time for the unmodified sequence to 0 and 10 min for the 4N-butylcytidine modified sequence. B indicates point of modification

Minor Groove Studies.

Marx *et al*[30] carried out minor groove hydration studies that showed that alkyl groups covalently attached to the 4'-positions of deoxyribose residues point towards the minor grooves of DNA duplexes. They suggested that steric hindrance by these substituents prevents the formation of ordered spine of hydration in the minor groove. We investigated the effect on charge transfer in DNA by synthesizing and incorporating either 4′-isopropyl modified thymidines or 4'-hydroxymethyl modified thymidines in the DNA sequences in Figure 2.5b and comparing the result from the irradiation of these 5'-Anthraquinone linked modified sequences (DNA **17**, **19** and **21**) with unmodified sequences (DNA **16**, **18** and **20**). Modification was realized in the DNA by flanking the second CC step of the complementary strand on both ends with the 4'-isopropyl modified thymidine (DNA **17**) and for DNA **19** by flanking the second GG step on both ends with 4'-isopropyl modified thymidine. DNA **21** was modified by flanking the fourth single G on both ends with 4'-hydoxymethyl modified thymidines.

Results from the irradiation of these sequences also show little or no detectable difference between the hopping or trapping rate of the modified compared to the unmodified sequences. However, the quantum efficiency of strand cleavage of the duplexes that contain 4′-isopropyl modification is somewhat reduced, which may be as a result of slower reactivity of the modified sequences with water as seen in Figure 2.11 (DNA **17)**.

Interestingly, disruption of the DNA spine of hydration can also be effected by increasing the hydrogen bonding capabilities in the minor groove, and this is evident when DNA (**21**), Figure 2.12, is considered. Experiments with the single G sequence DNA (**21**) indicate that the 4'-hydroxymethyl modified thymidines can reduce the extent of the reaction of $G^{+\bullet}$ with water and strand cleavage. The modified sequence shows reduced reaction.

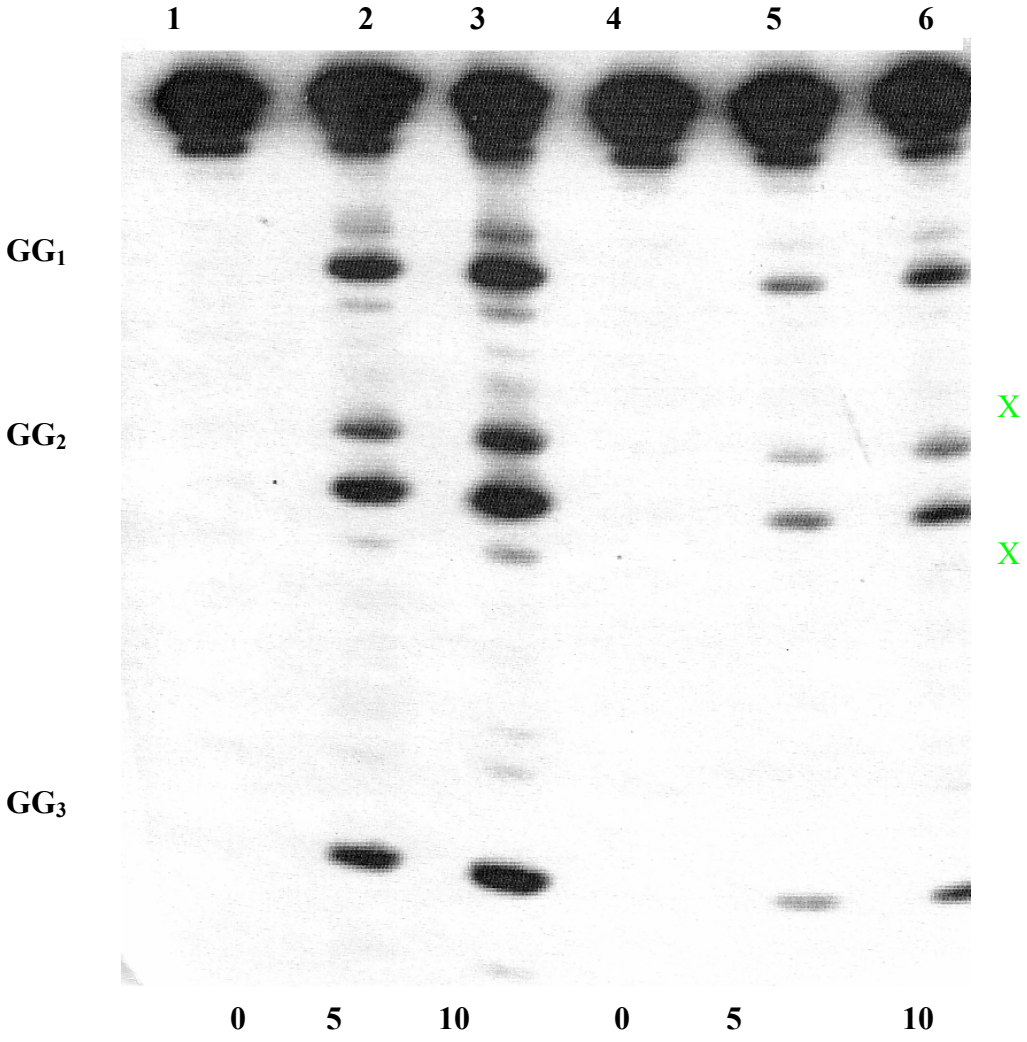

Figure 2.11 Autoradiogram showing the result of irradiation of DNA (17). The lanes from left to right show 0, 5, and 10 min of irradiation for the unmodified sequence and 0, 5 and 10 min of irradiation for the modified sequence. X indicates 4'-isopropyl modified thymidine

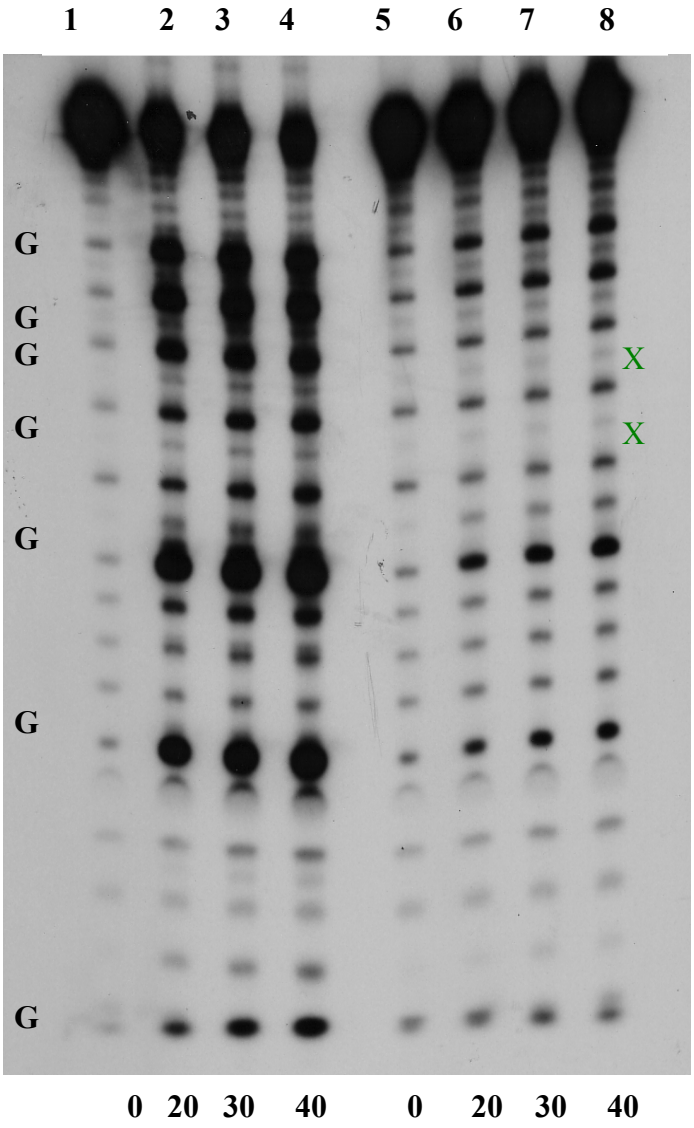

Figure 2.12 Autoradiogram showing the result of irradiation of DNA (21). The lanes from left to right show 0, 20, 30, and 40 minutes of irradiation for the unmodified sequence and 0, 20, 30, and 40 minutes of irradiation for the modified sequence. X indicates 4'-hydroxymethyl thymidine

According to reports by Sunderalingam et al,[7] complete exclusion of water from the DNA major groove by modification of the N4 of cytosine would result in only a 30% reduction in water binding sites at the CG base pair. From our experimental results, Pettit's[14] work and molecular dynamic calculations from Gunsteren,[12] it is evident that

exclusion of water from DNA major groove by modification of only the N4 of cytosine or from minor groove by modification of only 4′-position of thymidine with alkyl groups would result in a minimal observable overall effect on water binding sites of the major groove. Evidently, the remaining water molecules are sufficient to effectively trap the guanine radical cation. While increasing the number of modified nucleosides in a sequence may increase the possibility of excluding more water molecules from the major groove, thereby slowing the reaction of guanosine radical cation with water and resulting in a reduced damage pattern, it may not change the trapping or hopping rate since there is no observable damage ratio difference between the proximal and distal GG steps. An increase in the number of modified nucleosides in the duplex can only result in further dehydration of the duplex and probably a change from B-form DNA to A-form DNA with time.

To determine the extent of $G^{+\bullet}$ reaction with water leading to 8-oxoG formation in our modified sequences, we treated the irradiated samples with iridium salt to further oxidize the 8-oxoG and result in strand cleavage without piperidine treatment[38]. We reasoned that inhibition of the reaction of $G^{+\bullet}$ with water to form 8-oxoG should result in less 8-oxo-G formation in the modified sequences, leading to less strand cleavage, but the result of iridium treatment of these sequences also showed no difference in the proximal to distal ratio of the GG damage . Also, for the above reason and because formamidopyrimidine glycosylase (FPG) is known to cleave oligonucleotides at damaged guanines[9] and specifically 8-oxoG, we treated the irradiated samples with FPG to determine the relative amount of 8-oxoG that is formed by the inhibition of water in the minor groove. The results of the gel electrophoresis (autoradiography not shown)

indicate approximate amount of damage compared to sequences treated with piperidine by quantitative analyses and no difference in damage between the modified and unmodified sequences. The data from the autoradiography of DNA 1-6 and 13-17 are summarized as a histogram in Figure 2.13.

NMR spectroscopy studies of the *trp* operator fragment d-$(TAGCGTACTAGTACGCT)_2$ by Gunsteren *et a*[12] show that water molecules in the major and minor groove bind with residence times not longer than 1 ns at 277 K before they are exchanged by other water molecules. Consequently, it is expected that the rate of exchange of water molecules will be much faster than trapping of the guanine radical cation; this may explain the absence of an alkyl substitution effect in excluding water from the major or minor groove. Our findings suggest that the relative rate of the reaction of water with guanosine radical cation may be slower than the rate at which water molecules exchange with each other. It is also to be noted that since the molecular dynamic simulation studies by Gunsteren *et al.*[12] show that only water molecules that are 0.35 nm to the major/minor groove or less can be effected by N4 substitution on cytosine or 4'-position on thymidine, it may be that the water molecules in this proximity do not participate in the trapping or hopping mechanism.[39]

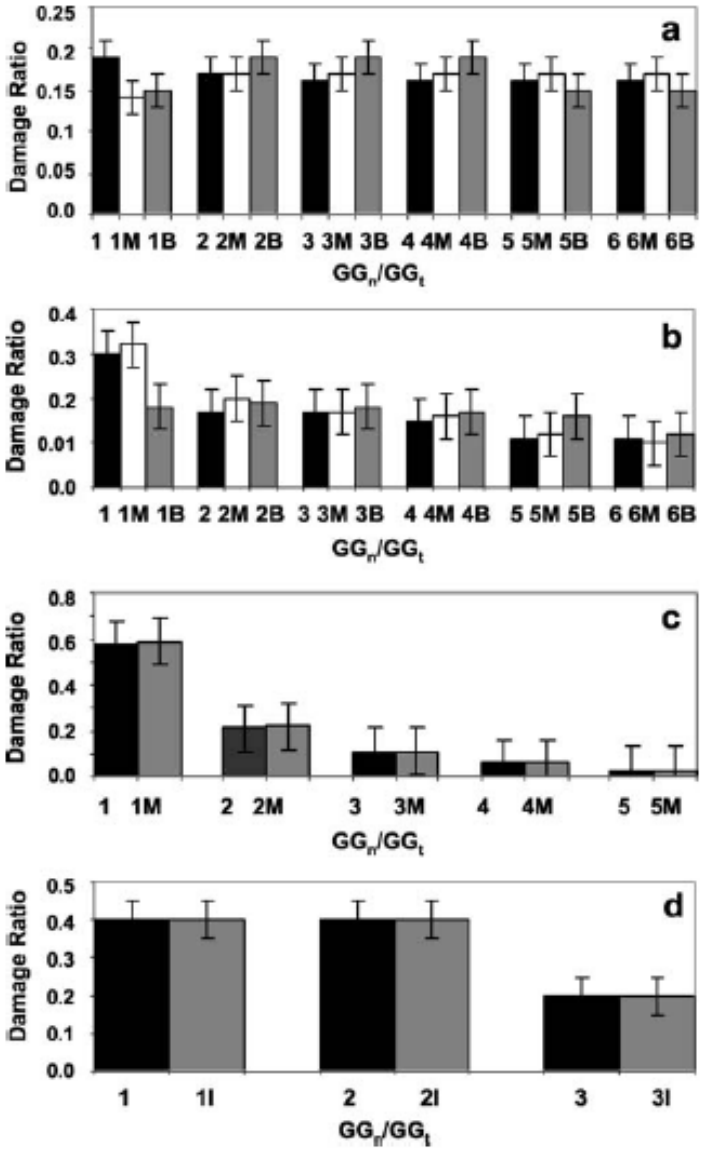

Figure 2.13 Histograms showing the relative amount of reaction at GG sites as ratios of the amount of strand cleavage (proportional to the number of counts at that 5'-G position in the autoradiograms, which is referred to in the caption as G_n) divided by the total number of counts at all 5'-G cleavage sites (G_t) in that oligomer. Panel (a): DNA (1-3), Panel (b): DNA (4-6), Panel (c): DNA (13,14) and Panel (d): DNA(16,17). In the legend, B stands for the position of the N4-*n*-butyl modified cytosine, M stands for the position of N4-methyl modified cytosine, and I stands for 4′-isopropyl modified thymidine.

Conclusions

Within the sensitivity of our experimental technique, we have demonstrated that alkyl modification of the major or minor groove of DNA duplexes results in no change in the trapping or hopping rate of charge transfer in DNA. However, we do not rule out the possibility that there may be observable differences as a result of these modifications when these sequences are probed with more sensitive techniques.

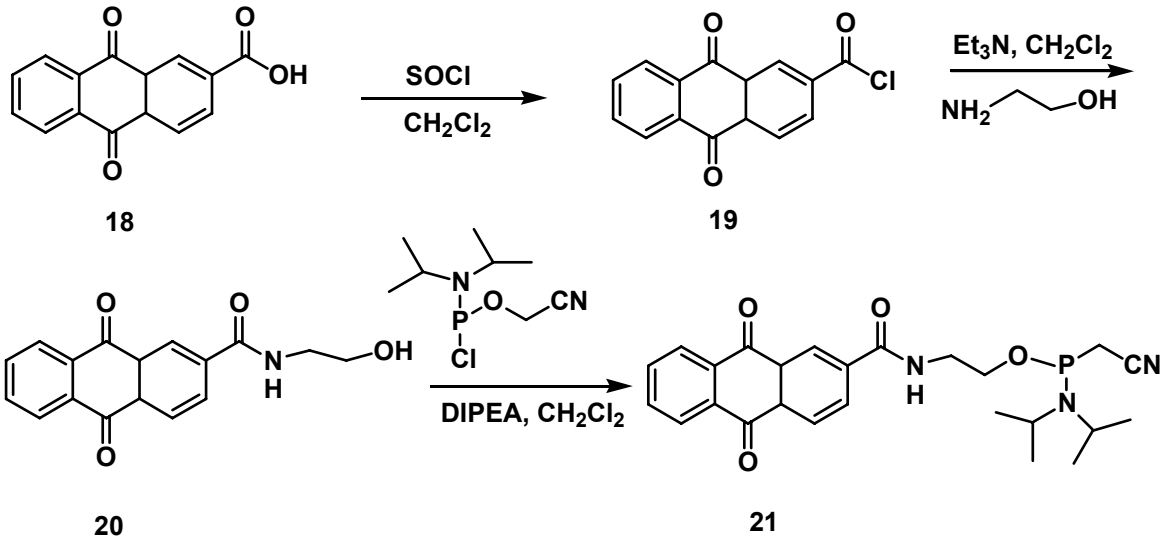

Scheme 2.3 Synthesis of Anthraquinone phosphoramidite

SYNTHESIS

Synthesis of 4′-isopropylthymidine [30-34]

5'-DMT-thymidine: Thymidine (1.0 g, 4.0 mmol) and 4,4′-dimethoxytrityl chloride (DMTCl) (2.0 g, 6.0 mmol) were added in a flask and purged with N_2 for 15 min, after which anhydrous pyridine (15.0 mL) was added under nitrogen . To the above mixture was added catalytic amount of N,N-Dimethyl amino pyridine (DMAP) and the reaction mixture was stirred at room temperature overnight. Afterwards, reaction mixture was poured into ice cold H_2O (100 mL) and extracted with CH_2Cl_2 (3 x 100 mL). The combined organic extracts were dried ($MgSO_4$) and concentrated under vacue. Column chromatography with Hexane and EtOAc 1:4 afforded 1.9 g, 3.5 mmol white solid product **2**, 87% yield. Spectral data is in agreement with literature report.

3'-O-tertbutyl dimethyl silyl-5'-O-DMT-thymidine: To a solution of 5'-DMT-thymidine **1** (6.9 g, 12.6 mmol) and imidazole (2.6 g, 37.8 mmol) in anhydrous DMF was added tertbutyl dimethyl silylchloride (2.1 g, 13.9 mmol). Reaction mixture was stirred for 48 hours at room temperature under argon and quenched with H_20. Organic residue was extracted with CH_2Cl_2 (3x100 mL), washed with brine and dried ($MgSO_4$). Column chromatography with Hexane EtOAc 1:1 gave 8.0 g, 12.1 mmol white foam **2**, 96% yield. Spectral data is in agreement with literature report.

3'-O-tertbutyl dimethyl silyl thyimidine : 3′-tertbutyl dimethyl silyl-5'-DMT-thymidine (8.0 g, 12.1 mmol) was dissolved in 80% acetic acid in H_20 (46.0 mL) and THF (11.5 mL) and the reaction mixture was stirred at room temperature for 24 hours. The reaction mixture was cooled to 0^oC and neutralized with NH_4OH 33% (30.0 mL).

The organic layer was extracted with CH_2Cl_2 (4x100 mL) and the combined extracts was washed with $NaHCO_3$, dried ($MgSO_4$) and evaporated by vacue. Column chromatography with EtOAc/Hexane 1:1 afforded 3.3 g, 9.30 mmol white foam, 77% yield. Spectral data is in agreement with literature report.

4'-5'-dihydroxy-3'-O-tertbutyl dimethyl silyl thymidine ***(5)***: 3'-tBDMSthymidine (3.0 g, 8.60 mmol) was dissolved in anhydrous DMSO (15.0 mL) and DCC (1.7 g, 8.0 mmol), pyridine (7.1 g, 34.3 mmol) and TFA-Py (357 mg/373 mg, 4.7 mmol) were added to the reaction mixture under argon atmosphere at room temperature. The reaction mixture was stirred for 5 hours at room temperature and cooled to 0^oC. To the cooled reaction mixture was added oxalic acid (405 mg, 4.50 mmol in 4 mL of methanol). After 5 minutes, the reaction mixture was filtered and diluted with CH_2Cl_2 (40.0 mL). The organic layer was washed with H_2O (80.0 mL) and the H_2O was back extracted with CH_2Cl_2 (2 x 50.0 mL). Organic extracts were combined, dried ($MgSO_4$) and the solvent was evaporated. The crude reaction mixture was redissolved in dioxane (20.0 mL) and formaldehyde (10.0 mL of 37 % solution in H_2O), NaOH (10.0 mL of 2M) were added. After stirring at room temperature for 2 hours, tartaric acid (4.0 g) was added. After stirring for another 10 minutes, the solvent was removed by vacuum and H_2O (80.0 mL) was added. The organic phase was extracted with CH_2Cl_2 (3 X 60.0 mL) and the combined extracts was dried $MgSO_4$ and evaporated. The concentrate was dissolved in EtOH (30.0 mL) and $NaBH_4$ (357 mg, 9.4mmol) was added. After stirring for 15 minutes at room temperature, tartaric acid (4.0 g in 3 mL of acetic acid) was added and stirring was continued for additional 5 minutes, after which the solvent was evaporated. To the concentrate was added H_2O (100.0 mL) and the organic layer was extracted with CH_2Cl_2

(4 x 60.0 mL), dried ($MgSO_4$) and evaporated. Column chromatography on silica gel with EtOAc gave the desired white powder **5** in 60 %. Spectral data is in agreement with literature report.

4'-methyl-O-dimethoxytrityl-5'-hydroxy-3'-O-tBDMS-thymidine: 4'-5'-dihydroxy-3'-tertbutyl dimethyl silyl thyimidine **4** (2.0 g, 5.2 mmol) was dissolved in anhydrous pyridine (20.0 mL). To this solution was added DMTCl (1.8 g, 5.2 mmol) and catalytic amount of N,N-dimethyl amino pyridine under argon at room temperature. The reaction mixture was stirred at room temperature for 24 hours and poured into ice cold H_2O (200 mL). The organic layer was extracted with CH_2Cl_2 (3 x 100 mL), dried ($MgSO_4$) and concentrated. Column chromatography on silica gel with hexane and ethyl acetate (2:1) afforded white solid foam (2.6 g, 73 %). Spectral data is in agreement with literature report.

4'-methyl-O-dimethoxy trityl- 5'-tertbutyl diphenyl silyl-3'-O-tBDMS-thymidine: To a solution of 4'-methyl-O-dimethoxy trityl- 5'-hydroxy-3'-O-tBDMS-thymidine (2.0 g, 2.90 mmol) and imidazole (592 mg, 8.7 mmol) in DMF (7 mL) was added *tert*-Butyl diphenyl silyl chloride (877 mg, 3.2 mmol) at room temperature. After stirring for 24 hours, reaction mixture was poured into H_2O (60.0 mL) and extracted with CH_2Cl_2 (3 X 60 mL) and dried ($MgSO_4$). The residue was concentrated by vacue and column chromatography on silica gel with Hexane and EtOAc (2:1) gave 2.1g white foam, 48 % yield. Spectral data is in agreement with literature report.

4'-hydroxymethyl-5'-tert-butyldiphenylsilyl-3'-O-tert-butyldimethylsilyl-thymidine **(6)**: 4'-methyl-O-dimethoxy trityl- 5'-tert-butyldiphenyl silyl-3'-O-tBDMS-

thymidine (1.0 g, 1.11 mmol) was dissolved in 80% acetic acid in H_20 (16.0 mL) and THF (4.0 mL) and the reaction mixture was stirred at room temperature for 24 hours. Reaction mixture was cooled to 0^oC and neutralized with NH_4OH 33% (12.0 mL). Organic layer was extracted with CH_2Cl_2 (4 X 100 mL) and the combined extracts was washed with $NaHCO_3$, dried ($MgSO_4$) and evaporated by vacue. Column chromatography with EtOAc/Hexane 1:1 afforded (550 mg, 0.87 mmol white foam **7**, 80% yield. Spectral data is in agreement with literature report.

3'-O-[(tert-Butyl)dimethylsilyl]-5'O-[(tert-butyl)diphenylsilyl]-4'-C-formylthymidine **(7)**: To solution of trichloroacetic anhydride (384 mg, 1.2 mmol) in CH_2Cl_2 (6.0 mL) DMSO (13 μL 2.2 mmol) was added at -78°C. After stirring for 15 minutes at -78°, a solution of 4'-hydroxymethyl- 5'-tert-butyldiphenylsilyl-3'-O-tert-butyldimethylsilyl-thymidine (520 mg, 0.83 mmol in 2 mL CH_2Cl_2) was added. After stirring for another 30 minutes at -78 °C, Et_3N (567 μL, 4.10 mmol) was added and the mixture warmed up gradually to room temperature within 30 minutes. Reaction mixture was poured unto H_2O (60.0 mL) and the organic layer was extracted with CH_2Cl_2. The combined extracts was dried ($MgSO_4$) and concentrated. Column chromatography with hexane and EtOAc (2:1) gave 370 mg white foam, 71% yield. Spectral data is in agreement with literature report.

3'-O-[(tert-Butyl)dimethylsilyl]-5'O-[(tert-butyl)diphenylsilyl]-4'-C-(1-hydroxymethyl)thymidine: To a solution of the starting material from above, **7**(370 mg, 0.59 mmol) in THF (8 mL) was added CH_3MgCl (3M in THF, 0.7 mL) at 0°C. After stirring for 2.5 hours, saturated aqueous NH_4Cl (2.0 mL) was added and organic phase

was extracted with CH_2Cl_2, and washed with water, dried ($MgSO_4$) and evaporated as a diasterioisomer. Product was used in the next step without further purification.

4′-C-Acetyl-3′-O-[(tert-Butyl)dimethylsilyl]-5'O-[(tert-butyl)diphenylsilyl]thymidines, **(8)** : To a solution of 1,1,1-triacetoxy-1,1-dihydro-1,2-benziodoxol-3(1H)-one (1.2 g, 2.7 mmol) in CH_2Cl_2 (10 mL) was added 3'-O-[(tert-Butyl)dimethylsilyl]-5'O-[(tert-butyl)diphenylsilyl]-4'-C-(1-hydroxymethyl)thymidines (850 mg, 2.7 mmol) in CH_2Cl_2 (8 mL) at room temperature. After stirring for 1 hour, the reaction mixture was poured into saturated aqueous sodium hydrogen carbonate/saturated aqueous NaS_2O_3 1:1 (100 mL, v/v). The organic layer was extracted with ether (3 X 100 mL), dried (MgSO4) and evaporated. Flash chromatography (Hexane ethyl acetate 3:1) gave 530 mg of product as a colorless form. 64 % yield. Spectral data is in agreement with literature report.

4′-C-(Isopropenyl)-3′-O-[(tert-Butyl)dimethylsilyl]-5'O-[(tert-butyl)diphenylsilyl]thymidine **(9):** CH_3PPh_3Br (850 mg, 2.40 mmol) and potassium *tert*-butoxide (234 mg, 2.1 mmol) were dissolved in dry THF (7.0 mL) under argon and stirred for one hour at room temperature. To this mixture was added 4′-C-Acetyl-3′-O-[(tert-Butyl)dimethylsilyl]-5'O-[(tert-butyl)diphenylsilyl]thymidines from above (380 mg, 0.59 mmol in 5 mL of THF). After stirring overnight at room temperature, the reaction mixture was quenched with concentrated aqueous NH_4Cl solution, extracted with dichloromethane, dried ($MgSO_4$) and concentrated. Concentrate was column chromatographed on silica gel (ethyl acetate/ hexane 1:3 to afford colorless foam 300 mg, 80% yield. Spectral data is in agreement with literature report.

4′-C-(Isopropyl)thymidine **(1)**: Compound **9** (600 mg, 0.94 mmol) was dissolved in THF (10 mL), and TBAF solution in THF (2.26 mL, 2.26 mmol) was added at room temperature. After stirring for four hours, the reaction mixture was poured on a silica gel column without further work up. Column chromatography on silica gel (ethyl acetate and then ethyl acetate/ methanol (10:1)) afforded the crude product, which was used directly in the next step. The residue was dissolved in methanol (15 mL) and 10% Pd/C (approximately 150 mg) was added under argon. The reaction mixture was then floated with hydrogen (balloon). After stirring for 5 hours, the reaction mixture was poured on silica gel column without further work up. Elution with ethyl acetate/hexane 10:1 and then ethyl acetate/methanol 10:1 gave the desired compound as a colorless form, 250 mg, 94% yield. The spectral data is in agreement with literature report.

5′-O-Dimethyoxytrityl-4′-C-(isopropyl)thymidine . Compound **1** (250 mg, 0.88 mmol) was co-evaporated twice with pyridine and dissolved in pyridine (5 mL). To the coevaporated compound was added DMTCl (595 mg, 1.76 mmol, 2 equivalents) and catalytic amount of DMAP at room temperature. After stirring for 12 hours, the reaction mixture was quenched with methanol and stirring continued for another 30 minutes. Mixture was then poured into saturated sodium hydrogen carbonate solution and extracted with dichloromethane. Extracts were combined, dried ($MgSO_4$) and evaporated. Column chromatography on silica gel (ethyl acetate/ hexane (2:1)→ ethyl acetate/Hexane (3:1) containing 1% triethyl amine afforded the product as a colorless foam 350 mg, 68% yield. Spectral data is in agreement with literature report.

5′-O-Dimethyoxytrityl-3′-phosphoramido-4′-C-(isopropyl)thymidine **(11)**: 5′-O-Dimethyoxytrityl-4′-C-(isopropyl)thymidine (140 mg, 0.20 mmol) was coevaporated

twice with toluene and dissolved I dichloromethane (6 mL). To this solution was added N-ethyldiisopropylamine (208 μL, 1.20 mmol, 5 equivalents) and 2-Cyanothyl-N,N-(diisopropylamino)chlorophosphite (113 mg, 0.48 mmol, 2 equivalents) at room temperature. Reaction mixture was stirred for 5 hours and quenched with saturated sodium hydrogen carbonate solution and extracted with dichloromethane, dried ($MgSO_4$) and concentrated. Column chromatography on silica gel (ethyl acetate/hexane 2:1→ethyl acetate/hexane 3:1 containing 1% triethylamine gave the desired product as colorless foam (130 mg, 69% yield). Spectral data is in agreement with literature report. This product was incorporated into a DNA sequence using automated DNA synthesizer.

Synthesis of N4-alkyl-deoxycytidine

3',5'-di-O-acetyl-2'-deoxyuridine (**12)**: deoxyuridine (3.0 g, 13.00 mmol) was dissolved in anhydrous pyridine (20 mL) and DMAP (10% mol equivalent) was added. To the solution mixture was added acetic anhydride (5.4 mL, 53.00 mmol). Reaction mixture was stirred overnight and quenched with water. Residual product was extracted with dichloromethane three times. Flash chromatography on silica gel with hexane/ethyl acetate (1:1) gave a white foam (3.5g 86% yield). Spectral data is in agreement with literature report.

3',5'-di-O-acetyl-4-thio-2'-deoxyuridine **(13):** Compound **12** (2.6g, 6.40 mmol) was taken in a round bottom flask and dissolved in pyridine (50 mL) and this solution was treated with phosphorus pentasulfide (8.5g, 19.20 mmol). After stirring for 5 minutes, 0.1% H_2O was added and the reaction mixture was stirred at refluxing condition for 4 hours. Reaction was allowed to stand at room temperature overnight after which the pyridine was decanted and evaporated. The solid residue was dissolved in a large volume

of water and after stirring vigorously for 45 minutes at room temperature, reaction mixture was filtered. The solid was redissolved in dichloromethane and filtered. Combined filtrates (aqueous and organic) was mixed and separated. Aqueous layer was further washed with dichloromethane (2X). Organic extracts were combined and washed with H_20, dried ($MgSO_4$) and concentrated by vacue. Column chromatography on silica gel with ethyl acetate/hexane afforded yellow crystals (1.5g, 71% yield). Spectral data is in agreement with literature report.

4N-methyl-2'-deoxycytidine **(3)**: Compound **13** (600 mg, 1.80 mmol) was taken in 250 mL flask and 33% methylamine in ethanol (6 mL) was added under argon. Reaction mixture was stirred for 24 hours afterwards excess solvent was evaporated and residual product was recrystalized from ethanol to afford a white solid (300 mg, 69% yield).

5'-O-dimethoxytrityl-4N-methyl-2'-deoxycytidine **(14)**: Compound **13** (280 mg, 1.2 mmol) was evaporated 3 times with pyridine and dissolved in pyridine (15.0 mL). To this solution was added DMTCl (589 mg, 1.70 mmol) under argon. Reaction mixture was stirred at room temperature overnight and quenched with methanol. Aqueous $NaHCO_3$ and dichloromethane were added to the mixture and the organic layer was further extracted with dichloromethane (3 x 50.0 mL). Organic layers were combined, dried ($MgSO_4$) and evaporated. Column chromatography on silica gel with ethyl acetate →ethyl acetate/MeOH (10:1) and 1% triethylamine gave 410g product as a white solid (65% yield). Spectral data is in agreement with literature report.

3'-2-cyanoethyldiisopropylphosphoramidite-5'-dimethoxytrityl-(N4-methyl)-2'-deoxycytidine **(16)**: Compound **14** (400 mg, 0.74 mmol) was coevaporated twice in toluene and dissolved in anhydrous dichloromethane (8.0 mL). To this solution was

added N,N-diisopropylethylamine (475 mg, 3.70 mmol, 5 equivalent) and 2-cyanoethyl-N,N-(diisopropylamino) chlorophosphite (0.35 mL, 1.50 mmol, 2 equivalents) at room temperature. Mixture was stirred for 3 hours and quenched with saturated $NaHCO_3$. Product was extracted with dichloromethane, dried ($MgSO_4$) and concentrated. Column chromatography on silica gel(ethyl acetate →ethyl acetate/ methanol (20:1) with 1% triethylamine afforded the final compound as a white foam(400 mg, 73% yield) ready to be incorporated into DNA sequence. Spectral data is in agreement with literature report.

4N-butyl-2'-deoxycytidine **(4)** compound **13** (900 mg, 2.70 mmol) was dissolved in ethanol (5.75mL) and butyl amine (3.15 mL) was added to bring the mixture to 35% butyl amine in ethanol. Reaction mixture was stirred at room temperature for 48 hours and excess solvent was removed by vacue. Flash chromatography on silica gel (10% methanol in ethyl acetate) gave the desired product as colorless foam (450 mg, 59% yield. Spectral data is in agreement with literature report.

5'-O-dimethoxytrityl-4N-butyl-2'-deoxycytidine **(15)**: Follows the same procedure as in compound **14**. Spectral data is in agreement with literature report.

3'-2-cyanoethyldiisopropylphosphoramidite-5'-dimethoxytrityl-(N4-butyl)-2'-deoxycytidine **(17)**: Follows the same procedure as in compound **16**. Spectral data of final compound is in agreement with literature report.

Synthesis of Anthraquinone phosphoramidite (Scheme 2.3)

2-Carbonylanthraquinone chloride **(19)** 5.5 mL thionyl chloride was added to anthraquinone-2-carboxylic acid (2.0 g, 18.60 mmol) in a round bottom flask fitted with water condenser leading to 1 M NaOH solution. The reaction mixture was heated at

reflux for 5 hours while a yellow solid was formed. The solid was collected with a glass frit and was rinsed several times with cyclohexane (5.0 mL) to wash off excessive thionyl chloride. 2-charbonylanthraqunione chloride was obtained as pale yellow needles after air-drying overnight (2.0 g, 95% yield): Spectral data is in agreement with literature report.

N-(2-hydroxyethyl)-2-anthraquinonecarboxamide **(20)** A solution of 687 mg (2.5 mmol) of anthraquinone-2-carbonyl chloride in 20.0 mL of dry methylene chloride was added dropwise to a solution of 610 μL (10.00 mmol) of 2-aminoethanol and 370 μl (2.7 mmol) of triethylamine in 90 ml of methylene chloride. The reaction mixture became

cloudy upon complete addition of the anthraquinone-2-carbonyl chloride solution. The reaction mixture was stirred overnight at room temperature. Afterwards the solution was filtered and a pale yellow solid was isolated. Recrystallization from hot isopropyl alcohol gave N-(2-hydroxyethyl)-2-anthraquinonecarboxyamide as a dull yellow powder (545 mg, 73% yield). Spectral data is in agreement with literature report.

N-(2-(O-methoxydiisopropylphosphityl)ethyl)-2- antraquinonecarbox-amide **(21)**. N-(2-hydroxyethyl)-2-anthraqhinonecarboamide (259 mg, 0.89 mmol) was dissolved in anhydrous CH_2Cl_2 (2.0 mL), followed by addition of DIEA (670 μL). The mixture was stirred under nitrogen until complete dissolution. To this flask, 2-cyano diisopropylethylphosphoramidite (170 μL, 0.88 mmol) was added dropwise; yielding a clear orange-red solution upon complete addition, and the reaction was stirred at room temperature for additional 30 min. The reaction mixture was poured into 5 ml of ethyl acetate containing 0.5 ml of triethylamine. The organic layer was washed twice with 5 ml of 5% aqueous sodium bicarbonate, twice with 5 ml of brine and dried over anhydrous

sodium sulfate. Solvent was removed by vacua and then applied directly to silica gel column. Elution with CH_2Cl_2/EtOAc/Et_3N (45:45:10) afforded the desired fraction. The solvent was removed under reduced pressure to give dark red oil which was used directly in the DNA synthesis.

REFERENCES

(1)Saenger, W. *Principles of Nucleic Acid Structure*. Cantor C. Ed. Springer-Verlag. New York. 1984

(2)Berendson, H. J. C.; Postma, J. P. M.; van Gunsteren, W. F.; DiNola, A.; Haak, J. R. *J. Chem. Phys*. **1984**, *81*, 3684

(3) Vlieghe, D.; Turkenburg, J. P.; van Meervelt, L. *Acta. Cryst*. **1999**, *D55*,1495

(4)Solar-Lopez, M., Malinina, L., Liu, J., Huynh-Dinh, T. and Subirana, J. A. *J. Biol. Chem.* **1999**.. *274*(34), 23683

(5)Falk, M.; Poole, A. G.; Goymour, C. G. *Can. J. Chem*. **1970**, *48*, 1536

(6)Tippin, D. B.' Sunderalingam, M. *Biochemistry*. **1997**, *36*, 536

(7) Kasai, H., Yamaizumi, Z., Berger, M. and Cadet, J. *J. Am. Chem. Soc.* 1992, **114**, 9692

(8) Frelon, S., Douki, T., Ravanat, J. L., Pouget, J. P., Tornabene, C. and Cadet, J. *Chem*. *Res*. *Toxicol* 2000, **13**(10), 1002

(9) Krokan, H. E.; Standal, R.; Slupphaug, G. *Biochem. J*. **1997**, *326*, 1

(10) Di Ventra, M. and Zwolak, M. In *Nalwa*, H. S. (ed.), *Encyclopedia of Nanoscience and Nanotechnology*. American Scientific Publishers, Stevenson Ranch, California. 2003

(11) Steeken, S.; Jovanovic, S. V. *J. Am. Chem. Soc*. **1997**, *119*, 617

(12) Bonvin, A. M. J. J.; Sunnerhagen, M.; Otting, G.; Gunsteren, W. F. *J. Mol. Biol*. **1998**, *282*, 859

(13) Feig, M.; Pettitt, B. M. *J. Mol. Biol*. **1999**, *286*, 1075

(14) Feig, M.; Pettitt, B. M. *Biopolymers*. **1998**, *48*, 199

(15) Schuster, G. B.; Landman, U. *Top. Curr. Chem*. **2004**, *236*, 139

(16) Henderson, P. T.; Jones, D.; Hampikian, G.; Kan, Y. Z.; Schuster, G. B. *Proc. Natl. Acad. Sci*. *USA* **1999**, *96*, 8353

(17) Ly, D.; Kan, Y.; Armitage, B.; Schuster, G. B. *J Am. Chem. Soc*. **1996**, *36*, 118, 8747

(18) Armitage, B.; Yu, C.; Devadoss, C.; Schuster, G. B. *J. Am. Chem. Soc*. **1994**, *116*, 9847

(19) Ma, J-H.; Lin, W.; Wang, W.; Han, Z.; Yao, S.; Li, N. J. *Photoch. Photobiol. B*. **2000**, *57*(1), 76

(20) Lewis, F. D.; Liu, J.; Weigel, W.; Rettig, W.; Kurnikov, I. V.; Beratan, D. N. *Proc. Nat. Acad. Sci*. *USA*. **2002**, *99*, 12536

(21) Fukuzumi, S.; Nishimine, M.; Ohkubo, K.; Tkachenko, N. V.; Lemmetyinen, H. *J. Phys. Chem. B.* **2003**, *107*(45), 12511

(22) Kobayashi, K.; Tagawa, S. *J. Am. Chem. Soc*. **2003**, *125*, 10213

(23) Candeias, L. P.; Steenken, S. *J. Am Chem. Soc*. **1989**, *111*, 1094

(24) Candeias, L. P.; Steenken, S. *J. Am Chem. Soc*. **1992**, *114*, 699

(25) (a) Stemp, E. D. A.; Arkin, M. R. ; Barton, J. K. *J. Am. Chem. Soc*. **1997**, *119*, 2921. (b) Wagenknecht, H. A.; Pajski, S. R.; Pascaly, M.; Stemp, E. D. A.; Barton, J. K. *J. Am. Chem. Soc*. **2001**, *123*, 4400

(26) Shafirovich, V.; Dourandin, A.; Huang, W.; Geacintov, N.E. *J. Biol. Chem.* **2001**, *276*, 24621

(27) Hildebrand, K.; Schulte-Frohlinde, D. *Free Radical Res. Commun*. **1990**, *11*, 195

(28) Schiemann, O.; Turro, N. J.; Barton, J. K. *J. Phys. Chem. B* **2000**, *104*, 7214

(29) Sriram, M.; Wang, A. H.-J. *in Bioorganic Chemistry: Nucleic Acids*, ed. Hecht, S. M. Oxford Univ. Press, New York, **1996**, pp. 105-143.

(30) Detmer, I.; Summerer, D.; Marx, A. *Chem. Comm*. **2002**, 2314-2315

(31) Kraszewski, A.; Delort, A. M. *Tetrahedron Lett*. **1986**, *27*(7), 861

(32) O-Yang, C.; Wu, H.Y.; Fraser-Smith, E.B.; Walker, K. A. M. *Tetrahedron Lett*. **1992**, 33, 37

(33) Jones, G. H.; Taniguchi, M.; Tegg, D.; Moffatt, J. G. *J. Org. Chem.* **1979**, 44 (8) 1309

(34) Detmer, I.; Summerer, D.; Marx, *A. Eur. J. Org. Chem*. **2003**, 1837-1846

(35) Wempen, I.; Duschinsky, R.; Kaplan, L.; Fox, J. *J. Am. Chem. Soc.* **1961**, 83, 4755

(36) Liu, C.-S., Hernandez, R. and Schuster, G. B. *J. Am. Chem. Soc*. **2004,** *126*(9), 2877-2884.

(37) Butkus, V.; Klimasauskas, S. L. P.; Maneliene, Z.; Minchenkova, L. E.; Schyolinka, A. K. *Nucleic Acids Res*. **1987**, *15*, 8467

(38) Müller, J. G.; Duarte, V.; Hickerson, R. P.; Burrows, C. J. *Nucleic Acids Res*. **1998**, *26*, 2247

(39) Schuster, G. B. *Acc. Chem. Res*. **2000**, *33*, 253

CHAPTER 3

DNA METHYLATION AND THE ROLE OF CHARGED NUCLEOSIDES DNA CHARGE TRANSFER

Background and Significance

The initial product of DNA oxidation by a wide variety of oxidizing agents is guanine radical cation. The radical cation can react further with O_2 or H_2O to form 8-oxoG and other oxidation products. It can also recombine with the anionic sensitizer by rapid back electron transfer to regenerate the starting material[1-4]. While the backbone of natural DNA strands are saturated with negatively charged phosphate groups, DNA bases are uncharged and interact through their π-electrons. DNA methylation which is a natural process in biological systems can also lead to mutation. Alkylation of the electron rich sites of nucleobases, especially guanine's N7 and adenine's N1 and N3 can lead to charged nucleobases resulting in DNA mutation[5]. We synthesized N-methyl pyridinium nucleoside to investigate the effect of charged nucleobases on DNA charged transfer.

Our choice of a charged nucleoside for the study of the role of charged nucleobases on DNA charge transfer was based on the stability of the nucleosides in their charged states. The N1, N3, or N7 positions of the nucleobases are susceptible to alkylation leading to cleavage of the glycosidic bonds of these nucleosides (Figure 3.1),

therefore we opted for an unnatural nucleoside with a carbon-carbon bond between the base and the ribose as a model compound, which when alkylated is stable enough to be incorporated into a DNA (Figure 3.2).

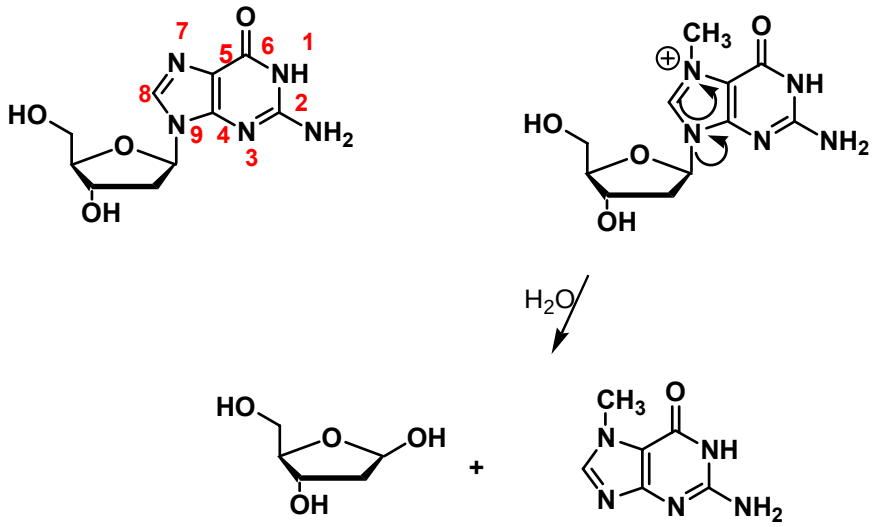

Figure 3.1

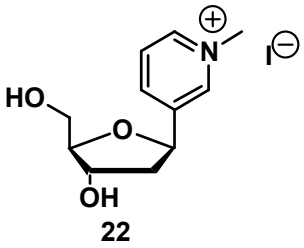

22

Figure 3.2 Target Compound

Chemistry

Our initial synthetic approach was the formation of a carbon-carbon bond between a glycal and a base using Heck coupling conditions.[6] This approach however was unsuccessful in our hands and we had to find a new route after several attempts

(scheme 3.1). Two other methods that have been used for the construction of C-nucleoside are nucleophilic displacement of a halogen group from C-1 of a ribose by a functionalized precursor or heteroaryl moiety, and reaction of a C-nucleophile at C-1 with spontaneous or chemically mediated ring closure to reform a furanose.[7-8] We chose the latter for our syntheses (scheme 3.2).

The starting material was a 2-Deoxy-D-ribose which was converted to the methyl-2-deoxyribose using methanolic HCl. Protection of the C-3 and C-5 hydroxyl groups with p-toloyl chloride in pyridine afforded **28** in good yield. **28** was treated with ethanethiol in the presence of zinc bromide in dichloromethane at room temperature to afford the straight chain thioacetal **29**. Deprotection of the tolyl protecting groups of the thioacetal with sodium methoxide in methanol afforded the trialcohol **30** which was subsequently protected with three equivalents of *p*-methoxy benzyl (PMB) protecting group to afford **31**. Oxidation of the thioacetal group to aldehyde using I_2 in H_20 and $NaHCO_3$ provided the aldehyde **32** ready to be coupled to the base. The key intermediate **32** has the appropriate functionality for the introduction of the 1-substituent and for the subsequent cyclization of the ribose moiety. Thus, reaction of **32** with 3-bromopyridine in *n*-BuLi at -78^{0}C in ether gave the intermediate **33**, which was cyclized with methanesulphonyl chloride in pyridine at room temperature to provide compound **34** and its isomer after separation by column chromatography. Deprotection of the PMB protecting groups afforded compound **35** in 5% overall yield starting from 2-deoxy-D-ribose. The 5′ alcohol of compound **35** was again protected with a trityl protecting group to enable the phosphoramidation of the 3′ alcohol followed by methylation of the imine nitrogen of the pyridine base with methyl iodide.

Attempts to phosphoramadite the 3′ alcohol of N-methylated version of **36** by standard procedures proved difficult. Since methylation of the imine nitrogen after phosphoramidition will result in uncontrolled reactions on the trivalent phosphorus, we sought to find other ways of forming a phosphate ester bond that will be less reactive to methyl iodide, and a more stable and pentavalent phosphorus was the chemistry of choice.[9-11] The reaction of **36** with dibenzyl phosphite in pyridine followed by hydrolyses with water and triethylamine afforded the H-phosphonate **37** (78% yield), which was then methylated with methyl iodide to yield the desired monomer **38** ready to be incorporated into DNA strands.

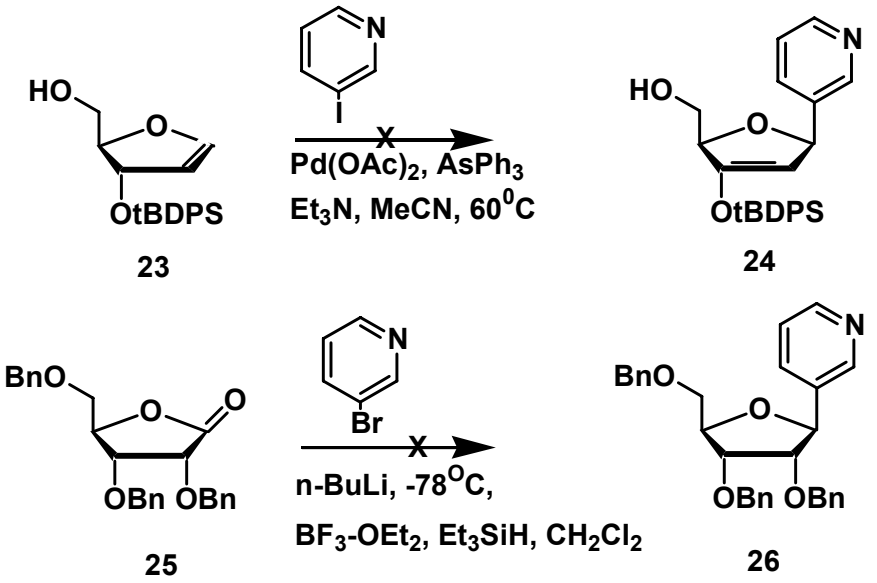

Scheme 3.1 Attempted synthetic routes to Pyridinium Nucleoside

MATERIALS AND METHODS

ATP radioactive isotope [α^{32}P] and terminal dinucleotide transferase (TDT) were purchased from Amersham Bioscience. DNA oligonucleotides containing anthraquinones were prepared by standard solid phase methods on an Applied Biosystems DNA

synthesizer using standard phosphoramidite chemistry, while the complementary strands were prepared using H-phosphonate chemistry, and purified by reverse phase HPLC using a C18 Varian Column.

Melting temperature (T_m) measurements of 2 μM duplexes were determined in 10 mM sodium phosphate buffer solution at pH 7.0 using a Cary 1E 3C spectrophotometer. Circular dichroism (CD) measurements were obtained using a JASCO (J-720) CD spectrophotometer. Images from gels were quantified using a Fuji 2340 BAS-image reader. All chemicals and reagents for the synthesis of the modified nucleosides were purchased from either Fisher Scientific or from Sigma Aldrich.

Preparation of radiolabeled DNA.

Oligomers were radiolabeled at the 3'-end using α-^{32}P ATP and TDT enzyme. The single DNA strands were mixed with α-^{32}P ATP and the TDT enzyme. The mixture was diluted to 20 μL and incubated for 45 min at 37^{o}C after which it was purified using a 20% denaturing polyacrylamide gel.

UV Irradiation and analyses

A 5 μM sample of the complementary strand was mixed with 10,000 c.p.m radiolabeled AQ-linked oligonucleotide in a 10 mM sodium phosphate buffer at pH 7.0 and hybridized by heating at 90^{0}C for 10 min, followed by slow cooling to room temperature. Samples were irradiated for 10, 15 or 20 min at ca 30^{o}C in microcentrifuge tubes in a Rayonet Photoreactor equipped with eight 350 nm lamps. Irradiated samples were then precipitated with cold absolute ethanol (100 μL) and glycogen (2 μL), after

which the samples were washed twice with 100 µL 80 % ethanol. The samples were dried and treated with 1 M piperidine (100 µL) for 30 min at 90 ^{0}C and afterwards the samples were dried and co-evaporated twice with H_2O (20 µL). Samples were then dissolved in a loading dye and loaded in a 20 % 19:1 acrylamide/bis-acrylamide gel. Drying of gels enabled the visualization of the cleavage sites by autoradiography

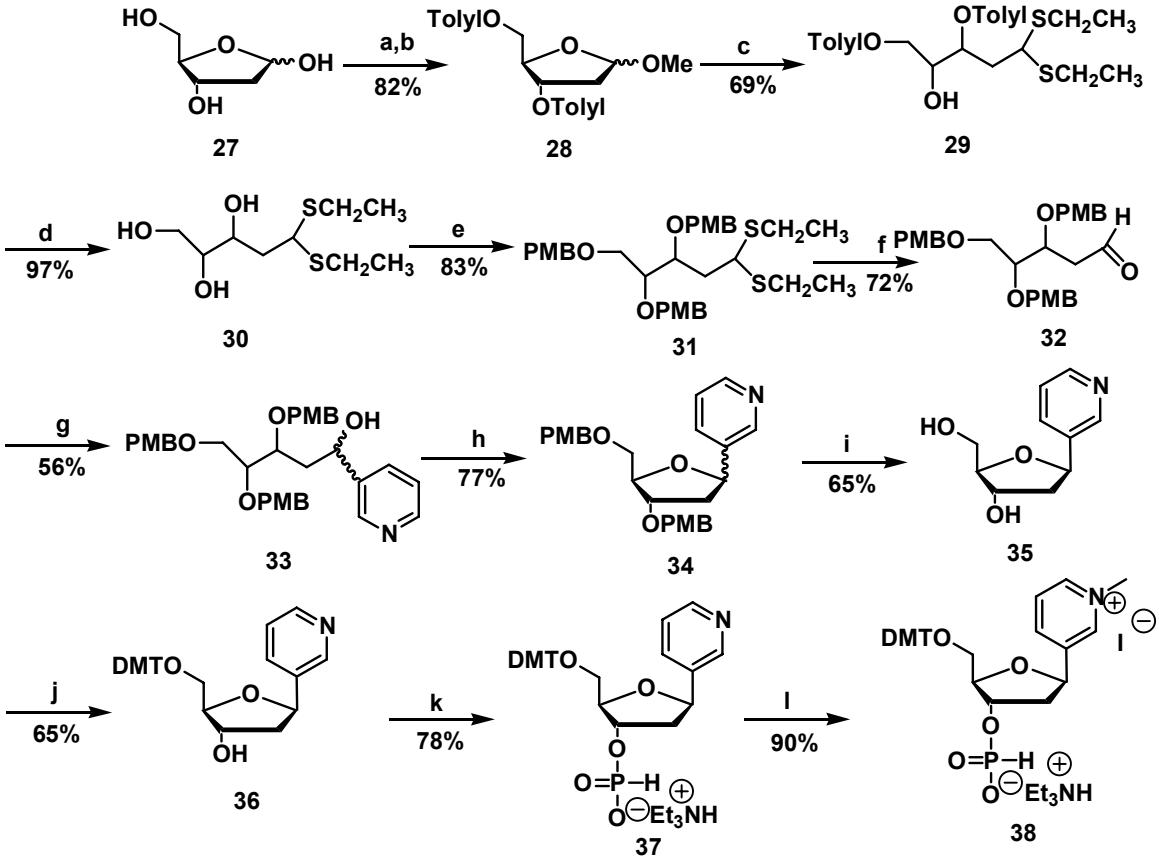

Reagents and condition: (a) MeOH/HCl, MeOH (b) Tolyl chloride, pyridine (c) excess EtSH, $ZnBr_2$, $NaHCO_3$, CH_2Cl_2 (d) K_2CO_3, MeOH (e) PMBCl, DIPEA, DMF (f) I_2, acetone, $NaHCO_3$, H_2O (g) n-butyl lithium, 3-bromopyridine, THF, -78^{o}C (h) methanesulfonylchloride, DIPEA, pyridine (i) Ph_3CBF_4, CH_2Cl_2, (j) DMTCl, pyridine, DMAP (k) Diphenyl phosphite, Pyridine, H_2O/Et_3N (l) MeI, CH_2Cl_2, 6h

Scheme 3.2 Synthesis of Pyridinium Nucleoside

RESULTS AND DISCUSSION

DNA sequences with known kinetic and thermodynamic behavior, where the magnitude of *k* hop and *k* trap are similar[12] were synthesized, with the modified nucleoside paired with adenine bases after the third GG steps (Figure 3.3).To determine the impact of the positively charged moiety introduced into the ring nitrogen of the modified oligomers on duplex stability and structure, we performed CD and T_m analyses of the duplexes. The CD spectra (Figure 3.4) show that the modified duplex with positively charged nucleobase maintains a predominant B-form structure. The T_m of the pyridinium modified 30 base pair duplex (DNA 2) is 3^0C lower than the unmodified DNA sequence (DNA1) (Figure 3.5). If the modified nucleoside is intrahelical, then the difference in melting temperature can only be attributed to lack of hydrogen bonding properties of the pyridinium base. Alternatively, if the modified nucleoside is extrahelical, then the difference in T_m can be attributed to both the absence of π electron stacking and lack of hydrogen bonding.

DNA
(1) 5′-AQ-ATA AGG AAG GAA GGA AGG AAG GAA GGT ATA-*3′ **3′-TAT TCC TTC CTT CCT TCC TTC CTT CCA TAT-5′** **(2) 5′-AQ-ATA AGG AAG GAA GGA AGG AAG GAA GGT ATA-*3′** **3′-TAT TCC TTC CTT CCt^+ TCC TTC CTT CCA TAT-5′**

Figure 3.3 DNA Sequences. t^+ = N-methyl pyridinium nucleoside

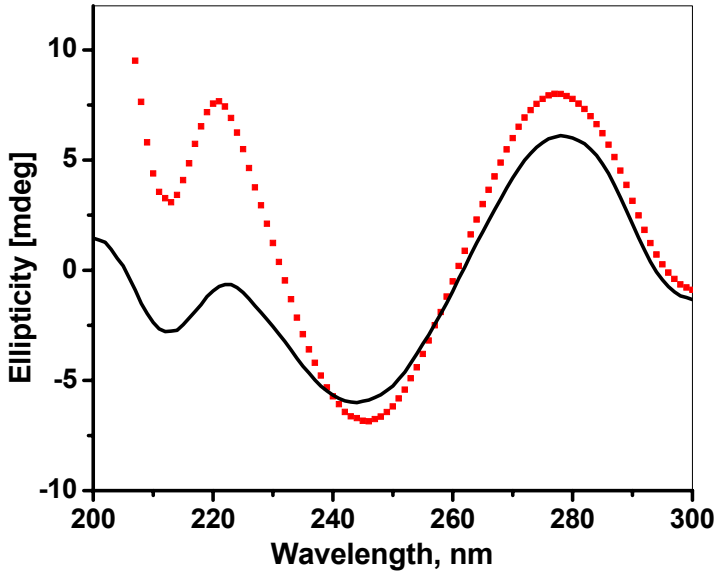

Figure 3.4 Circular dichroism spectra of pyridinium modified duplex in red dotted line and unmodified duplex in black solid line.

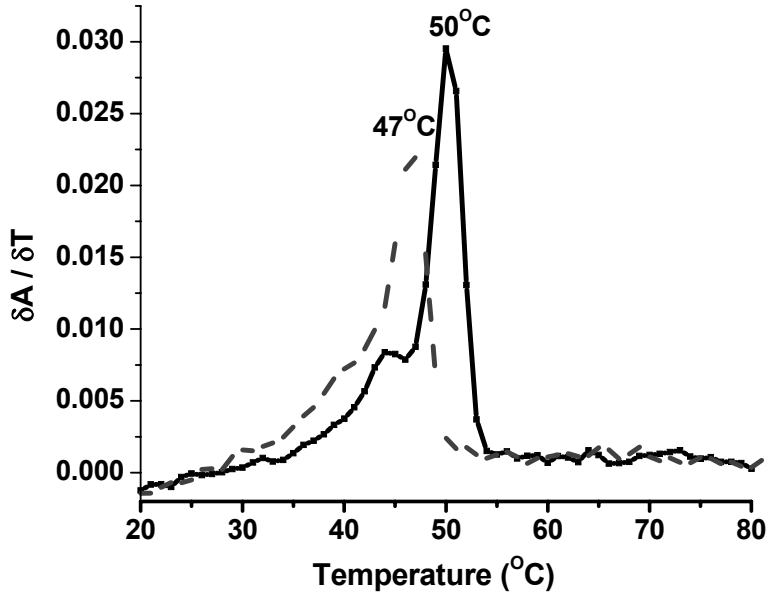

Figure 3.5 Thermal denaturation studies of DNA duplexes. The dotted line is the pyridinium modified duplex and the solid line is the unmodified DNA duplex

To probe the helical structure of the DNA duplex, we substituted the nucleoside opposite the modified base with an abasic site allowing the modified base a greater degree of freedom and better π-stacking in the absence of a complementary base (DNA 4).We also prepared a control strand with abasic site on the complementary strand. The abasic site is shown in Figure 3.6 (DNA 3 and 4) as a*. Thermal denaturation studies of DNA 3 and 4 (Figure 3.7) indicate just 1^0C difference in melting temperature.

DNA
(3) 5′-AQ-ATA AGG AAG GAA GGa* AGG AAG GAA GGT ATA-*3′ **3′-TAT TCC TTC CTT CCT TCC TTC CTT CCA TAT-5′** **(4) 5′-AQ-ATA AGG AAG GAA GGa* AGG AAG GAA GGT ATA-*3′** **3′-TAT TCC TTC CTT CCt^+ TCC TTC CTT CCA TAT-5′**

Figure 3.6 DNA sequences. t^+= N-methyl pyridinium nucleoside, a*= abasic site

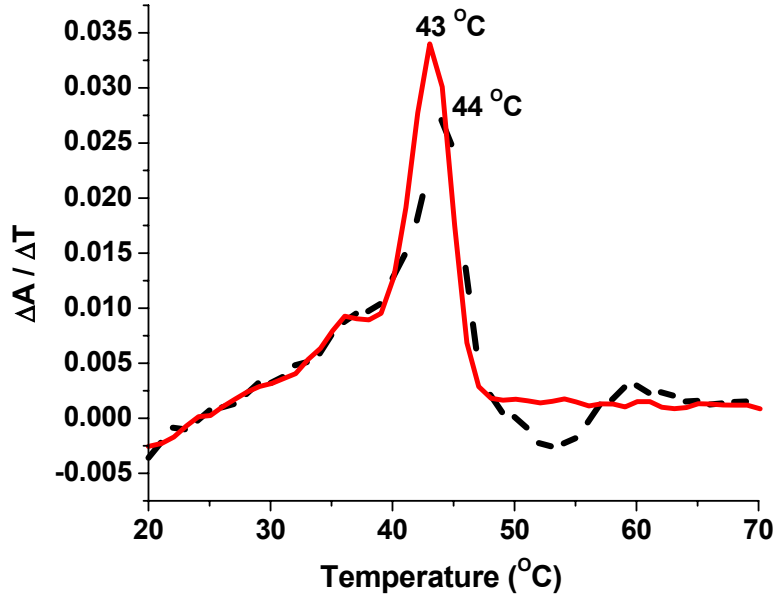

Figure 3.7 Thermal denaturation studies of DNA duplexes: Black dotted line is the modified sequence with abasic site and red solid line is the unmodified sequence with abasic site

A comparison between the T_m of the modified base, DNA 2 ($T_m = 47^0C$), DNA 3 with abasic site on the opposite strand ($T_m = 43^0C$) and DNA 4 with abasic site opposite pyridinium modified strand ($T_m = 44^0C$) indicate a 4^0C melting temperature difference between DNA 2 and DNA 3. If the pyridinium modified duplex is extrahelical, then it will be expected that the Tm of DNA 2 should be the same with the T_m of DNA 3 since they will both lack a base pair stacking along the helix. In contrast, the result from the T_m experiments show that the duplex with N-methyl modified base (DNA 2) is 4^0C higher in T_m compared to the duplex with abasic site on the complementary sequence. The difference in melting temperature is as a result of the π-cation interaction and π-π interaction between the charged nucleoside and the aromatic rings of the adjacent bases in the helix. This can be interpreted as evidence that the pyridinium modified duplex is intrahelical.

The Effect of Charged Nucleosides on Charge Migration

We analyzed the role of charged nucleoside on charge transfer in DNA by synthesizing duplex DNA's 1-4 with six GG steps in each DNA duplex separated by AA segments(Figure 3.3 and 3.6). The strands containing the GG steps are covalently linked to anthraquinone phosphoramidite (AQ) at 5′-end and are labeled at the 3′- terminus with ^{32}P. The irradiation of these AQ linked DNA strands at 350 nm introduces a base radical cation into the duplex, which can then migrate across the sequence until it encounters the charged base cation or it is irreversibly trapped by water. DNA duplex 1 is a control duplex with AQ attached to one strand. DNA duplex 2 has a pyridinium modified

nucleoside on the 15th position of the complementary strand opposite adenine base. DNA 3 contains an abasic site on one strand while DNA 4 contains an abasic site opposite a pyridinium modified nucleoside. Treatment of the irradiated strands with hot piperidine reveals damages on the GG steps of each of the DNA strands after gel electrophoresis and visualization by autoradiography (Figure 3.8 and 3.9).

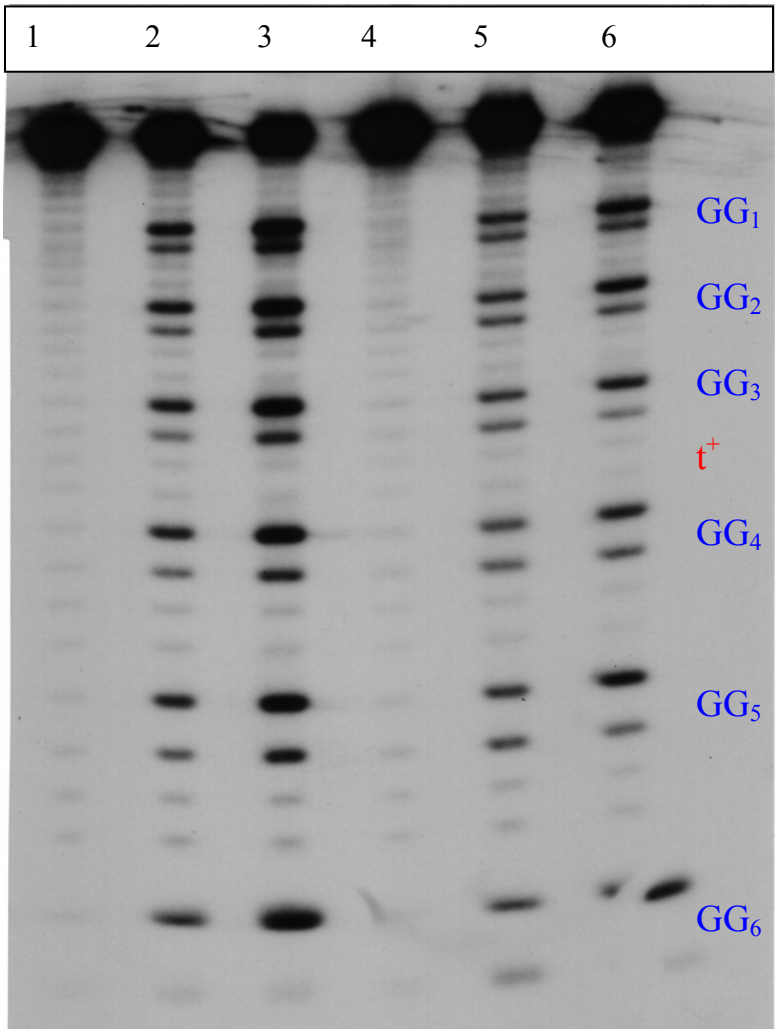

Figure 3.8 DNA's 1 and 2. Lanes 1-3 are the unmodified duplex. Lanes 4-6 are modified duplexes t^+ = N-methyl pyridinium nucleoside

Surprisingly, examination of the polyacrylamide gel electrophoresis (PAGE) results of DNA 2 and its control sequence DNA 1 (Figure 3.8) show very little effect of the charged nucleoside incorporated after the third GG step of DNA 2 from repelling the migrating radical cation. The steric effect of the N-methyl modified pyridinium in the duplex DNA should result in either the expansion of the H-boding core of the double stranded DNA to accommodate the extra carbon and three hydrogens extending from the ring nitrogen or an alignment with distortion of the π-π stacking arrangement of the aromatic rings that will force the modified ring away from the helix i.e. to result in extrahelical orientation of the modified base.

To begin to understand the orientation of the modified base in the helix, we synthesized DNA strands that incorporated an abasic site opposite the modified base (DNA 4) and a control DNA double strand with abasic site on one strand and a thymine base on the opposite strand (DNA 3). This adjustment should enable the modified base to stack fittingly into the core of the helix. PAGE analyses of the duplex with an abasic site opposite the pyridinium modified base (DNA 4) show that the charged nucleoside indeed has a local effect on the migrating radical cation (Figure 3.9, DNA 3 and 4). Figure 3.10 is a histogram of a quantitative analyses of DNA 3 and 4 showing a one third reduction in damage on the fourth GG step of DNA duplex 4 when compared to the control duplex (DNA 3). This reduction in damage is as a result of incorporation of the charged nucleoside after the third GG step of the complementary strand of DNA 4.

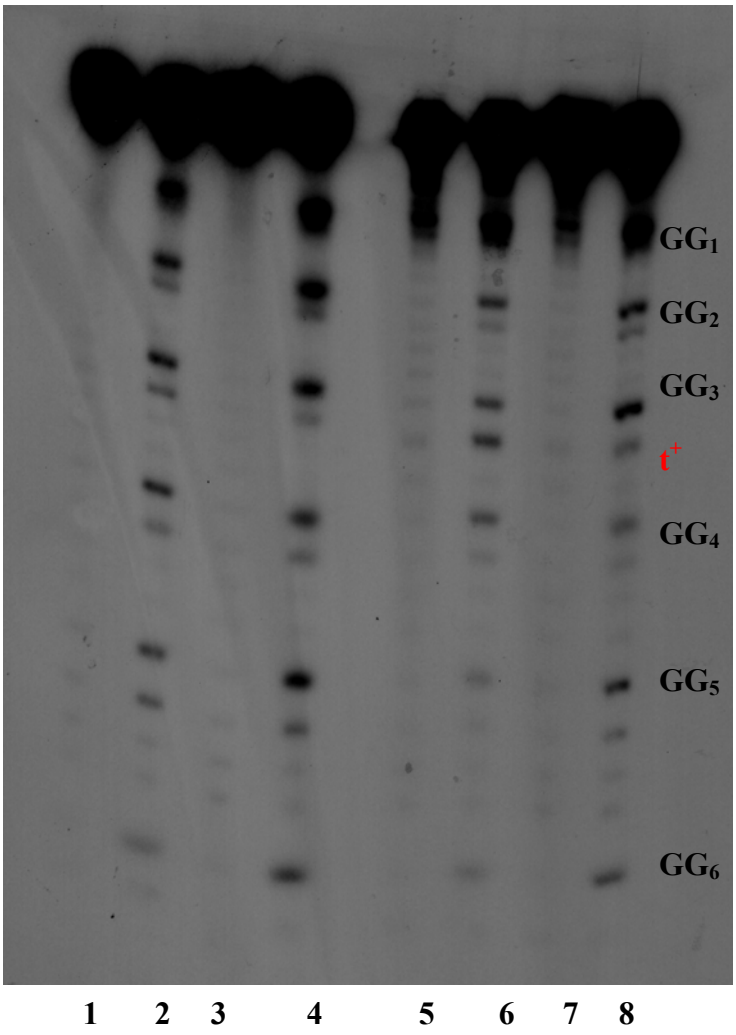

Figure 3.9 DNA's 1- 4. t^+ = N-methyl pyridinium nucleoside. Lanes 1 and 2 correspond to 0 and 10 minutes of irradiation (DNA 1). Lanes 3 and 4 are 0 and 10 minutes of irradiation (DNA 2). Lanes 5 and 6 are 0 and 10 minutes of irradiation (DNA 3), and lanes 7 and 8 are 0 and 10 minutes of irradiation (DNA 4)

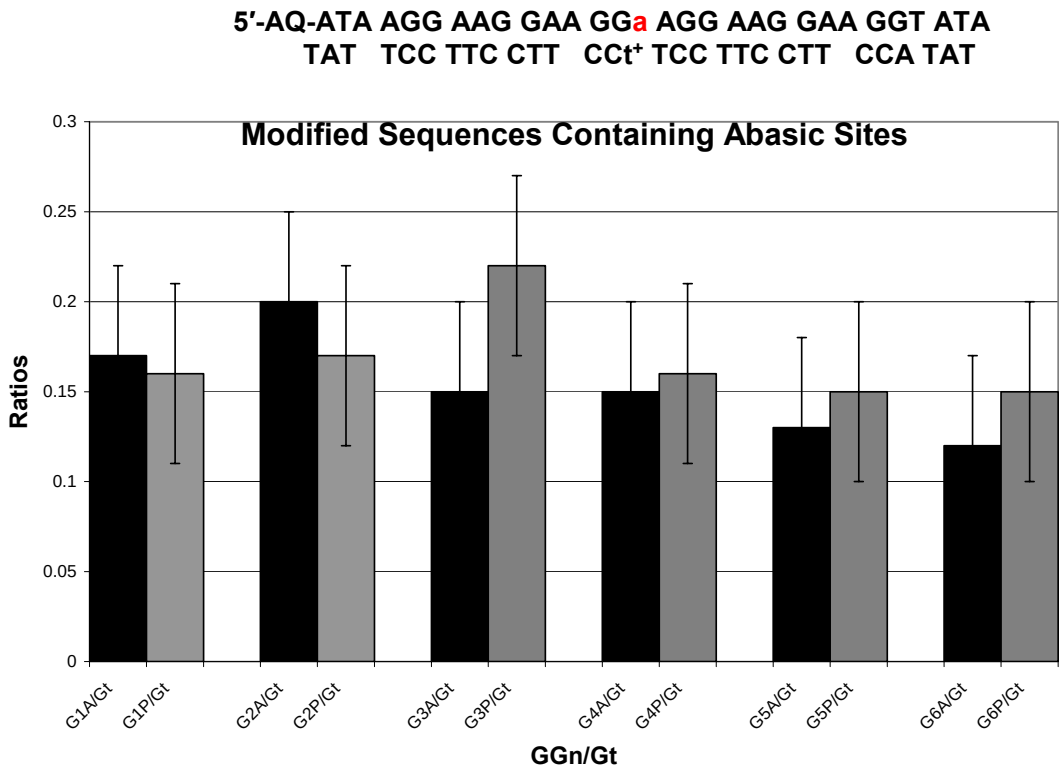

Figure 3.10 Histogram of DNA sequences 3 and 4. t^+ = pyridinium nucleoside. a = abasic site

With AA segments between GG steps, the sequences are designed as such that rate of hopping of the radical cation across the bases will be greater than the rate of trapping by water. Hence it is expected that there should be equal damage across the six GG steps, and at most minimal distance dependence from margin of error when the damage on the proximal GG step is compared to the damage on the distal GG step. The damage on the third GG step increases by some fraction when compared to damage on the second GG step. The damage then reduces by one third on the fourth GG step. The increase in the damage ratio on the third GG step can be attributed to a local distortion to the structure of the DNA due to the repelling of the migrating radical cation by the positively charged nucleoside. This distortion does not extend over many bases so that it is no longer a B-form DNA, but instead helps in stabilizing the DNA as a result of the

stabilizing energy gained from delocalization of the radical cation across the bases. The energy of the system is further reduced by the surrounding negative anions and solvent molecules that provide electron density to the cation and radical cation. The damage rations observed between the GG steps indicate that while there is a local effect of the pyridinium nucleoside on the approaching radical cation, neither k_{hop} nor k_{trap} is changed as a result of the modification.

Conclusions

The results discussed above indicate that using pyridinium base as a model, the introduction of a positive charge on ring nitrogen of a DNA can result in a local distortion of the structure of the DNA without affecting the B-form of the DNA. The rate of hopping of the radical cation across the GG steps is not affected, but reactivity around the charged nucleoside is reduced. Thermal experiments indicate that the positively charged nucleoside if accommodated along the π-π stacking core of the DNA impart extra stability to the duplex by lowering the energy of the duplex.

Synthesis of Pyridinium Nucleoside

D-erythro-pentafuranoside methyl-2-deoxy-3,5-bis(4-methylbezoate) **28**: To a solution of 2-deoxy-D-ribose (10.0 g, 74.5 mmol) in MeOH (120 mL) was added 1 % methanolic hydrogen chloride (20.0 mL), formed by reaction of acetyl chloride (1.7 mL) with MeOH 100 mL). The reaction mixture was stirred at room temperature for 25 minutes and neutralized by adding solid sodium carbonate (4.0 g). After filtration, the methanol was removed by coevaporation with pyridine (1 x 50.0 mL and 2 x 25.0 mL).

Afterwards, the residual syrup was dissolved pyridine (60.0 mL), cooled to 0 °C and *p*-Toloyl chloride (22.0 mL, 160.0 mmol) was added dropwise. Reaction mixture was stirred at room temperature overnight and diluted with cold water (150 mL) and the organic layer was extract CH_2Cl_2 (3 X 100 mL). Organic layers were combined and washed with saturated sodium carbonate twice and then with HCl (2.0 M) and with H_2O (150 mL). Organic extract was dried ($MgSO_4$) and evaporated. Column chromatography with 10% ethyl acetate in hexane gave 23.2 g of white solid product, 81% yield. Spectral data was in agreement with literature report.

1,2-Dideoxy-3,5-di-O-p-toluoyl-D-ribose diethyl dithioacetal **29**: D-erythro-pentafuranoside methyl-2-deoxy-3,5-bis(4-methylbezoate **28** (21.2 g, 55.2 mmol) was dissolved in anhydrous CH_2Cl_2 (40.0 mL) and ethanethiol (15.9 g, 256 mmol) was added. After 3 minutes, zinc bromide (12.4 g 55.2 mmol) was added gradually in several portions. After stirring for 45 minutes at room temperature, the reaction mixture was poured into aqueous NaOH (5% w/v, 250.0 mL) and the organic layer was extracted with CH_2Cl_2 (4 x 100 mL). Organic extracts were combined and washed with brine, dried ($MgSO_4$) and concentrated under reduced pressure. Residual oil was chromatographed on silica gel with hexane and ether (4:1) to afford 18.1g clear oil, 69% yield. Spectral data was in agreement with literature report.

1,2-Dideoxy-D-ribose diethyl dithioacetal **30***:* The thioacetal **29** (13. 9 g, 29.1 mmol) was dissolved in dry MeOH (35.0 mL) and solid sodium methoxide (3.97 g 73.5 mmol) was added. The reaction mixture was stirred at room temperature for one hour and neutralized with NH_4Cl. The ammonium chloride was then filtered and the filtrate was concentrated under reduced pressure. Column chromatography on silica gel with

dichloromethane and methanol 95:1 afforded a clear oil (6.1, g 25.4 mmol), 97% yield. Spectral data was in agreement with literature report.

2-Deoxy-3,4,5-tris-O-(4-methoxybenzyl)-D-ribose **31**: 1,2-Dideoxy-D-ribose diethyl dithioacetal **30** (5.0 g, 20.8 mmol) was dissolved in dry DMF (48 mL) and cooled to 0°C. To this mixture was added NaH (1.65 g, 68.8 mmol). After 10 minutes, *para*methoxybenzyl chloride (10.8 g, 68.8 mmol) was added gradually, Reaction mixture was stirred at room temperature for additional 3 hours and excess NaH was quenched with methanol. Reaction mixture was concentrated and partitioned between ethyl acetate and water. Aqueous layer was extracted twice with ethyl acetate and organic layers were combined and dried ($MgSO_4$) and concentrated. Column chromatography (ethyl acetate/ hexane 1:3) gave 10.4 g clear oil 83% yield. Spectral data was in agreement with literature report.

2-Deoxy-3,4,5-tris-O-(4-methoxybenzyl)-D-ribose aldehyde **32**: 2-Deoxy-3,4,5-tris-O-(4-methoxybenzyl)-D-ribose aldehyde **31** (10.0 g, 16.7 mmol) was dissolved in H_2O (100 mL) and acetone (25 mL). To this solution was added sodium hydrogen carbonate (3.o1g, 36.7 mmol). The reaction mixture was cooled in an ice bath and iodine (9.3g, 36.7 mmol) was added in portion-wise over a 10 minute period. Reaction mixture was allowed to warm up to room temperature and stirring for about 1.5 hours, a solution of saturated sodium thiosulfate (100.0 mL) was added and mixture was stirred for additional 5 minutes. After evaporation of acetone, the reaction mixture was poured into saturated sodium bicarbonate (150.0 mL) and the organic layer was extracted with dichloromethane (3 x 100 mL). The organic extracts were combined and dried ($MgSO_4$), and concentrated. Column chromatography on silica gel with ether/hexane 4:1

afforded 5.9 g of the title compound **32** as colorless oil, 72% yield. Spectral data was in agreement with literature report.

2-Deoxy-3,4,5-tris-O-(4-methoxybenzyl)-1-(3-pyridyl)-D-altro- and D-allo-ribitol **33:** Anhydrous diethyl ether (100.0 mL) was taken in 500 mL round bottomed flask and cooled to -78°C (CO_2/ acetone) under argon atmosphere. To the cooled ether was added butyl lithium [1.6M in hexane (14.9 mL, 23.9 mmol)]. After stirring for 10 minutes, 3-bromopyridine (3.8 g, 2.4 mL, 23.9 mmol) was added dropwise and the solution was stirred for another 10 minutes at -78°C. To the brown cold reaction mixture was slowly added tri-protected *para*-methoxybenzyl aldehyde **32** (5.9 g, 11.9 mmol) in dry ether (20.0 mL). The reaction mixture was allowed to warm up to room temperature within 3 hours. Afterwards the brown suspension was poured into aqueous sodium hydrogen carbonate (5% w/v, 150 mL) and the organic layer was extracted with dichloromethane (3 X 75.0 mL). The extract was dried ($MgSO_4$) and concentrated. Column chromatography with ether and ethanol 95:5 gave a clear yellow oil, 3.8 g, 56% yield. Spectral data was in agreement with literature report.

1,2-Dideoxy-3,5-bis-O-(4-methoxybenzyl)-1-(3-pyridyl)-α-andβ-D-ribofuranose **7**: Compound **34** (3.3 g, 5.8 mmol) was dissolved in anhydrous pyridine (70.0 mL) and ethyl diisopropylamine (1.9 g, 2.6 mL, 15.0 mmol) was added. The reaction mixture was stirred for 10 minutes followed by slow addition of methanesufonyl chloride (1.7g, 1.2 mL, 15.0 mmol). The reaction mixture was stirred at room for 2 hours and poured into aqueous sodium hydrogen carbonate (100 mL). The organic layer was extracted with dichloromethane (3 X 100 mL), dried (MgSO4) and concentrated. Column chromatography with hexane/ethyl acetate 2:1, 1:1 and then 1:4 afforded 800 mg of the α

anomer as a slight yellow oil and 1.00 g of the β anomer also as slight yellow oil. 71% overall yield. Spectral data was in agreement with literature report.

1,2-dideoxy-1-(3-pyridyl)-β-D-ribofuranose **(35):** Compound 7 (280 mg, 0.64 mmol) was dissolved in dry dichloromethane (15.0 mL) and triphenyl carbenium tetrafluoroborate (1.27g, 3.86 mmol, 6 equivalents) was added. The reaction mixture was stirred at room temperature for one hour and afterwards water (20 mL) was added. Stirring was continued for another 45 minutes at room temperature. Aqueous layer was separated and the organic layer was washed four times with water and the aqueous layers were combined and concentrated by vacue. Column chromatography on silica gel with dichloromethane → dichloromethane/methanol (95:5) afforded 104 mg, 83% yield of light yellow foam. Spectral data was in agreement with literature report.

5′-O-(dimethoxytrityl)-1,2-dideoxy-1-(3-pyridyl)-D-ribofuranose **(36):** Compound **35** (125 mg, 0.64 mmol) was co-evaporated twice with pyridine and dissolved in dry pyridine (5 mL). To this mixture was added DMTCl (325 mg, 0.96 mmol) and DMAP (0.2 equivalents). Mixture was stirred at room temperature for five hours and excess DMTCl was quenched with methanol. After evaporation of excess solvent by vacue, residual oil was poured directly on a silica gel column without further work up. Elution with ethyl acetate → ethyl acetate/methanol (9:1) gave the desired 5′-O-protected product as colorless foam (200 mg, 63% yield). Spectral data was in agreement with literature report.

5′-O-(dimethoxytrityl)-1,2-dideoxy-1-(3-pyridyl)-D-ribofuranose-H-phosphonate Triethyl ammonium Salt **(37):** 5′-O-(dimethoxytrityl)-1,2-dideoxy-1-(3-pyridyl)-D-ribofuranose **36** (200 mg, 0.41 mmol) was dissolved in anhydrous pyridine (4 mL) and

diphenyl phosphite (0.7g, 2.80 mmol) was added dropwise at room temperature. After stirring for 20 minutes, a 1:1 mixture of Et_3N and water was added. Reaction mixture was stirred for additional 20 minutes and afterwards the mixture was concentrated and redissolved in CH_2Cl_2 and aqueous $NaHCO_3$. Organic layer was extracted and washed twice $NaHCO_3$ solution, dried ($MgSO_4$) and concentrated under reduced pressure. Column chromatography on silica gel on silica gel with dichloromethane →10 % methanol in dichloromethane afforded the desired product as a white foam (210 mg, 79% yield). ^{1}H NMR ($CDCl_3$) δ 8.45 (m, 2H, aromatic), 7.84 (d, 1H, aromatic), 7.61 (m, 1H, aromatic) 7.05-7.42 (m, 9H, aromatic), 6.75 (m, 4H, aromatic), 5.10 (dd, 1H, *J*= 6, 10 Hz), 4.80 (m, 1H), 4.25 (m, 1H), 3.65 (s, 9H), 3.20 (m, 2H), 2.90 (m, 6H), 2.58 (m, 1H), 1.95 (m, 1H), 1.22 (m, 9H). ^{13}C NMR ($CDCl_3$) δ 159.5, 149.8, 147.5, 145.0, 138.8, 1.36.5, 134.0, 130.0, 128.0, 127.5, 126.9, 123.5, 113.0, 86.8, 85.0, 78.0,75.9, 64.0, 55.1, 45.9, 42.5, 8.7. P NMR (CD_3OD) δ 3.51. HRMS (Ion mode: TOF, 70 eV) *m/z* $[M+H]^+$ Calcd. for $C_{31}H_{32}O_7NP$, 562.5635; found, 562.5001.

3-(5′-O-dimethoxytrityl-4-methyl-phosphinoyloxy-tetrahydro-furan-2-yl)-1-methyl-pyridinium: Triethyl ammonium Salt **(38):** 5′-O-(dimethoxytrityl)-1,2-dideoxy-1-(3-pyridyl)-D-ribofuranose-H-phosphonate Triethyl ammonium Salt **37** (110 mg, 0.20 mmol) was dissolved in anhydrous CH_2Cl_2 (4 mL) and CH_3I (30 equivalents) was added at room temperature and reaction mixture was stirred for 6 hours. Excess solvent was evaporated and product was recrystalized from EtOAc to afford yellow crystals (120 mg, 88% yield). ^{1}H NMR (CD_3OD) δ 9.00 (s, 1H, aromatic), 8.80 (d, 1H, aromatic) 8.99 (d, 1H, aromatic), 8.05 (m, 1H, aromatic) 7.40 (m, 2H, aromatic), 7.18-7.36 (m, 7H, aromatic), 6.85 (m, 4H, aromatic), 5.39 (m, 1H), 4.90 (m, 1H) 4.40 (s, 3H), 4.22 (m, 1H)

3.78 (s, 6H), 3.33-3.39 (m, 2H), 3.20 (m, 6H), 2.65 (m, 1H), 2.10 (m, 1H), 1.30 (m, 9H). ^{13}C NMR (CD_3OD) δ 159.5, 145.8, 144.0, 143.1, 142.5, 130.6, 130.0, 128.0, 126.8, 113.0, 87.2, 86.5, 76.5, 62.2, 56.1, 55.2, 47.0, 46.1, 41.6, 8.8. HRMS (Ion mode: TOF, 70 eV) *m/z* $[M+H]^+$ Calcd. for $C_{32}H_{35}O_7NP$, 576.2228, found 576.2204.

REFERENCES

(1) Schuster, G. B. (ed) Long Range Charge Transfer in DNA I, II in *Topics in Current Chemistry*. 2004, 236, 237. Springer-Verlag, Heidelberg.

(2) Frelon, S.; Douki, T.; Ravanat, J. L.; Pouget, J. P.; Tornabene, C.; Cadet, J. *Chem. Res. Toxicol*. **2000**, *13*(10) 1002

(3) Kasai, H.; Yamaizumi, Z.; Berger, M.; Cadet, J. *J. Am. Chem. Soc*. **1992**, *114*, 9692

(4) Luo, Wenchen.; Muller, J. G.; Rachlin, E. M.; Burrows, C. J. *Org. Lett*. **2000**, *2*(5) 613-616.

(5) For a list of pertinent references see Jones, J. W.; Robins, R. K.; *J. Am. Chem. Soc.* **1962**, *84*, 1914

(6) Searls, T.; Chen, D. L.; Lan, T.; McLaughlin, L. W. *Biochemistry*. **2000**, *39*, 4375

(7) Eaton, M. A.W.; Millican, T. A. *J. Chem. Soc. Perkin Trans. 1*. **1988**, 545.

(8) Buchanan, J. G. *Fortschr. Chem. Org. Naturst*. **1983**, *44*, 245

(9) Jankowska, J.; Sohkowski, M.; Stawilrskif, J.; Kraszewski, A, *Tet. Lett.*, **1994**, 35, (20), 3355

(10) Froehler, B. C.; Ng, P. G.; Matteucci, M. D. *Nucleic Acids Res*. **1986**, *14*(13), 539

(11) Lin, C.; Fu, H.; Tu, G.; Zhao, Y. *Syn. Comm*. **2003**, *33*(14), 2553

(12) Liu, C.-S., Hernandez, R. and Schuster, G. B. *J. Am. Chem. Soc*. **2004,** *126*(9), 2877

APPENDIX A

DESIGN AND SYNTHESIS OF CHEMOTHERAPEUTIC AGENTS

DNA methylation is an enzyme-induced modification to DNA structure without alteration of the specific sequence of the base pairs responsible for encoding the genome.[1] One of the group of enzymes that mediates this process is known as DNA methyltransferases. The methyl group is provided by S-adenosyl methionine (SAM), which is converted to S-adenosyl homosysteine (SAH) in the process. SAH breaks down to generate adenosine and homocysteine, which then recycles back to SAM in a folate- and cobalt- amine dependent pathway. While DNA methylation is known to be an essential and normal component of mammalian embryogenesis, altered methylation patterns are known to occur in the DNA of cancer cells. Thus, inhibition of such altered DNA methylation patterns can be achieved directly by inhibition of DNA methase, or indirectly by inhibition of SAH.[2] Both of these enzymes are known cellular targets for antiviral, antiparasitic, and anticancer agents[3-9] as a result of their involvement in nucleotide metabolism and DNA synthesis. The goal of this research is to synthesize series of carbocyclic analogues of natural nucleosides that will be more stable than the natural nucleosides while retaining the ability to inhibit the active site of SAHase.

The main classes of purine and pyrimidine nucleosides that have been identified as differentiation inducers include: those that interfere with the de novo synthesis of DNA and RNA precursors like antifolates and inhibitors of rate-limiting enzymes, those that

disrupt DNA methylation by inhibiting DNA MeTase and/or the enzyme SAHase, and those that inhibit DNA synthesis. The work discussed herein is focused on the second class of inhibitors.

Chemistry

The target compounds (Figure A.1) are structurally modified nucleosides that are expected to inhibit DNA methylation. The structural modification was introduced by replacing the furanose oxygen of the sugar moiety with a methylene group and by replacing the N-3 of the base with a carbon to form a carbon-carbon bond for the deazaAdenosine. For the IsoAdenosine isoAdenosine (isoA), the structural modification was done by replacing the furanose oxygen with a methylene group and retaining the glycosidic bond (Figure A.1). IsoA is a structural isomer of adenosine with the glycosidic bond attached to the N-3 instead of N-9 of the base. This structural modification will impart an increased level of stability as a result of the transformation of the unstable hemiaminal glycosidic bond to a stable tertiary amine, thereby increasing the ability of the modified nucleosides to resist cleavage by enzymes and also their overall lipophilicity, which helps to increase their uptake into the cells.[2]

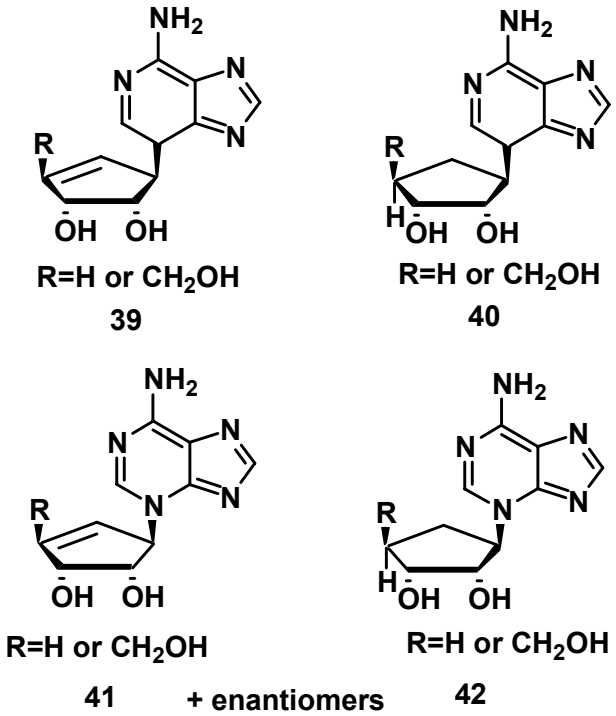

Figure A.1 Target compounds

Four of the carbocyclic moieties required for the synthesis of the inhibitors are shown in Figure A.2. The synthetic routes to the carbocyclic moieties are shown in scheme A.2. The methoxymethyl ether protected enone **52** was synthesized according to the method by Schneller et al.[10] in six steps starting with cyclopentadiene with 18 percent overall yield (scheme A.1).

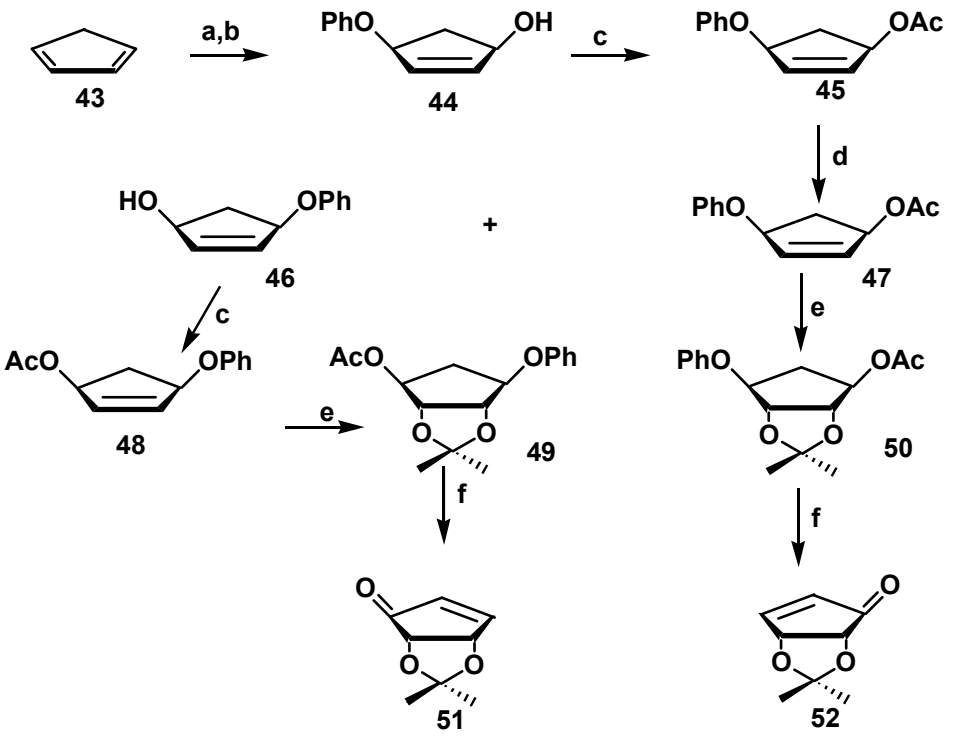

Reaction conditions: (a) Na_2CO_3/CH_2Cl_2, O^0C, paracetic acid, NaOAc. (b) $Pd(PPh_3)_4$/THF,phenol, O^0C (c) AC_2O, pyridine/catalytic DMAP, CH_2Cl_2. (d)pseudomonas capacia lipase/phospate buffer, 25^0C. (e) i, N-methylmorpholine N-oxide/catalyst OsO_4,acetone/H_2O ii, 2,2-dimethoxypropane/acetone, catalytic *p*-TsOH. (f) i, KOH/MeOH ii, pyridinium chlorochromate/molecular sieves 4-anstromes powder/CH_2Cl_2.

Scheme A.1 Synthesis of *(4R, 5R)-4,5-(isopropylidenedioxy-2-cyclopentenone ((-)-* **and *(4S, 5S)-4,5-(isopropylidenedioxy-2-cyclopentenone ((+)-***

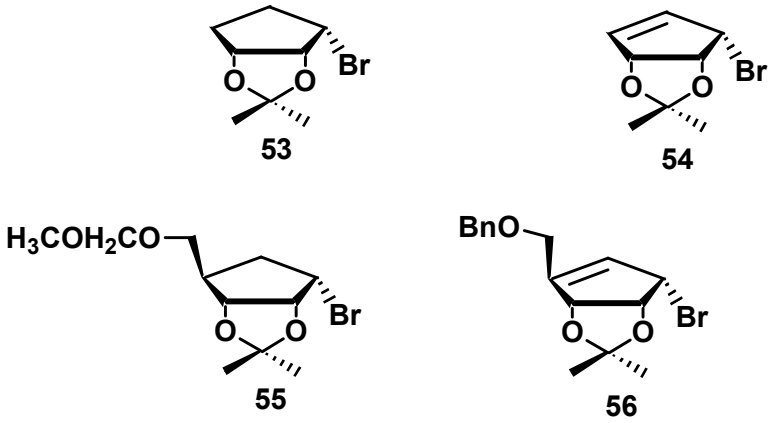

Figure A.2 Carbocyclic moieties

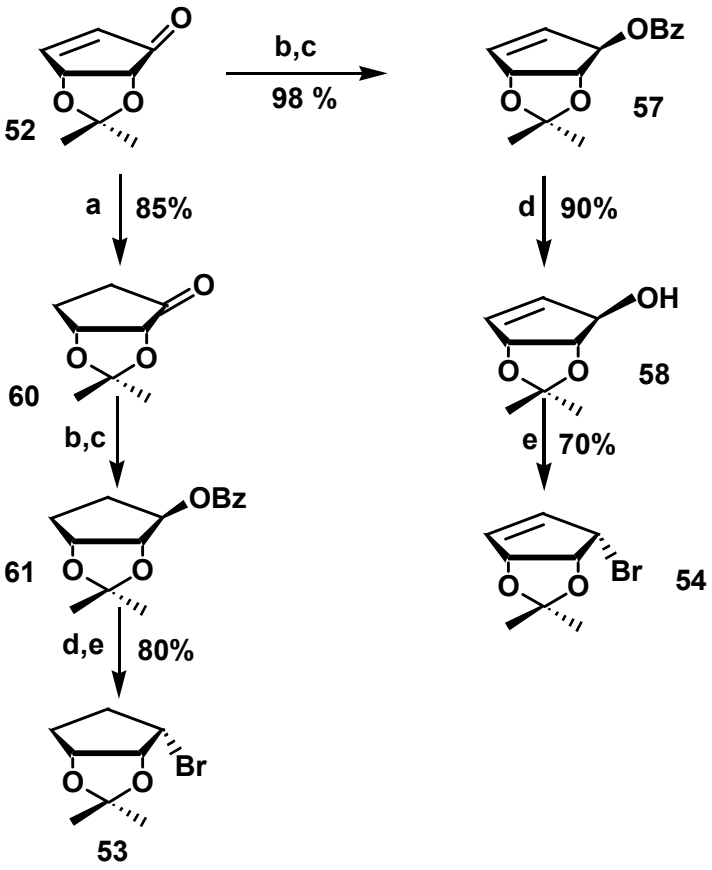

Reagents and conditions: (a) Pd/C, H_2, EtOH (b) $CeCl_3$, $NaBH_4$, MeOH (c) *p*-Nitrobenzoic acid, PPh_3, DIAD, THF, 55^0C, 48h (d) KOH, $MeOH/H_2O$ (e) PPh_3, NBS, DMF

Scheme A.2 Synthesis of Carbocyclic Moieties

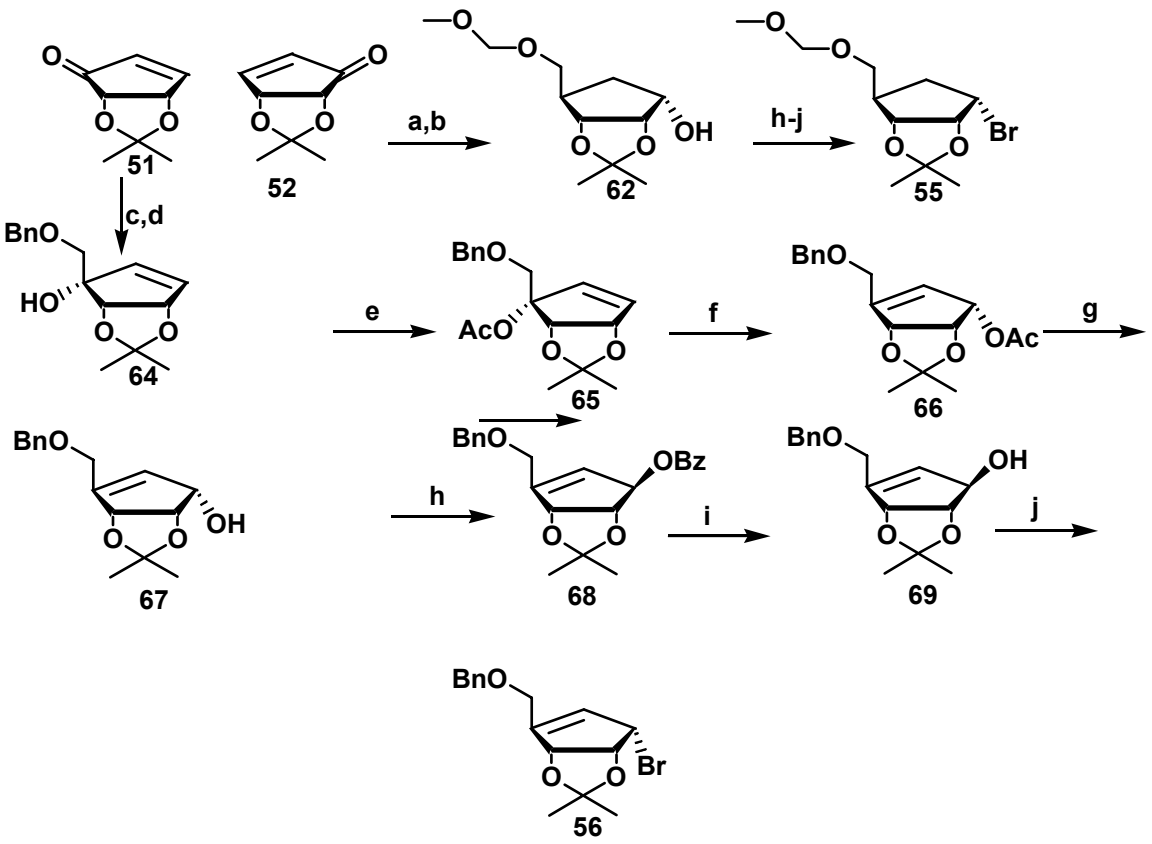

Reagents and conditions (a) $CuBr.Me_2S$, i-PMgCl, $Bu_3SnCH_2OCH_2OCH_3$,n-BuLi, CuBr, BF_3, (b) $CeCl_3$,$NaBH_4$, MeOH (c) ICH_2I, ZnCu, Bu_3SnCl, Benzyl alcohol, NaH/THF (d) n-BuLi, -78^{0}C, THF (e) Ac_2O, DMAP, Et_3N, CH_2Cl_2, (f) Benzoquinone, $PdCl_2(CH_3CN)_2$, THF, reflux (g) KOH/MeOH, H_2O (h) PPh_3, DIAD, p-NBzOH, 55^{0}C, 48h, (i) KOH, MeOH/H_2O (j) PBr_3, ether, 0^{0}C.

Scheme A.3 Synthesis of compounds 55 and 56

Compound **54** was obtained in 80% yield from **52** (scheme A.2). Compound **56** is formed by stannylation of benzylalcohol[11] and the subsequent reaction of the stannylated compound with **52** in 62% yield (scheme A.3). Protection of the resultant alcohol followed by treatment with a catalytic amount of benzoquinone and palladium-acetonitrile complex under refluxing conditions afforded compound **66**, which was deprotected using standard hydrolysis conditions to obtain compound **67**. Attempts to synthesize **62** by the method of Johnson et al.[12] resulted in a very low yield (10%) after several trials (scheme A.3). To couple the carbocyclic moieties to the bases, the α-alcohols were converted to the β-alcohols using Mitsunobu conditions. Hydrolysis of the Mitsunobu products followed by bromination of the resultant alcohols afforded carbocyclic compounds **53**, **54**, **55**, and **56** (scheme A.2 and A.3), which are ready to be coupled to the bases.

Initial attempts to build the isoA nucleosides from pyrimidine using the method of Denayer et al. (scheme A.4)[13] were unsuccessful. It was later found that direct alkylation of adenine at the 3 position can be accomplished under non-basic conditions using dimethylacetamide as solvent and at 110 ^{o}C.[14] The stage was now set for coupling and deprotection to yield the final compounds. The construction of the bases for the 3-deaza C-nucleosides proved to be more challenging. Several substituted pyridines were synthesized to enable the formation of the imidazole part of the heterocyclic ring after coupling to the carbocyclic moieties, but only 5-bromo-2-methoxy pyridine appeared to be the less complicated compound for the coupling. Coupling of compound **54** and 5-bromo-2-methoxy pyridine resulted in the formation of two isomers **71a** and **71b** (scheme A.5), which were difficult to separate. This separation problem resulted in a search for

better coupling methods that will allow an addition only on the allylic position instead of a 1,4 addition on compound **52**.

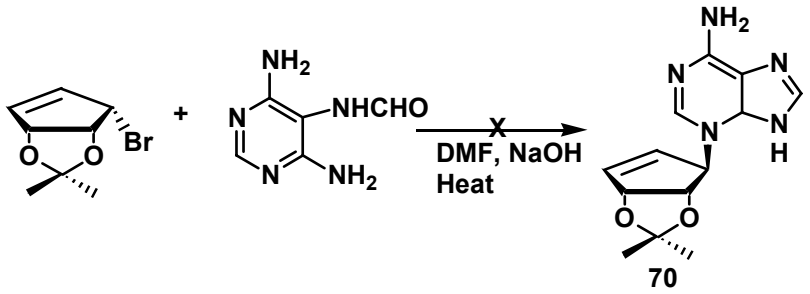

Scheme A.4 Attempted synthetic route

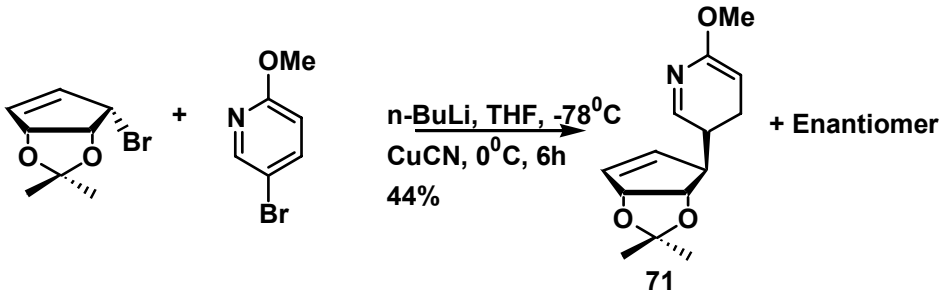

Scheme A.5 Synthesis of 5((-)-2,3-isopropylidenedioxy-4yl-cyclopenta)-2-methoxy pyridine

APPENDIX B

SYNTHESIS OF CHEMOTHERAPEUTIC AGENTS

*(3R, 5S)-3-Acetoxy-5-phenoxycyclopentent-1-ene((+)-**44**) and (3S,5R)-3-hydroxy-5-phenoxycyclopent-1-ene ((-)-**44b**)*. To an ice cooled suspension of Na_2CO_3 (1 kg) and freshly cracked cyclopentadiene (200g, 3.03 mol) was added 32% paracetic acid (500 mL, 2.17 mol pretreated with 25 g of NaOAc) dropwise over a period of 1.5 hours. The reaction mixture was stirred at room temperature for 3 hours. Afterwards the inorganic salts where removed by filtration and product was washed with CH_2Cl_2 (1L). The resultant filtrate was used in the next step after preparation of solution 2.

Solution 2.(tetrakis(triphenylphosphine)Pd: A mixture of $PdCl_2$(1.11 g, 6.25 mmol), PPh_3(8.20 g, 31.2 mmol) and DMSO (75.0 mL) was heated at 170 ^{0}C under argon until solid is completely dissolved in the mixture. The oil bath was then taken away and the solution was rapidly stirred for 5 minutes. Hydrazine monohydrate (1.25 g, 25 mmol) was added with a syringe. The dark solution was immediately cooled with an H_2O bath. Crystallization began to occur at about 125^{0}C and mixture was allowed to continue cooling at room temperature until the temperature of reaction mixture cooled down to room temperature. Reaction mixture was filtered and under N_2 atmosphere on a coarse sintered glass funnel. The solid was washed with EtOH (2 X10 mL) and Et_2O (2 X 10 mL). Product was dried by passing a slow stream of N_2 through a capped flask and the bright yellow crystalline product was used in the next step.

To a solution of *tetrakis(triphenylphosphine)Pd* (6.0 g, 5.19 mmol) in dry THF at 0^0C was added Phenol (235 g, 2.44 mol). After stirring at 0^0C for 5 minutes, filtrate from above was added over a 30 minutes period while maintaining the reaction at 0^0C. Reaction mixture was stirred at room temperature for 24 hours followed by evaporation of excess solvent. The brown residue was redissolved in Et_2O (1L) and washed with H_2O/brine (2 x 500 mL), dried with Na_2SO_4 and evaporated to dryness. The crude product was purified by silica gel chromatography. Column was eluted first with hexane and then with a mixture of ethyl acetate/hexane (1:4). The product (±)-3-hydroxy-5-phenoxycyclopent-1-ene was eluted was eluted with ethyl acetate/hexane (1:1) to afford a clear syrup (280.4 g) a part of which was used in the next step.

To a solution of (±)-3-hydroxy-5-phenoxycyclopent-1-ene (180.4 g, 0.79 mol), 4-dimethylaminopyradine (0.64 g, 0.0052 mol) and pyridine (77.5 g, 0.98 mol) in dry CH_2Cl_2 (750 mL) at 0^0C was added Ac_2O (94.4 g, 0.92 mol). After stirring for 2 hours, the reaction mixture was stirred at room temperature for 17 hours. The reaction mixture was stirred vigorously with saturated aqueous $NaHCO_3$ solution (3 x 400 mL) maintained at 0^0C and H_2O (500 mL), dried with $MgSO_4$ and evaporated to dryness. Residual brown oil was crystallized to pentane to afford (±)-3- acetoxy-5-phenoxycyclopent-1-ene. Spectral data was in agreement with literature report.

To a 3 liter (three-necked with Hirschberg stirrer, dropping funnel and pH electrode) was added (±)-3- acetoxy-5-phenoxycyclopent-1-ene (126.0 g, 0.58 moles) and NaH_2PO_4 (0.2 moles), pH 4.20, 1 L) and acetone (300 mL). Mixture was adjusted to pH 7 with NaOH (2 M). To the stirred suspension was added Pseudomonas Cepacia lipase (2.6 g) in one portion. pH of mixture was then maintained between pH 7.0 and 7.3 by

continuous addition of NaOH (260 mL, 1.1 moles) solution. After approximately 2.5 hours more lipase PS (0.6 g) was added. After all the NaOH had been (in approximately 18 hours), mixture was diluted with 700 mL of AcOEt and filtered through celite. The celite pad was washed with additional amount of EtOAc (1 L). Organic layer was extracted with EtOAc (4 x 250 mL) and combined organic phases were dried with $MgSO_4$ and evaporated to dryness. Recovered residual brown oil weighed 119 g. Residual brown oil was purified by silica gel chromatography. The column was first eluted with hexane EtOAc (9:1) to afford (+)-3R, 5S-3-Acetoxy-5-Phenoxycyclopent-1-ene (74.3 g) which was recrystalized from pentane. The column was next eluted with hexane/EtOAc (6:1) and (1:1) to give (3S, 5R)-3-Hydroxy-5-Phenoxycyclopent-1-ene (94g) as a hygroscopic yellow oil. Spectral data was in agreement with literature report.

(*1R, 2S, 3R, 4S)-1-Acetoxy-4-phenoxy-2, 3-(isopropylidienedioxy)-cyclopentane ((-)-**50**)*. To a solution of (+)-3R, 5S-3-Acetoxy-5-Phenoxycyclopent-1-ene (74.0 g, 0.34 mol) and N-methylmorpholine N-oxide (150 mL) of 60% aqueous solution, 0.769 moles) in acetone (500 mL) and H_2O (150 mL) cooled to 0^0C was added OsO_4 (250 mg). Solution was stirred at room temperature for approximately 22 hours and the acetone was removed by rotary evaporation. The residue was cooled to 0^0C and saturated aqueous $NaHSO_3$ solution (150 mL) was added. After stirring for an hour at 0^0C, the mixture was extracted with EtOAc (5 x 200 ml). The organic phase was washed with ice cold 1M HCl, (2 x150 mL), dried MgSO4 and evaporated to dryness to afford the diol products (78.0 g). Spectral data was in agreement with literature report.

To a solution of the diol (78.0 g) in dry acetone (300 mL) containing 2, 2-dimethoxypropane (200 mL) was added *p*-Toluenesulfonic acid (1.5 g). Mixture was

stirred for approximately 20 hours at room temperature and then was neutralized with saturated aqueous sodium carbonate. The volatile solvents were evaporated without heating. Product was dissolved in EtOAc (750 mL) and washed with brine (5 x 150 mL). Residual product was dried with $MgSO_4$, evaporated to afford brown oil which was purified by silica gel column chromatography. The column was first eluted with hexane/ethyl acetate (9.5:0.5) and then hexane/ethyl acetate (4:1). Solvent was evaporated and pentane was added to product which solidified in the freezer. Final compound weighed 46g. Spectral data was in agreement with literature report.

*(3S, 5R)-3-Acetoxy-5-phenoxycyclopent-1-ene((-)-**48**)* To a solution of (3S,5R)-3-Hydroxy-5-Phenoxycyclopent-1-ene (44g, 0.25 mol) , 4-dimethoxy pyridine (250 mg, 2.0 mmol) and pyridine (28.0 g, 0.36 mol) in dry dichloromethane (240.0 mL) was Ac_2O (30.0 g, 0.29 mol) at 0^0C. Mixture was stirred at the same temperature for 2 hours and then stirred at room temperature for approximately 20 hours. Reaction mixture was then cooled to 0^0C and stirred vigorously with saturated aqueous sodium hydrogen carbonate solution (3 x 250 mL). The organic phase was separated and washed with 1 molar HCl (2 x 250 mL) and H_2O (250 mL), dried $MgSO_4$ and evaporated to dryness. The residual brown oil was recrystalized from pentane to afford 45 g, 0.208 moles of white solid, 83% yield. Spectral data was in agreement with literature report.

(*1S, 2R, 3S, 4R)-1-Acetoxy-4-phenoxy-2, 3-(isopropylidienedioxy)-cyclopentane ((+)-**49**)*. To a solution of (3S, 5R)-3-Acetoxy-5-phenoxycyclopent-1-ene (-) (45.0 g, 0.208 mol) and N-methylmorpholine N-oxide (85.0 mL, 0.437 mmol of 60% aqueous solution) in acetone (300 mL) and H_2O (100 mL) cooled to 0^0C was added OsO_4 (250 mg). Solution mixture was stirred at room temperature for approximately 24 hours and

the acetone was removed by rotary evaporation. The residue was cooled to 0^0C and saturated aqueous $NaHSO_3$ solution (100 mL) was added to the solution mixture. After stirring for 15 minutes at 0^0C, the mixture was extracted with EtOAc (5 x 150 ml). The organic phases were combined and washed with ice cold 1M HCl, (2 x 120 mL), dried $MgSO_4$ and evaporated to dryness to afford the crude diol products (45.0 g).

To the solution of the crude diol from above (45.0 g) in dry acetone (200 mL) containing 2, 2-dimethoxypropane (120 mL) was added *p*-Toluenesulfonic acid (1.0 g). The reaction mixture was stirred for approximately 20 hours at room temperature and then was neutralized with saturated aqueous sodium carbonate. After removal of the volatile solvents by rotary evaporation without heating, residual product was dissolved in EtOAc (500 mL) and washed with brine (5 x 100 mL). Product was dried with $MgSO_4$ and evaporated to afford brown oil which was purified by silica gel column chromatography. The column was first eluted with hexane/ethyl acetate (9.5:0.5) and then hexane/ethyl acetate (4:1) to afford 25.0 g of white solid product. To a solution of the protected acetoxy-phenoxycyclopentane from above (25.0 g, 86 mmol) in MeOH (50.0 mL) was added a solution of KOH (6.0 g, 110 mmol) in MeOH (70.0 mL). The reaction mixture was stirred at room temperature for 3 hours and then neutralized to pH 7 by the dropwise addition of concentrated HCl. Excess methanol was then removed by evaporation and residual product was redissolved in ethyl acetate (250 mL) and washed with brine (3 x 70.0 mL). Resultant product was dried $MgSO_4$ and solvent was removed by vacue to afford 20.0 g colorless syrup which was used in the next step without further purification.

*(4R, 5R)-4,5-(isopropylidenedioxy-2-cyclopentenone ((-)-**52**)*. To a stirred suspension of molecular sieves (70.0 g) and pyridinium chlorochromate (60.0 g, 0.28 mol) in dry dichloromethane (750 mL) was added slowly 20.0 g of the syrup from above. Reaction mixture was stirred at room temperature for approximately 24 hours and then diluted with Et_2O (500 mL). The product was filtered through a celite pad and the filtrate was evaporated to dryness. Silica gel column chromatography with hexane/ethyl acetate (8:2) afforded a solid crystal which was recrystalized from pentene/Et2O (8:1) to afford 6.1 g white crystal product. Spectroscopic data was in agreement with literature report.

*(4S, 5S)-4,5-(isopropylidenedioxy-2-cyclopentenone ((+)-**51**)*: using the same procedure for the converting *(-)-**50*** to *(-)-**52***, compound **51** was obtained in 85% yield.

((-)-2,3-isopropylidenedioxy)-4-cyclopenten-1α-ol. To a stirred solution of cyclopentenone from above (4.0 g, 26 mmol) and cerium (III) chloride heptahydrate (9.68 g, 260 mg) at 0^0C was added $NaBH_4$ (2.95 g, 78.0 mmol) in small portions under argon atmosphere. At the completion of the addition of $NaBH_4$, reaction mixture was stirred for 1 hour and neutralized to pH 7 with concentrated HCl (4.0 g). After evaporation of excess solvent, residual product was redissolved in brine and extracted with Et_2O (3 x 150 mL). Organic layers were combined, dried with $MgSO_4$ and evaporated by vacue to afford yellow syrup (3.5 g, 87% yield). Spectral data was in agreement with literature report.

4-*Nitro-benzoic cid 2,2-dimethyl-4,6a-dihydro-3aH-cyclopenta[1,3]dioxol-4-yl ester **57**:*. To a solution of *p*-Nitrobenzoic acid (8.57 g, 51.0 mmol) and triphenylphosphine (13.45 g, 51.0 mmol) in dry THF (100 mL) flushed with argon for 10 minutes was added diisopropyl azodicarboxylate (7.78 g, 38.0 mmol). Reaction mixture

was stirred under argon for 15 minutes at room temperature and a solution of *((-)-2,3-isopropylidene)-4-cyclopenten-1-ol* (4.0 g, 26.0 mmol) in dry THF ((150 mL) was added with a syringe. Stirring was continued at 55^0C for 4 days. Afterwards, excess THF was removed by vacue and residual product was purified by silica gel column chromatography. Column was first eluted with hexane and then hexane/ethyl acetate (9:1). Fractions containing product were collected with hexane/ethyl acetate (6:1) and evaporation of the fractions afforded 6.55 g of crystalline solid, 84% yield. Spectral data was in agreement with literature report.

((-)-2,3-isopropylidenedioxy)-4-cyclopenten-1β-ol ***58***: To a solution of 4-Nitro-benzoic cid 2,2-dimethyl-4,6a-dihydro-3aH-cyclopenta[1,3]dioxol-4-yl (0.80 g, 2.60 mmol) in MeOH (40.0 mL) was added H_2O (50.0 mL). To this mixture was added KOH (300 mg, 5.3 mmol dissolved in 2.0 mL). Reaction mixture was stirred for 45 minutes and methanol was evaporated completely. Aqueous layer was extracted with dichloromethane (7 x 30.0 mL). Organic layers were combined was dried (MgSO4), evaporated and dried overnight in a vacuum oven to afford 350 mg of colorless syrup, 86% yield. Spectral data was in agreement with literature report.

((-)-2,3-isopropylidenedioxy)-4α-bromocyclopentene ***54***: A solution of ((-)-2,3-isopropylidenedioxy)-4β-cyclopenten-1β-ol (584 mg, 3.7 mmol) and triphenylphosphine (1.77 g, 6.7 mmol) in DMF (8.0 mL) was stirred for 10 minutes at room temperature under argon and cooled to 0^0C. To this mixture was added N-Bromosuccinimide (1.33 g, 7.5 mmol), and the reaction mixture was stirred for 3 hours at room temperature under argon. Afterwards, reaction mixture was quenched with H_2O (20.0 mL). Residual product was extracted with ethyl acetate (3 x 25 mL), dried ($MgSO_4$) and evaporated by vacue.

Column chromatography on silica gel with hexane/ethyl acetate (6:1) gave 405 mg of colorless brominated oil, 50% yield. Spectral data was in agreement with literature report.

5((-)-2,3-isopropylidenedioxy-4yl-cyclopenta)-2-methoxy pyridine ***71*** : To a solution of 5-bromo-2-methoxypyridine (214 mg, 1.14 mmol) in dry THF (4.0 mL) was added *n*-Butyl lithium (902 μL, of 2.5 M in hexane) at -78^{0}C under argon atmosphere. After 30 minutes of stirring at -78^{0}C, the reaction mixture was added to CuCN (2 mL solution prepared in dry THF under argon at -78^{0}C). Reaction mixture was allowed to stir at 0^{0}C until all the CuCN had gone into solution and then cooled back to -78^{0}C. To this mixture was added ((-)-2,3-isopropylidenedioxy)-4α-bromocyclopentene (100 mg, 0.45 mmol) under argon atmosphere. Reaction mixture was allowed to warm up to 0^{0}C and then stirred at 0^{0}C for 6 hours and then quenched with 10% ammonium hydroxide/aqueous ammonium chloride. Reaction mixture was stirred for additional 15 minutes at room temperature and then extracted with ethyl acetate (3 x 15 mL). Organic layers were combined and washed with H_2O and dried with $MgSO_4$. Column chromatography in hexane/ethyl acetate (5:1) afforded yellow syrup confirmed by proton NMR as a mixture of the desired compound (80.0 mg, 72% yield). Spectral data was in agreement with literature report.

(Benzyloxymethyl)tributylstannane. To a three neck round bottom flask was added cupric acetate (0.5g) in hot glacial acetic acid (50.0 mL). To this solution was added zinc granules (33.0 g, 0.5 mol), and the hot mixture was shaken for approximately 2 minutes. The acetic acid was decanted from the metal and an additional fresh acetic acid (50.0 mL) was added. This process was repeated again, and the cooled ZnCu couple was then washed three times with diethyl ether (50.0 mL). Afterwards, the residual brown solid

was dried with nitrogen. To the ZnCu couple was added a solution of diiodomethane (100 g) in THF through a dropping funnel after the reaction had been initiated with few drops of concentrated diiodomethane and THF (50.0 mL). An exothermic reaction is an indication that the reaction has been initiated. The content of the dropping funnel was then added dropwise for about three hours while maintaining the temperature at 40^0C with heating at the last hour. After most of the zinc had been consumed, the reaction mixture was cooled to 0^0C and filtered under nitrogen using schlenk-type filter with coarse fritted disc. The solution was a cloudy purple. To the purple solution was added tributyltin chloride (67.4 mL, 81.0 g, 0.25 mol) dropwise over a period of 30 minutes, and the reaction was let to stir for 18 hours under nitrogen. The reaction mixture was then poured into 300 mL of petroleum ether and washed with H_2O (2 x 200 mL), dried ($MgSO_4$) and evaporated to give crude Bu_3SnCH_2I (98.0 g).

Sodium hydride (8.2 g, 0.34 mol) was suspended in anhydrous THF (330 mL) under nitrogen atmosphere and benzyl alcohol (27.0 g, 0.25 mol) was added dropwise with stirring. Stirring was continued at room temperature for approximately one hour past the time when gas evolution ceased and Bu_3SnCH_2I from above was added. Reaction mixture was stirred for 72 hours at room temperature and afterwards it was treated with small amount of methanol. Reaction mixture was poured into petroleum ether (1.0 L) and washed with H_2O (2 x 250 mL), dried ($MgSO_4$), and evaporated by vacue. Column chromatography on silica gel treated with 5% triethylamine and elution ethyl acetate/hexane (9:1) gave 29.0 g of (Benzyloxymethyl)tributylstannane.

Compound ***64***: To a solution of (Benzyloxymethyl)tributylstannane (3.2 g, 7.8 mmol) in THF (15.0 mL) cooled to -78^0C was added n-Butyl lithium (3.1 mL, of 2.5M

in hexane). The reaction mixture was stirred for 15 minutes and a solution of (4S, 5S)-4,5-(isopropylidenedioxy-2-cyclopentenone ((+)-51) (1.0 g) in THF (3.0 mL) with a syringe under argon condition. The reaction mixture was stirred for 40 minutes at -78^{0}C and then quenched with saturated ammonium chloride (20.0 mL) and extracted with ethyl acetate. The extract was washed with H_2O and then brine, dried ($MgSO_4$) and evaporated. Column chromatography on silica gel with hexane/ethyl acetate (4:1) gave 1.2 g white solid, 62% yield. Spectral data was in agreement with literature report.

*Compound **65**:* To a solution of compound (5.5 g, 19.7 mmol) in dichloromethane (20.0 mL) at room temperature was added triethylamine (4.1 mL, 3.0 g, 29.6 mmol) and DMAP (500 mg, 3.9 mmol). Reaction mixture was stirred at room temperature for 5 minutes and Ac_2O (3. 0 mL, 29.6 mmol) was added to the mixture. The reaction mixture was stirred for 20 hours at room temperature and then cooled down to 0^{0}C, washed 3 times with saturated aqueous sodium hydrogen carbonate. The organic phase was washes further twice with ice cold HCl (0.5M) and H_2O, dried ($MgSO_4$) and excess solvent was evaporated. Column chromatography with hexane/ethyl acetate (4:1) gave 4.7 g white crystals 74%. Spectral data was in agreement with literature report.

*Compound **66***: Compound B (4.66 g, 14.7 mmol) was dissolved in THF (60.0 mL) under argon and pretreated with benzoquinone (0.4 equivalent, 633 mg) and $PdCl_2(CH_3CN)_2$ (10%, 379 mg). Reaction mixture was refluxed overnight under argon. Afterwards residual product was concentrated to approximately 1/5 volume by vacue. The product was poured into silica gel short column without further work up. Elution with ether and hexane afforded 3.5 g of the rearranged acetate product as a white solid, 75% yield. Spectral data was in agreement with literature report.

*Compound **67**:* Compound C (3.5g, 10.9 mmol) was dissolved in MeOH (40.0 mL) and H_20 (50.0 mL). To the above mixture was added KOH (1.3 g, 21.9 mmol dissolved in 10.0 mL of H_2O). Reaction mixture was stirred for about 45 minutes and excess methanol was evaporated. Product was extracted from aqueous layer with dichloromethane (5 x 40.0 mL), dried ($MgSO_4$) and concentrated. The solid crystalline product weighed 2.7g, 91% yield after drying overnight.

*Compound **68**: p*-Nitrobenzoic acid (3.3 g, 19.6 mmol) and triphenylphosphine (4.6 g, 17.7 mmol) were dissolved in dry THF (80.0 mL) and flushed with argon for 10 minutes. To this reaction mixture was added diisopropyl azodicarboxylate (3.0 g, 14.7 mmol). Reaction mixture was stirred under argon for 15 minutes at room temperature and a solution of compound D (2.7 g, 9.8 mmol in dry THF (30.0 mL)) was added with a syringe. Stirring was continued at 55^0C for 3 days. Afterwards, excess THF was removed by vacue and residual product was poured directly into a silica gel column. Fractions containing product were collected with hexane/ethyl acetate (6:1) and evaporation of the fractions afforded 3.8 g of crystalline solid, 92% yield. Identity of compound was confirmed by proton and carbon NMR.

*Compound **69***: Hydrolysis of compound E followed same procedure as compound **67** in 95% yield to afford the beta alcohol.

*Compound **56***: Compound **69** (430 mg, 1.6 mmol) was dissolved in ether (10.0 mL) and cooled down to 0^0C. To this solution was added PBr3 (584 mg, 2.0 mmol). Stirring was continued at the same temperature for three hours and then quenched with H_2O. Organic phase was extracted with ether (3 x 30 mL), dried ($MgSO_4$) and

concentrated. Column chromatography on silica gel with ethyl ether/hexane afforded the desired product in low yield (140 mg) confirmed by proton NMR and mass spec.

REFERENCES

1) Wajad, S. A.; Laid, P. W. DeMeester, T. R. *Annals of Surgery*. **2001**, *234*, 10

2) Dr. Katherine Seley's Research

3) Borchardt R. T.; Crevling, C. R.; Cleland P. M.; *Biological Methylation and Drug Design*; Humana Press: Clifton, New Jersey, 1996

4) Wolfe, M. S.; Lee, Y. Barlett, W. J. Borcherding D. R. ; Borcherdt R. T. *J. Med. Chem*. **1992**, *35*, 1782

5) Borchardt, R.T. Keller, B. T., Patel-Thombre, U. *J. Biol. Chem.* **1984**, *259*, 4353

6) Glazie, R. L.; Knode, M. C. *J. Biol. Chem*. **1984**, *259*, 12964

7) Saunders P. P. Tau, M. T. Robins, R. K. *Biochem. Pharmacol*. **1985**, *34*, 2749

8) Bocherding, D. R.; Scholtz, S. A.; Borcharelt, R. T. *J. Org. Chem*. **1987**, *52*, 5457

9) Bennet, L. L. Jr.; Allan, D. W.; Comber, R. N.; Rose, L. M.; Secrist, J. A. *Mol. Pharmacol*. **1986**, 29, 383

10) Johnson, C. R.; Medich, J. R. *J. Org. Chem*. **1998**, *53*, 4131

11) Schneller, S. W.; Siddiqi, S. M. Nucleoside and Nucleotides. **1993**, *12*, 185

12) Still, C. W. *J. Am. Chem*. *Soc*. **1978**, *100*, 1481

13) Denayer, R.; *Bull. Chem. Soc. Fr*. **1962**, 1358

14) Fujii, T.; Walker, Ca. C; Leonard, N. J. *J. Med. Chem*. **1979**, 22, 125

APPENDIX C

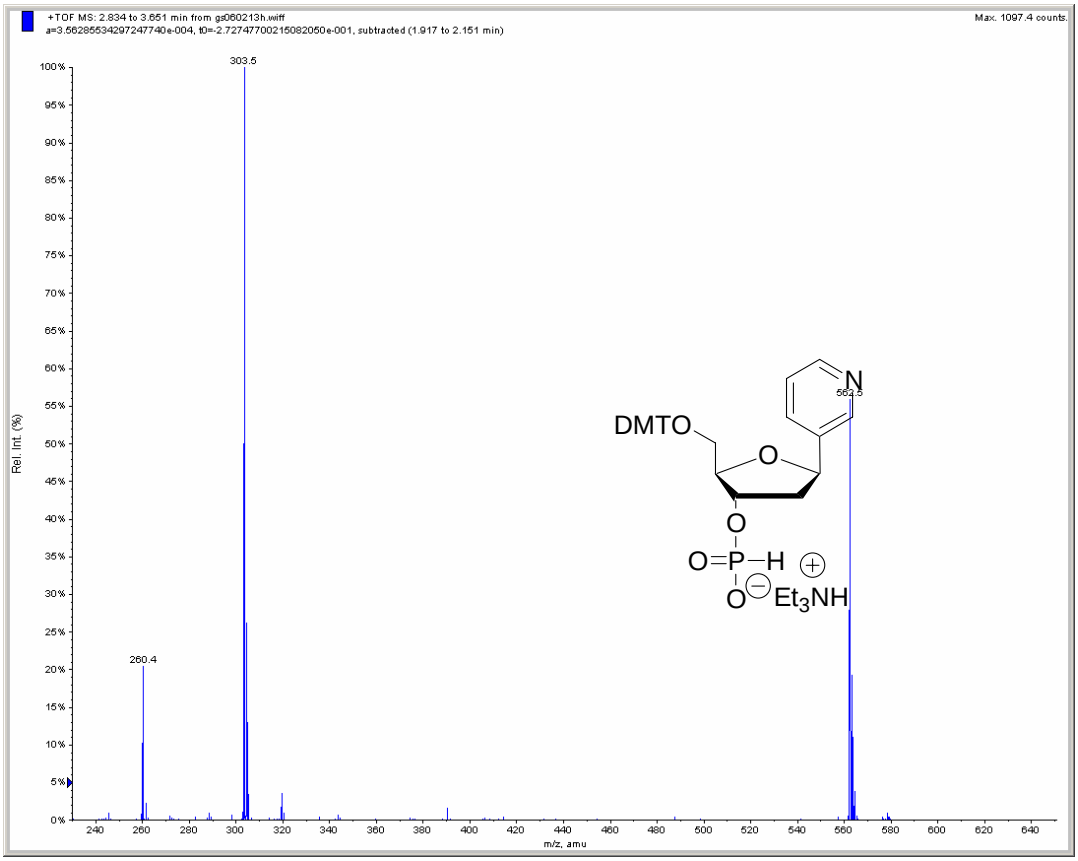

Figure C.1 Mass spectra of H-phosphonate pyridine nucleoside

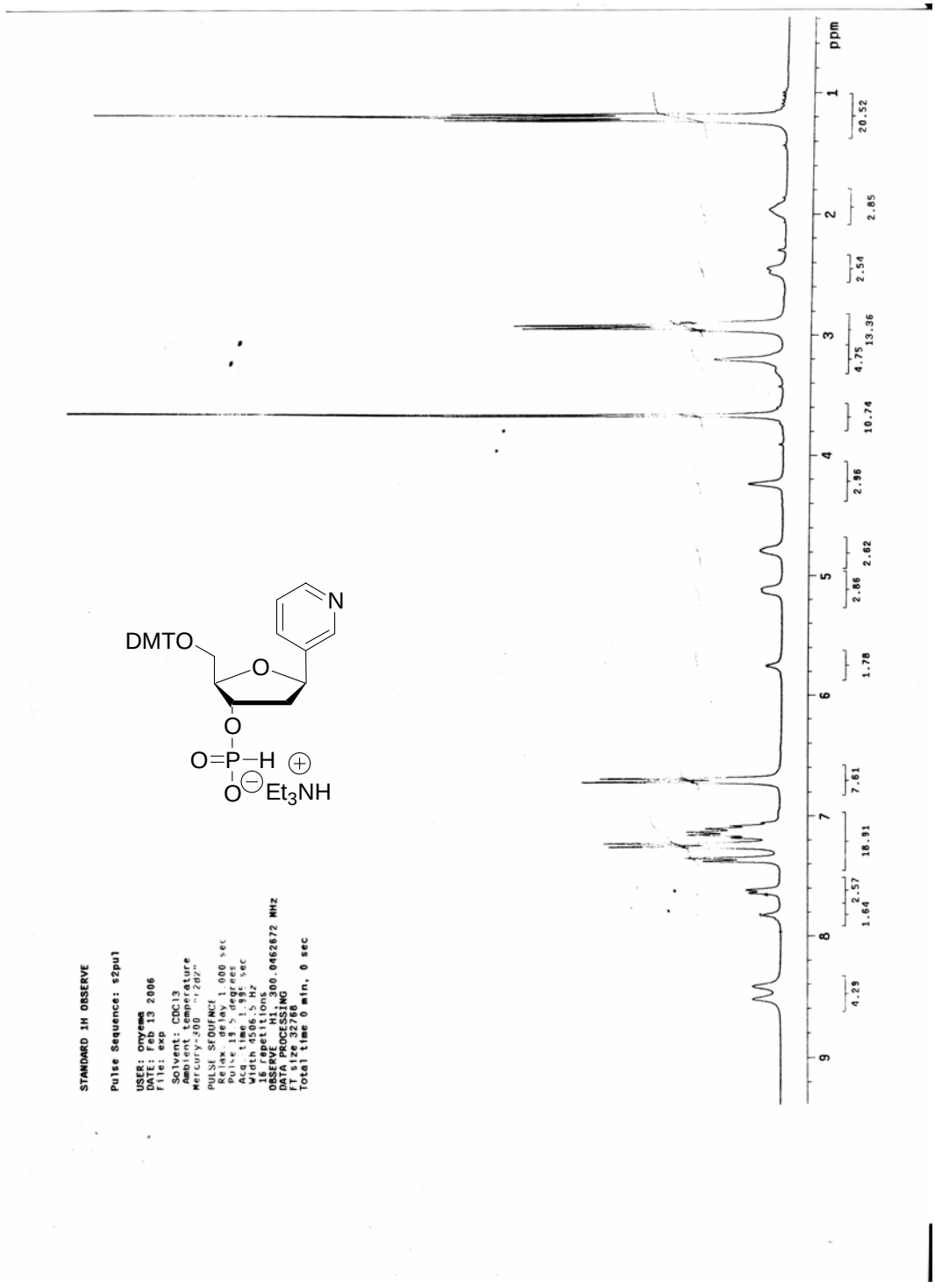

Figure C.2 HNMR spectra of H-phosphonate pyridine nucleoside

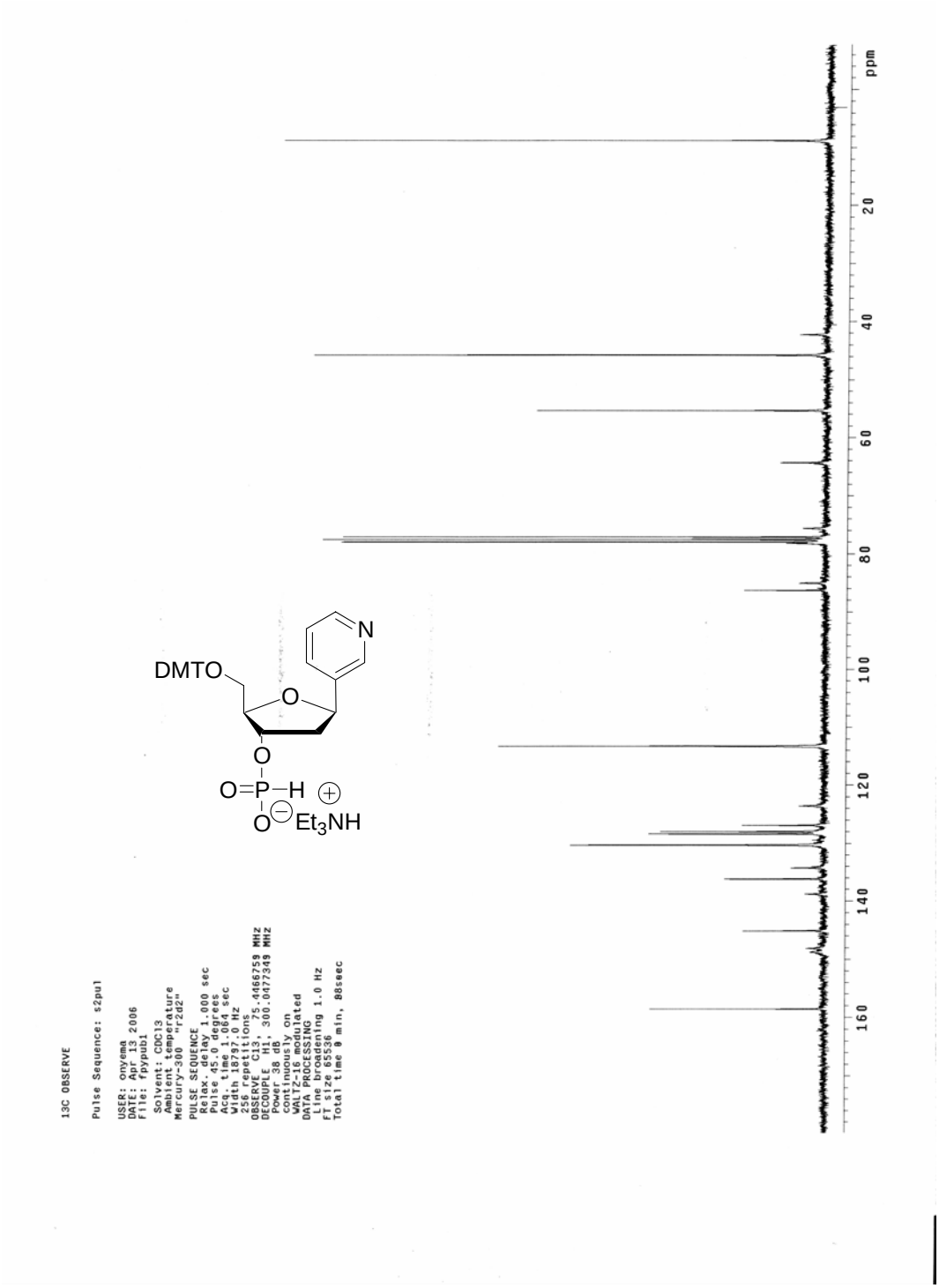

Figure C.3 13CNMR spectra of H-phosphonate pyridine nucleoside

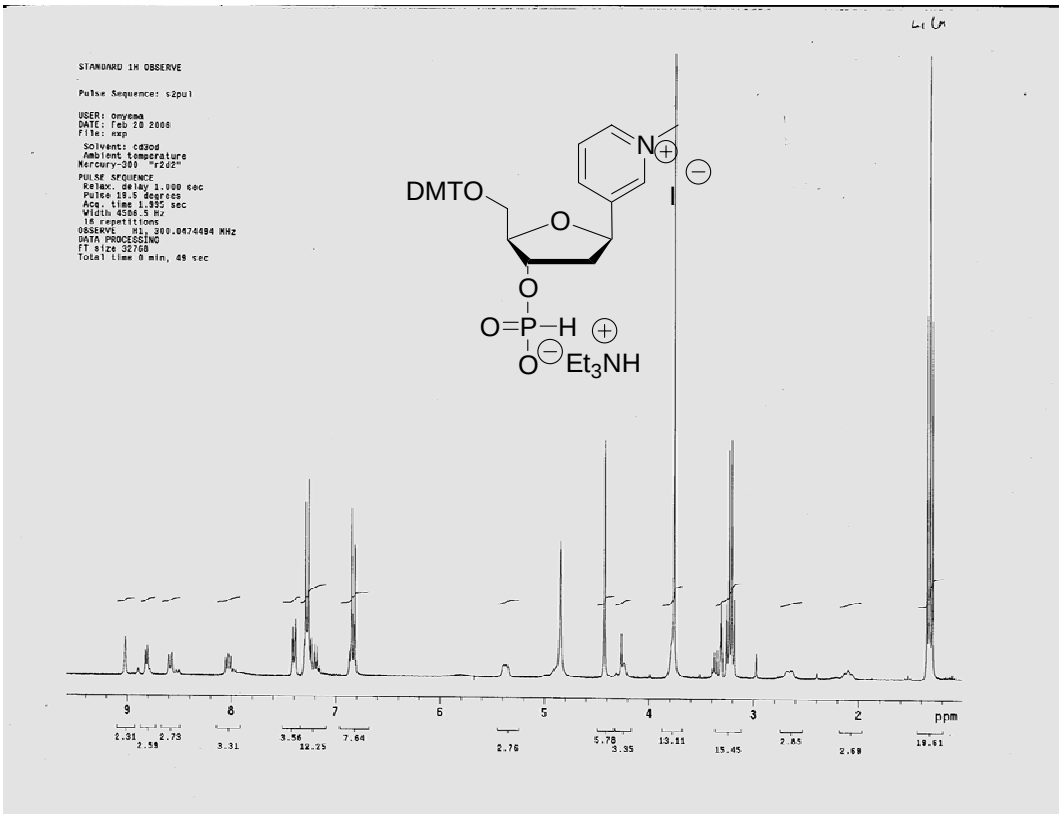

Figure C.4 HNMR spectra of pyridinium nucleoside

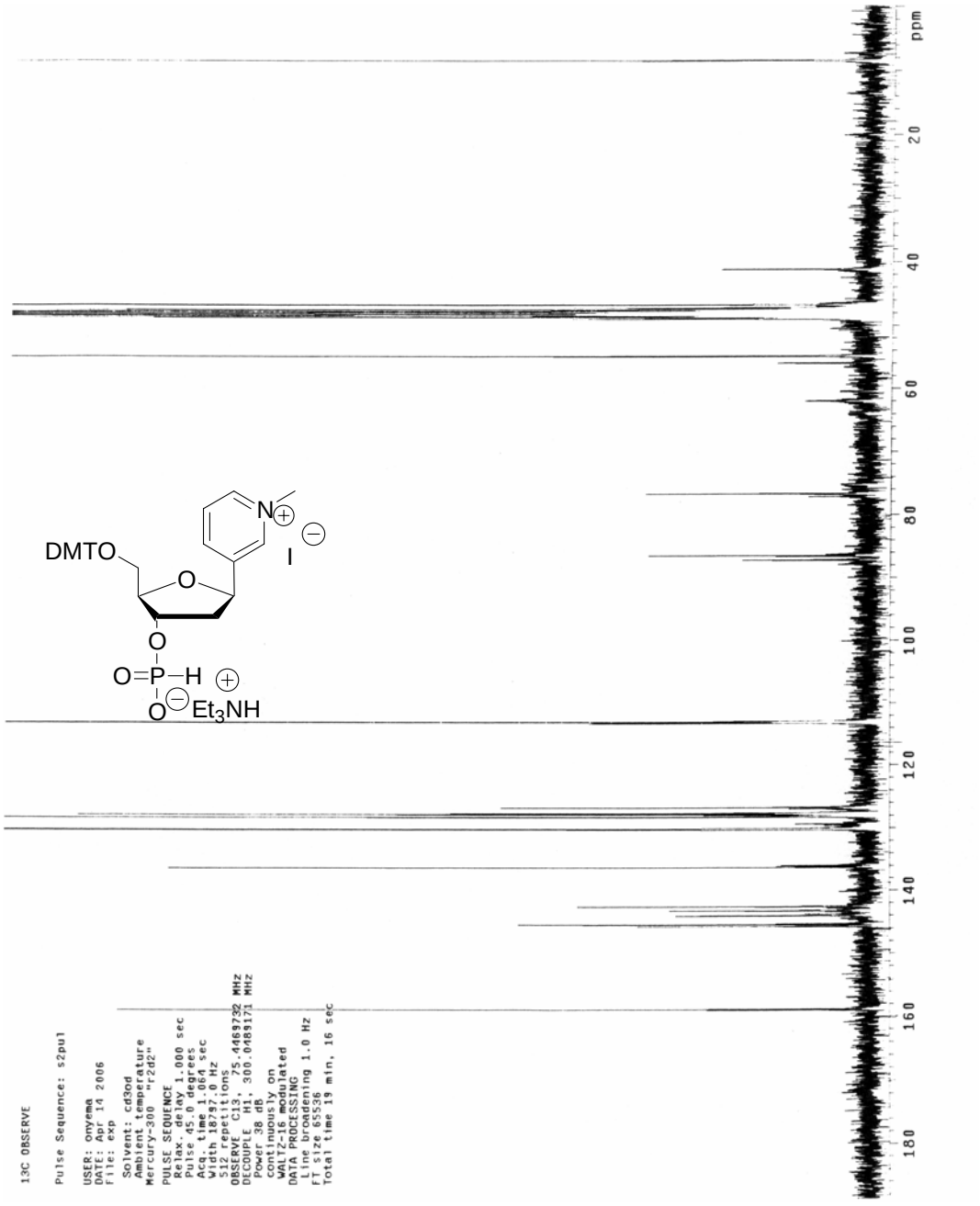

Figure C.5 13CNMR Spectra of pyridinium nucleoside

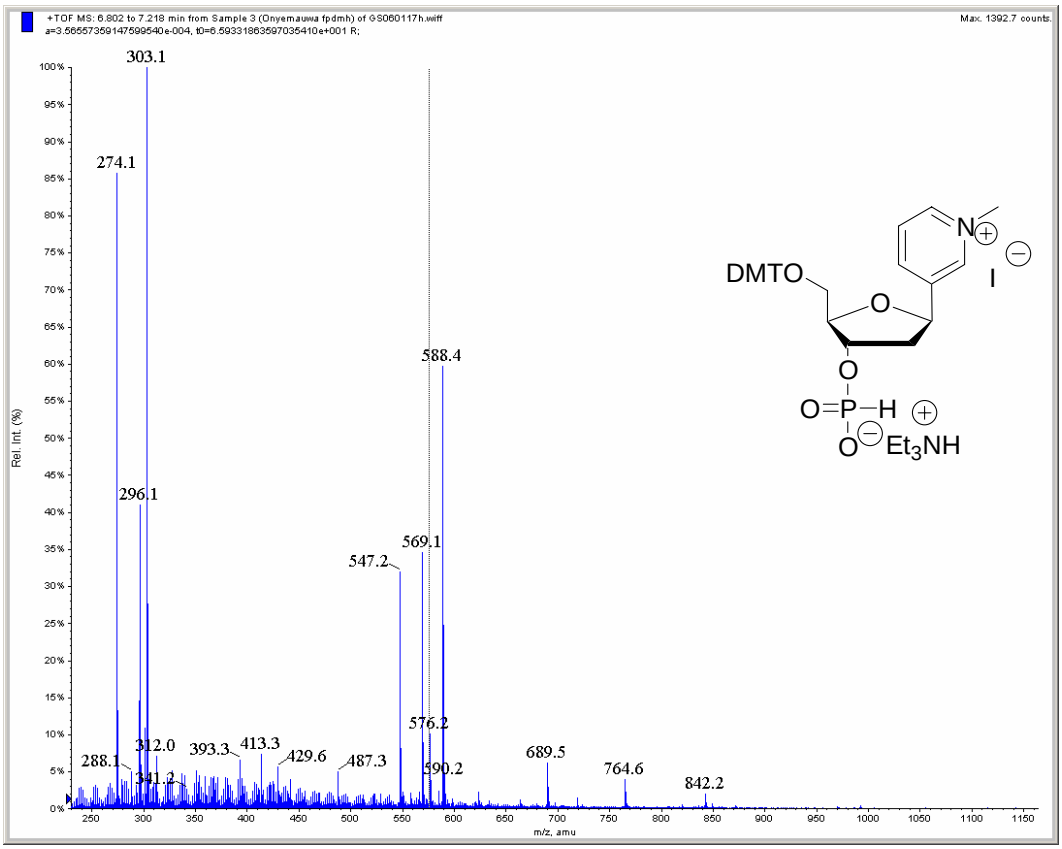

Figure C.6 Mass spectra pyridinium nucleoside

TAT TCC TTC CTT CCt^{+} TCC TTC CTT CCA TAT

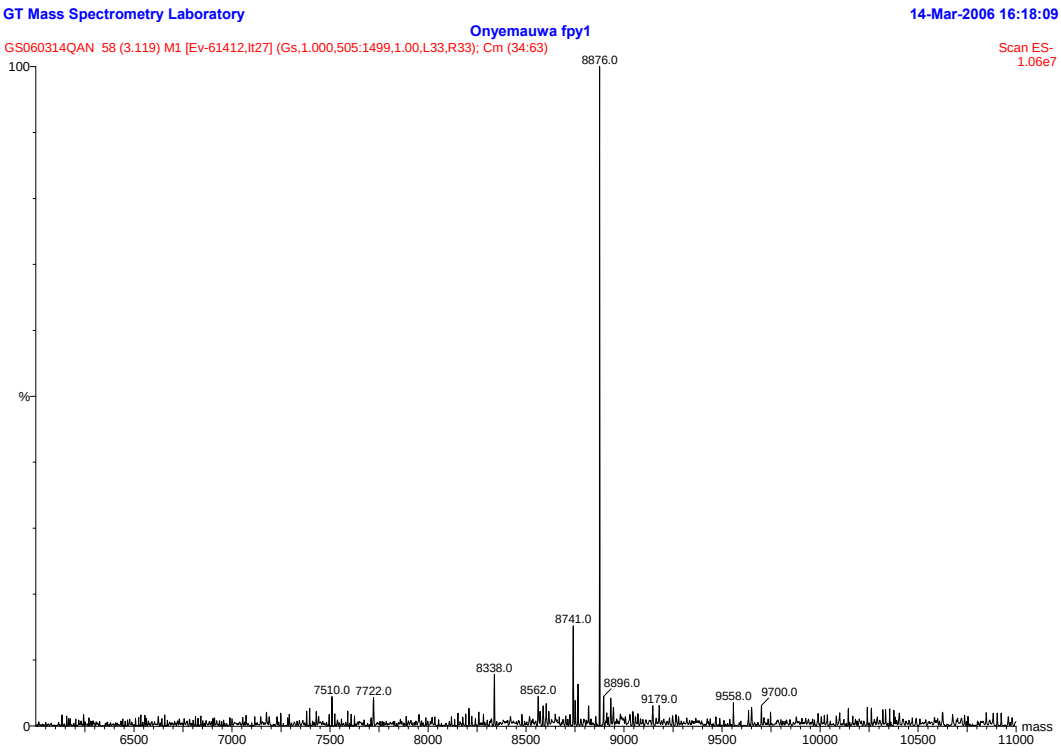

Figure C.7 Mass spectra of DNA sequence with pyridinium nucleoside

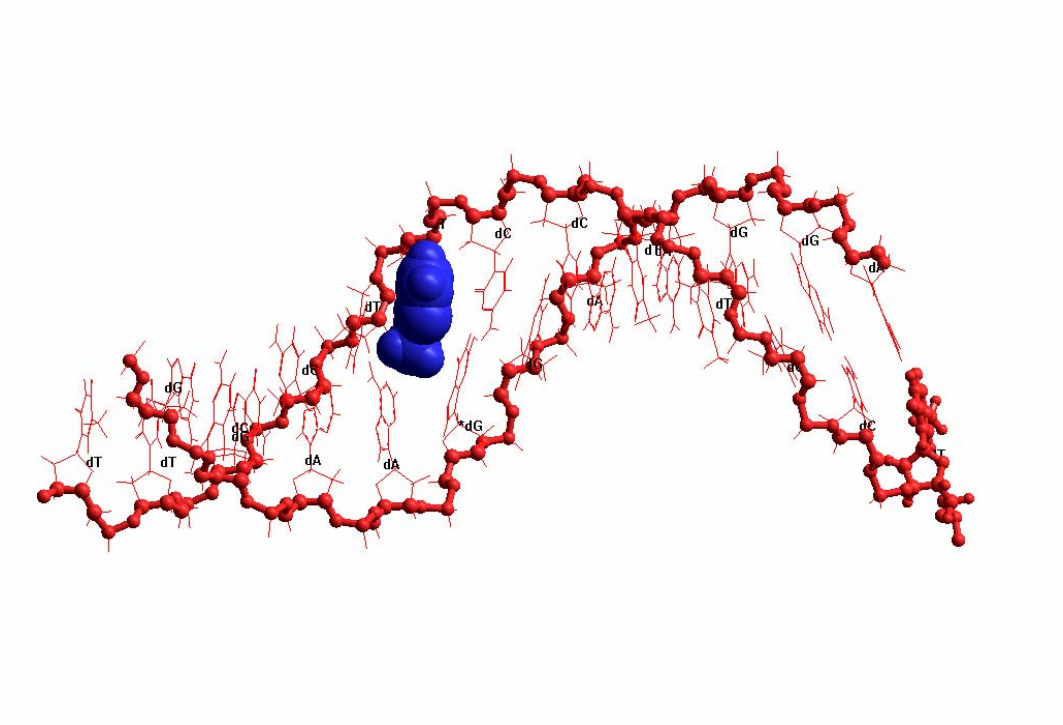

Figure C.8 Molecular model of DNA with pyridinium nucleoside